

INFORMATION TO USERS

This manuscript has been reproduced from the microfilm master. UMI films the text directly from the original or copy submitted. Thus, some thesis and dissertation copies are in typewriter face, while others may be from any type of computer printer.

The quality of this reproduction is dependent upon the quality of the copy submitted. Broken or indistinct print, colored or poor quality illustrations and photographs, print bleedthrough, substandard margins, and improper alignment can adversely affect reproduction.

In the unlikely event that the author did not send UMI a complete manuscript and there are missing pages, these will be noted. Also, if unauthorized copyright material had to be removed, a note will indicate the deletion.

Oversize materials (e.g., maps, drawings, charts) are reproduced by sectioning the original, beginning at the upper left-hand corner and continuing from left to right in equal sections with small overlaps.

Photographs included in the original manuscript have been reproduced xerographically in this copy. Higher quality 6" x 9" black and white photographic prints are available for any photographs or illustrations appearing in this copy for an additional charge. Contact UMI directly to order.

**ProQuest Information and Learning
300 North Zeeb Road, Ann Arbor, MI 48106-1346 USA
800-521-0600**

UMI[®]

University of Alberta

**Integrated protein analysis on microchips for capillary electrophoresis
electrospray mass spectrometry**

by

Can Wang 

A thesis submitted to the Faculty of Graduate Studies and Research in partial fulfillment
of the requirement for the degree of Doctor of Philosophy

Department of Chemistry

Edmonton, Alberta

Fall 2001



**National Library
of Canada**

**Acquisitions and
Bibliographic Services**

**395 Wellington Street
Ottawa ON K1A 0N4
Canada**

**Bibliothèque nationale
du Canada**

**Acquisitions et
services bibliographiques**

**395, rue Wellington
Ottawa ON K1A 0N4
Canada**

Your file Votre référence

Our file Notre référence

The author has granted a non-exclusive licence allowing the National Library of Canada to reproduce, loan, distribute or sell copies of this thesis in microform, paper or electronic formats.

The author retains ownership of the copyright in this thesis. Neither the thesis nor substantial extracts from it may be printed or otherwise reproduced without the author's permission.

L'auteur a accordé une licence non exclusive permettant à la Bibliothèque nationale du Canada de reproduire, prêter, distribuer ou vendre des copies de cette thèse sous la forme de microfiche/film, de reproduction sur papier ou sur format électronique.

L'auteur conserve la propriété du droit d'auteur qui protège cette thèse. Ni la thèse ni des extraits substantiels de celle-ci ne doivent être imprimés ou autrement reproduits sans son autorisation.

0-612-69012-1

Canada

University of Alberta

Library Release Form

Name of Author: Can Wang

Title of Thesis: Integrated protein analysis on microchips for capillary electrophoresis
electrospray mass spectrometry

Degree: Doctor of Philosophy

Year This Degree Granted: 2001

Permission is hereby granted to the University of Alberta Library to reproduce single copies of this thesis and to lend or sell such copies for private, scholarly or scientific research purpose only.

The author reserves all other publication and other rights in association with the copyright in the thesis, and except as herein before provided, neither the thesis nor any substantial portion thereof may be printed or otherwise reproduced in any material form whatever without the author's prior written permission.



3A, 9111, 112 ST

Edmonton, AB, T6G 2C5

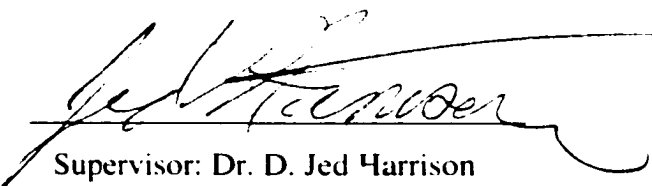
Canada

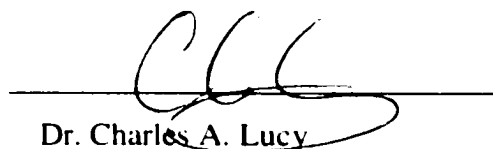
Date: June 28 2001

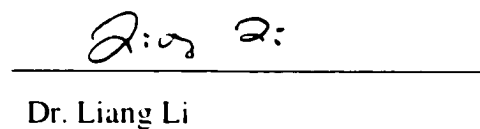
University of Alberta

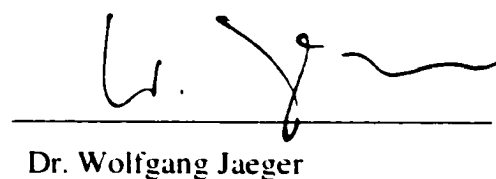
Faculty of Graduate Studies and Research

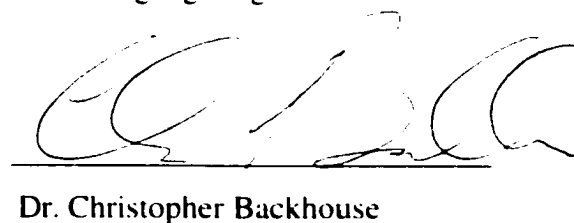
The undersigned certify that they have read, and recommend to the Faculty of Graduate Studies and Research for acceptance, a thesis entitled "**Integrated protein analysis on microchips for capillary electrophoresis electrospray mass spectrometry**" submitted by **Can Wang** in partial fulfillment of the requirements for the degree of **Doctor of Philosophy**.


Supervisor: Dr. D. Jed Harrison

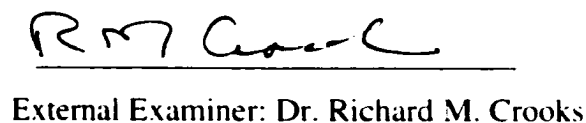

Dr. Charles A. Lucy


Dr. Liang Li


Dr. Wolfgang Jaeger


Dr. Christopher Backhouse

June 28 2009


External Examiner: Dr. Richard M. Crooks

**To my husband, my sisters, my parents and in-laws for their
love and concern**

Thesis abstract

We have developed an integrated system to combine protein processing steps such as protein digestion, preconcentration and peptide separation together with electrospray mass spectrometry detection. This thesis will present the development of the microchip-ESMS interface and its application to protein preparation and analysis on-chip.

Our first effort was to build a reliable interface to couple the microchip and mass spectrometer together. Different designs for spraying directly from the edge of the chip at the channel outlet were tested. Based on a low dead volume microchip-capillary coupling technique, a gold coated capillary tip was coupled to the end of the microchip channel and served as the electrospray tip. This design gave stable electrospray and was used for subsequent studies. Separation of protein and peptides was achieved. A large volume sample stacking method used to preconcentrate samples in the microchip system was developed. Standard peptides were tested and a 50-fold improvement on detection limit with bradykinin was achieved. This preconcentration method is a useful way to enrich analyte ions with high electrophoretic mobilities in the direction opposite to EOF.

Instead of traditional protein solution phase digestion in microcentrifuge tubes, proteins were digested directly in a microchip with immobilized trypsin beads. Two kinds of on-chip digestion methods were used: on-chip reservoir digestion and integrated packed bed digestion. The integrated packed bed appeared to be the fastest digestion method, compared to on-chip reservoir digestion and traditional solution phase digestion. A flow rate of 0.5-1 $\mu\text{l}/\text{min}$ was found adequate for complete consumption of cytochrome c or BSA, corresponding to a digestion time of 3-6 min at room temperature. The digests were separated in the microchip channel before mass spectrometry detection. A solid phase extraction step was then added. On-chip solid phase extraction of peptides was investigated, and it provided an efficient preconcentration method. A two-bed system for protein digestion and subsequent peptide SPE concentration was constructed on-chip. Submicromolar cytochrome c can be successfully digested and preconcentrated. This is the first time so many protein processing steps were integrated together on a microchip device with MS detection, which bump us closer to the final goal of a proteomic processing chip.

Acknowledgements

I give my first thanks to my supervisor, Dr. D. Jed Harrison, for his support, guide and encouragement in all of these years. I never saw any microchip and mass spectrometer before I joined the group. I appreciate that Jed introduced me to this interesting and exciting field. I learned a lot from him, which will make me more confident and stronger in my future life, personally and technically.

Thank Arlene Figley for helping me with grammar and organizing things in the group. I treasure the time spend together with all of the DJH group members, for their giving me company in the lab days and nights, for useful discussions and lots of jokes. I give special thanks to all of the people who worked with me at my beginning stage. Christa Colyer showed me how to use Beckman and set up optical stations. She leaded me to the door of this project. Cameron Skinner is the person who developed the drilling coupling process and brought light to this microchip-ESMS process. Based on this, I could move on for further experiments. I also learned from him lots of poor man's methods in the lab and they all worked well. I enjoyed talking with Nicholas Bings and appreciate lots of useful discussions. I give thanks to Pierre Thibault and Jianjun Li in National Research Council for cooperation, help and gold tip supply.

I give sincere thanks to all of my committee members, Dr. Charles A. Lucy, Dr. Wolfgang Jaeger, Dr. Liang Li, Dr. Christopher Backhouse, Dr. Richard M. Crooks, for their help. I appreciate their understanding and finishing my thesis in such a short time.

My appreciation also goes to the technical support stuff in machine shop, glass shop and electronic shop in the department. They were always so nice to me and gave me help whenever I wanted. I will always remember the bunny suits time spent in the student Fab and I give thanks Fahima Ouchen for helping me with device fabrication. I will never forget all of my friends in Edmonton, the time we spent together in this lovely northern city. Love you all.

Table of Contents

	page
Chapter 1. Introduction	
1.1. Introduction.....	2
1.2. Protein processing on microchip devices.....	3
1.3. Electrospray and nanoelectrospray mass spectrometry.....	7
1.3.1. Electrospray mechanism.....	8
1.3.2. Nanoelectrospray.....	11
1.4. Capillary zone electrophoresis	13
1.4.1. Electroosmosis and electrophoresis.....	13
1.4.2. Channel surface modification.....	16
1.5. Capillary electrophoresis electrospray mass spectrometry interface.....	18
1.6. Protein identification using mass spectrometry.....	21
1.7. Microchip Fabrication	24
1.8. Microchip-electrospray mass spectrometry.....	27
1.9. Outline of this thesis.....	29
1.10. References.....	32
Chapter 2. Interface Development for Coupling Microchip Capillary Electrophoresis to Mass Spectrometry Using Electrospray Ionization	
2.1. Introduction.....	38
2.2. Experimental	41
2.2.1. Joint preparation for coupling microchip to capillary tip.....	41
2.2.2. Capillary tip gold coating and chip channel modification with BCQ	44
2.2.3. Device and instrumental for microchip-ESMS detection.....	45
2.3. Results and Discussion.....	50
2.3.1. Electrospray directly from the edge of the chip.....	50
2.3.2. Capillary tip coupled to chip with minimal dead volume connection.....	55
2.3.3. Gold coated capillary tip coupled at channel outlet for microchip-ESMS.....	57
2.4. Conclusions.....	61
2.5. References.....	62

Chapter 3. Large Volume Sample Stacking to Preconcentrate Samples on Microchip

3.1. Introduction.....	66
3.2. Experimental.....	70
3.2.1. Large volume sample stacking on microchip using LIF detection.....	70
3.2.2. Large volume sample stacking on microchip using MS detection.....	72
3.2.3. Preparation of protein digests.....	75
3.3. Results and Discussion.....	76
3.3.1. Large volume sample stacking on microchip using LIF detection.....	77
3.3.2. Large volume sample stacking on microchip using MS detection.....	81
3.4. Conclusions.....	88
3.5. References	89

Chapter 4. Integration of Immobilized Trypsin Bead Beds for Protein Digestion Within a Microfluidic Chip Incorporating Capillary Electrophoresis Separations and an Electrospray Mass Spectrometry Interface

4.1. Introduction.....	92
4.2. Experimental.....	94
4.2.1. Chemicals and materials.....	94
4.2.2. Microchip device.....	95
4.2.3. Off-chip digestion in microcentrifuge tube.....	97
4.2.4. Digestion with immobilized trypsin within the chip reservoir.....	98
4.2.5. Integrated packed bed for on-chip digestion with immobilized trypsin.....	98
4.2.6. Microchip-CE/nanoESMS.....	100
4.3. Results and Discussion.....	101
4.3.1. Digestion with immobilized trypsin within the chip reservoir.....	101
4.3.2. Integrated packed bed for on-chip digestion with immobilized trypsin.....	104
4.3.3. Sample carry over evaluation.....	113
4.4. Conclusions.....	116
4.5. References.....	117

Chapter 5. Design of a Proteomics Chip: Integration of Protein Digestion, Preconcentration, Capillary Electrophoresis and a Nanoelectrospray Mass Spectrometry Interface Within a Microfluidic Chip

5.1. Introduction.....	122
5.2. Experimental.....	125
5.2.1. Chemicals and Materials.....	125
5.2.2. Microchip Device.....	126
5.2.3. On-Chip Digestion Using Immobilized Trypsin Bead Bed.....	128
5.2.4. Solid Phase Extraction within The Microchip.....	128
5.2.5. Integrated Packed Beds for On-Chip Digestion and Solid Phase Extraction.....	129
5.2.6. Integrated Protein Preconcentration Followed by Trypsin Digestion.....	130
5.2.7 Microchip-CE-nESMS.....	131
5.3. Results and Discussion.....	131
5.3.1. Waters Oasis HLB Beads.....	132
5.3.2. Solid Phase Extraction within the Microchip.....	134
5.3.3. Integrated Packed Beds for On-Chip Digestion and Solid Phase Extraction.....	139
5.3.4. Protein on Beads Preconcentration Followed by Trypsin Digestion within the Microchip.....	144
5.4. Conclusions.....	147
5.5. References	148

Chapter 6. Summary and Future Outlook

6.1. Further Development of Microchip-ESMS Interface.....	151
6.2. Improvement for Integrated Packed Bed Protein Digestion on Chip.....	152
6.3. More Thinking about Solid Phase Extraction on Microchip.....	153
6.4. References.....	158

List of tables

	Page
Table 3-1 Comparison of LOD with and without sample stacking.....	82
Table 4-1. Peptide sequences identified for trypsin digests.....	119
Table 4-2 BSA peaks and the corresponding sequences.....	120
Table 5-1. Comparison of 100 nM cytochrome c fragment intensity with and without SPE.....	137
Table 5-2. Comparison of 800 nM cytochrome c peptide recovery after digestion and SPE.....	141
Table 5-3. Comparison of 200 nM cytochrome c peptide recovery after digestion and SPE.....	143

List of figures

	Page
Chapter 1	
Figure 1-1. Schematic of major process occurring in electrospray.....	9
Figure 1-2. Two steps in covalent BCQ coating.....	17
Figure 1-3. Different types of CEME interface.....	19
Figure 1-4. Flow diagram for the identification of gel-separated proteins by mass spectrum and peptide-mass database searching.	22
Figure 1-5. The procedure for microchip fabrication using photolithography/wet- chemical etching.....	26
Chapter 2	
Figure 2-1. The microchip-capillary coupling process.....	42
Figure 2-2. Schematic diagram of drilling a flat bottomed hole into glass.....	42
Figure 2-3. Photos of flat and pointed hole for microchip-capillary connection.....	43
Figure 2-4. The microchip layout for ESMS from a PCRD-1 chip.....	46
Figure 2-5. Schematic layout of microchip design for (a) PCRD-1, (b)PCRD-2; (c) CEMS.....	47
Figure 2-6. Schematic diagram of the instrumental setup for microchip-ESMS.....	48
Figure 2-7. Block diagram of the high voltage supply system for reservoirs on chip.....	48
Figure 2-8. Different designs for electrospray directly from the flat edge of the chip.....	53
Figure 2-9. Total ion current for electroinfusion of a four peptide mixture.....	59
Figure 2-10. TIE and RIE for the separation of four peptides (500 ng/ml) with Selected Ion Monitoring.....	60
Figure 2-11. Separation of leu-enkephalin and cytochrome c on PCRD-2 chip with ESMS detection.....	60
Chapter 3	
Figure 3-1. Schematic drawing of small volume sample stacking.....	67
Figure 3-2. Large volume sample stacking with polarity switching.....	69
Figure 3-3. Procedures for large volume sample stacking using laser induced fluorescence detection on microchip.....	71

Figure 3-4. Laser induced fluorescence detection in the sample stacking step to trace the stacking profile.....	78
Figure 3-5. Comparison of separation profiles between large volume sample stacking and normal double T injection with stacking.....	80
Figure 3-6. API 3000 triple quadrupole analysis of 10 ng/ml peptide standards using various injection methods on microchip.....	83
Figure 3-7. 2-D gel electrophoresis separation of a 200 µg membrane protein from <i>H. influenzae</i> Rd ⁻ strain.....	86
Figure 3-8. Microchip-CE/Qq-TOF-MS analysis of tryptic peptides from spot 14 of figure 3-7 using large volume sample stacking.....	87

Chapter 4

Figure 4-1. Schematic representation of the on chip reservoir digestion device.....	96
Figure 4-2. Schematic representation of the integrated enzyme reaction bed and capillary electrophoresis chip.....	96
Figure 4-3. Total ion electropherogram (TIE) for 50 µg/ml melittin digested with beads loaded into reservoir for a 3 min “in-reservoir” digestion.....	102
Figure 4-4. Separation profile of off-line melittin digest at different digestion times.....	103
Figure 4-5. Comparison of electroinfusion melittin digestion profile with off-line digestion and in-chip packed bed digestion.....	105
Figure 4-6. Total ion electropherogram for digestion of 16 µM cytochrome c within the packed bead bed, using four different flow rates.....	106
Figure 4-7. Total ion electropherogram and reconstructed ion electropherogram for digestion of 16 µM cytochrome c within the immobilized trypsin bed.....	107
Figure 4-8. Electrokinetically driven infusion of 1 µM cytochrome c, following 3 min digestion of 3 µl of protein solution on the packed trypsin bed.....	108
Figure 4-9. Cytochrome c 10 µg/ml in solution digestion at room temperature.....	110
Figure 4-10. Total ion electropherogram for 6 µM bovine serum albumin (BSA) digested on-chip in the trypsin bed.....	111
Figure 4-11. Electrokinetically driven infusion of 3 µM BSA after 3 min digestion at 0.5 µl/min on the packed trypsin bed.....	112

Figure 4-12. Mass spectrum of infusion (a) digestion buffer passed through a fresh trypsin bead bed, (b) digestion buffer after washing a cytochrome c sample from the bead bed with 50 μ l of buffer at 25 μ l/min..... 114

Figure 4-13. Total ion electropherogram showing (a) the flushing of 3 μ M cytochrome c digest from the sample and separation channels with running buffer in reservoir E. (b) the TIE for digestion buffer after passing through a fresh trypsin bead bed..... 114

Chapter 5

Figure 5-1. Schematic representation of the integrated immobilized trypsin digestion bed, solid phase extraction preconcentration bed and capillary electrophoresis mass spectrometry chip..... 127

Figure 5-2. Comparison of adsorption effect for POROS R2 beads and Oasis HLB Beads..... 133

Figure 5-3. Comparison of mass spectrum for three peptides mixture with and without SPE..... 135

Figure 5-4. Comparison of 100 nM cytochrome c digest mass spectrum with and without SPE..... 137

Figure 5-5. Comparison of separation TIE for cytochrome c digest with and without SPE..... 138

Figure 5-6. Comparison of 800 nM cytochrome c digest mass spectrum with and without SPE..... 140

Figure 5-7. Comparison of 200 nM cytochrome c digest mass spectrum with and without SPE..... 141

Chapter 6

Figure 6-1. Schematic of a possible way for making a direct electrospray tip from a chip..... 151

Figure 6-2. Design of making multiple digestion beds to increase the total bed length.... 153

Figure 6-3. Solid phase extraction of peptides followed by gradient elution..... 154

Figure 6-4. Design for digestion and SPE followed by gradient elution..... 155

Figure 6-5. Solid phase extraction and CE elution or separation design..... 157

List of abbreviations

BCQ	[3-(methacryloylamino)propyl]trimethylammonium chloride
BSA	bovine serum albumin
CB	crystal bond
CE	capillary electrophoresis
CEC	capillary electrochromatography
CGE	capillary gel electrophoresis
CID	collision induced dissociation
CIEF	capillary isoelectric focusing
cps	counts per second
CZE	capillary zone electrophoresis
DTT	dithiothreitol
EOF	electroosmotic flow
ES	electrospray
ESMS	electrospray mass spectrometry
FASS	field amplified sample stacking
FITC	fluorescein isothiocyanate isomer I
FFE	free flow electrophoresis
FTMS	fourier transform mass spectrometry
HPCE	high performance capillary zone electrophoresis
HPLC	high performance liquid chromatography
IEF	isoelectric focusing
IET	ion evaporation theory
ITP	isotachopheresis
LIF	laser induced fluorescence
LOD	limit of detection
MALDI	matrix assisted laser desorption ionization
MAPTAC	[3-(methacryloylamino)propyl]trimethylammonium chloride
MS	mass spectrometry

μTAS	micro-total analysis system
nanoES	nanoelectrospray
NRC	National Research Council
PBS	phosphate buffered saline
PC	polycarbonate
PCR	polymer chain reaction
PMMA	polymethylmethacrylate
PMT	photo multiplier tube
PTFE	polytetrafluoroethylene
PVA	poly(vinyl alcohol)
Q-TOF	quadrupole- time of flight
RIE	reconstructed ion electropherogram
RPM	round per minute
SDS-PAGE	sodium dodecyl sulfate–polyacrylamide gel electrophoresis
SIDT	single ion in droplet theory
SIM	selected ion monitoring
SPE	solid phase extraction
TEMED	N, N, N', N'-.tetramethylethylenediamine
TIE	total ion electropherogram
TOF	time of flight
TPCK	L-1-tosylamino-2-phenylethyl chloromethyl ketone

Chapter 1

Introduction

	Page
Table of contents	
1.1. Introduction.....	2
1.2. Protein processing on microchip devices.....	3
1.3. Electrospray and nanoelectrospray mass spectrometry.....	7
1.3.1. Electrospray mechanism.....	8
1.3.2. Nanoelectrospray.....	11
1.4. Capillary zone electrophoresis	13
1.4.1. Electroosmosis and electrophoresis.....	13
1.4.2. Channel surface modification.....	16
1.5. Capillary electrophoresis electrospray mass spectrometry interface.....	18
1.6. Protein identification using mass spectrometry.....	21
1.7. Microchip Fabrication	24
1.8. Microchip-electrospray mass spectrometry.....	27
1.9. Outline of this thesis.....	29
1.10. References.....	32

1.1. Introduction

The microfluidic chip has been drawing more and more attention since the first introduction of the concept of micro-total analysis system (μ TAS) by Manz et al¹ in 1990. Sample processing including reaction,²⁻¹⁰ purification,^{11,12} separation¹³⁻²⁰ and detection^{3-7, 13-20} may all be done on a microchip, hence the systems have the name "lab on a chip". A microchip system provides fast and high throughput analysis with much less sample consumption. Most commonly, laser induced fluorescence,^{2-4, 13-19} absorbance^{21,22} and electrochemical^{23,24} detection have been used on chip. It is possible to expand the application realm of the microchip by using these chips for sample preparation for other analysis procedures. Such sample preparation devices may be connected to detection methods such as mass spectrometry.²⁵

Mass spectrometry (MS) is a powerful tool for structure analysis and identification of a large variety of compounds such as proteins,^{26,27} drugs^{28,29} or oligonucleotides.^{30,32} With the completion of human gene sequencing, studies in proteomics are drawing more and more attention. Mass spectrometry analysis in conjunction with database searching is the main method now used for protein identification. Electrospray (ES) is one of the widely used ionization methods for MS of proteins. It is compatible with on line separation techniques such as capillary electrophoresis (CE) and high performance liquid chromatography (HPLC). The flow rate on microchip-CE is usually in the submicroliter per min. range, so that it could be coupled to micro or nanoelectrospray ionization. Microchip-CE-ESMS can provide compact, fast and efficient protein analysis with minimal sample consumption and a better chance of automation. Importantly, protein

preparation could be integrated onto a microchip, facilitating more automated ESMS analysis.

The first report about microchip-ESMS was in 1997.³³ We started the project at about the same time. We are one of the few groups in the world who tried to combine microchips to mass spectrometry. Our goal is to build a microchip system that can integrate protein processing steps such as protein separation, digestion, preconcentration, digest separation before electrospray mass spectrometry detection. This thesis gives a detailed description on how we have been gradually working to get closer to this ambitious goal. We first used a method to couple a microchip to a mass spectrometer and get separation on chip with stable electrospray. We also built a novel on-chip fast protein digestion method. Two sample preconcentration techniques, large volume sample stacking and solid phase extraction, were integrated on-chip before the protein digest separation and MS detection.

In this introduction chapter, we will give some review and background information relevant to what we are going to talk in the following chapters. An overview of sample processing (especially protein analysis) on microchip and microchip-ESMS system will be presented. Electrospray, capillary electrophoresis, protein MS analysis and microchip fabrication are the basis of our experiments in all of the following chapters, and background information of all of these items will be introduced sequentially.

1.2. Protein processing in microchip devices

The microchip devices can be roughly divided into two categories: one is microfabricated structures such as microarrays, and the other one is microfluidic devices.

which have channels or reaction chambers for fluid manipulation. The development of a μ TAS or microchip system is aimed at integration, miniaturization and automation of chemical and biochemical analysis processes. The first capillary electrophoresis separation on a planar microfluidic device was reported by Harrison and coworkers¹³ in 1992. Since then, sample separation with microfluidic systems has been developed. Amino acids,^{14,15} nucleic acids,¹⁸ drugs,^{34,35} peptides and proteins³⁶⁻³⁹ could all be separated. Besides capillary zone electrophoresis (CZE), capillary electrochromatography (CEC),⁴⁰ open channel chromatography¹⁶, free flow electrophoresis (FFE)¹⁷ and capillary gel electrophoresis (CGE)^{18,41} have been demonstrated on microchip. In addition to separation, the beauty of the microchip system is that it could provide a convenient platform to integrate complex sample processing together, with shorter time and less sample consumption. DNA sequencing,^{42,43} polymer chain reaction (PCR)^{2,44-45} and DNA restriction digestion⁴⁶ were all performed on microchip. These studies showed that complex biochemical reactions can be performed on chip. Protein analysis such as sample purification, enzymatic reaction and preconcentration have also been explored on the microchip. We give a general review of protein processing on microchip in the following part of this section.

For analyzing complex bio-samples, initial sample cleanup increases the sensitivity and makes sample analysis much easier. Desalting is an important step in protein processing. Smith's group^{11,12} used microdialysis on microchip to purify protein samples. In their latest report¹², they used a device with two microdialysis membranes sandwiched between three polycarbonate layers. The polycarbonate layers had serpentine flow channels and the middle piece had an electrospray tip connected. Low molecular

weight matrix and salt in the sample diffused through the membrane and was removed by the flowing buffer solution. The purified protein sample was detected by electrospray mass spectrometry. The results showed that the membrane could effectively remove the salts in phosphate buffered saline (PBS) and the mass spectrum was improved. This design provides an efficient way to purify small amounts of liquid sample for electrospray detection.

Isoelectric focusing (IEF) is the traditional method to separate protein mixtures. In capillary isoelectric focusing (CIEF) of proteins, the whole capillary is filled with ampholyte and proteins. Upon application of an electric field, a pH gradient is formed and the proteins are separated according to their pI values. Conducting CIEF in a microchip reduces analysis time compared to traditional capillary or slab gel IEF. Recently, several groups have performed CIEF in both glass^{47,48} and plastic^{49,50} microchips. Their first approach was to make a single channel in the microdevice, with both ends connected to a capillary.^{47,48} Later on, more complex designs were used. Smith⁵⁰ and coworker showed their IEF chip with catholyte, anolyte and sample reservoirs, two connections for sheath liquid and sheath gas, and an electrospray tip at the end. This polycarbonate chip integrated the CIEF process and the ESMS detection together. Separation of simple protein mixtures was demonstrated. IEF in a microchip is still at the beginning stage. In the future, it may play an important role for protein separation and make contributions for total protein analysis on a microchip.

On-chip protein reactions have been studied by several groups. In our research group, Chiem et al.³ showed that competitive immunoassay of serum theophylline can be performed on-chip using integrated mixing, reaction and separation steps. Post separation

labeling of human serum proteins was studied by Colyer et al.⁴ Mangru et al.⁵ investigated horseradish peroxidase catalyzed reaction of luminol with peroxide using chemiluminescence detection. Cohen et al.⁶ studied protein kinase A catalysis of the transfer of a phosphate group to a serine residue. Hadd et al.⁷ described on-chip reactions between β -galactodidase and β -D-galactopyranoside. In all of these reactions, proteins, enzymes, or other reagents were driven by electroosmotic flow, mixed, reacted and analyzed in the channel networks. This demonstrates that rapid analysis with small amounts of proteins and reagents on microchip is feasible. These studies laid the groundwork for creating integrated protein digestion designs.

Protein digestion with MS detection and database searching is the most popular method used for protein identification. Based on this scheme, in the first stage, protein was digested off-line and the digest was separated on-chip for MS analysis.³⁶⁻³⁹ Traditionally, protein is digested in solution phase with a long digestion time (> 12 hours). When the digestion process was integrated on the chip, sample loss due to the transfer process could be avoided and much less amount sample could be used. The first on-chip digestion was reported by Xue et al.⁸ They used a chip with nine $25\ \mu\text{m} \times 60\ \mu\text{m}$ channels to perform in reservoir tryptic digestion of melittin, prior to direct ESMS from the edge of the chip. Although a syringe pump was used to drive the sample to the mass spectrometer, it was a novel starting step.

Varga et al.^{9,51} developed an immobilized enzyme reactor using the porous surface of a silicon device. After reduction/alkylation, protein was digested while passing through the enzyme reactor, then transferred to a microchip nanovial array MALDI (matrix assisted laser desorption ionization) target using piezoelectric microdispensing.

The protein identification was made by MALDI-TOF MS and database searching. The immobilized trypsin reactor provided very fast digestion (1-3 min) for a 1 μ l sample. This gives the system a throughput of 100 protein samples in 3.5 hours. In this system, microarray and microfluidic devices were all used. Microfabricated nanovials were also used for protein digestion.⁵²⁻⁵⁴ Fifteen nanoliter vials were made in a silicon chip to contain protein and enzyme for digestion. Solvent evaporation was minimized by using a closed humidity chamber or a thin film of octane on top of the sample. The reaction proved to be faster in the chip-based vials, compared to digestion performed in a conventional microcentrifuge tube. The authors proposed that the increased surface to volume ratio in the nanovials accelerated digestion through surface induced denaturing of the proteins.

Microchips can be used as a convenient tool for sample purification, protein separation and enzymatic digestion respectively. There is a need to combine several protein processes together in one microchip before mass spectrometry detection, to make it compact and multifunctional. This has been our goal and our progress will be presented in this thesis.

1.3. Electrospray and nanoelectrospray mass spectrometry

Electrospray (ES) is a method by which ions, present in a solution, can be transferred to the gas phase. It consists of the application of an electric field to the tip of a capillary containing a solution of electrolyte ions. The phenomenon of electrospray has been known for years. The first published report about the observation of electrospray is attributed to Zeleny in 1914.⁵⁵ Another publication by Zeleny⁵⁶ in 1917 included

impressive photographs and details of various operational modes of electrospray. Dole and co-workers⁵⁷ were the first to attempt to study charged particles produced by electrospray in 1968. Their goal was to produce a molecular beam of macro-ions and characterize them by ion mobility spectrometry. Electrospray ionization mass spectrometry (ESMS) was first introduced by Yamashita and Fenn⁵⁸ in 1984. A very similar, independent development was reported at approximately the same time by Aleksandrov and co-workers⁵⁹ in Russia. In 1987, Smith's group began to couple CE to ESMS.⁶⁰ Fenn and co-workers⁶¹ reported convincing results for large molecules such as proteins and polymers in 1989. After that, ESMS gained widespread attention. The high sensitivity of the electrospray technique and compatibility with liquid separation methods (HPLC or CE) gave rise to the popularity of ESMS. An advantage of electrospray ionization is that a high molecular mass compound could be multiply charged with great efficiency and readily detected on instruments previously considered to be restricted to the low mass range, such as quadrupole mass spectrometer. Since the end of 1980s, the volume of research in ESMS has risen exponentially. ESMS became a widely used technique in biological, biochemical, pharmaceutical and medical research.

1.3.1. Electrospray mechanism

Electrospray can be operated in either the positive ion mode for the generation of positive gas phase ion or the negative ion mode for the generation of negative ions. A schematic drawing of positive ions electrospray configuration is shown in Figure 1-1. When a high voltage is applied to the capillary tip, an electric field exists between the

capillary tip and a counter electrode. The magnitude of the electric field E at the capillary tip can be approximated by the following equation^{62,63}

$$E \approx \frac{2V}{r \ln(4d/r)} \quad 1-1$$

where V is the potential applied to the capillary tip, r is the outer radius of the capillary tip and d is the distance between the capillary tip and the counter electrode. Under the influence of an applied electric field the positive ions at the tip will migrate to the liquid surface. The solution at the capillary tip will have an overall positive charge and will be drawn towards the low field at the counter electrode. At relatively lower voltage, large droplets are emitted periodically from the capillary tip and this is referred to as a pulsed droplet mode. When the applied voltage increases, the frequency of the droplet formation increases with decreased droplet size. When the applied voltage is sufficiently high, the shape of the solution surface at the capillary tip changes and forms a cone. It was named the Taylor⁶⁴ cone because Taylor was the first to describe this cone in detail. From the tip of the Taylor cone a filament jet emerges, and from which charged droplets form. The

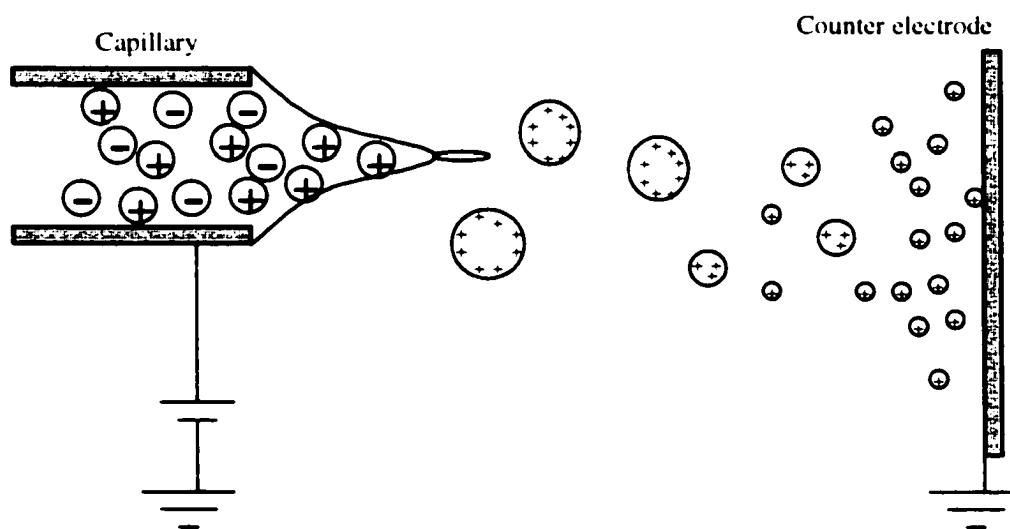


Figure 1-1. Schematic of major process occurring in electrospray. (not to scale)

droplets continue to evaporate and split to form gas phase ions. This is the normal working electrospray mode we use for mass spectrometry.⁶⁵ The result of further increases in the applied voltage causes discharge and it is sometimes called a bifurcated mode, which consists of two spray origins positioned at the tip of the capillary. Smith⁶⁶ derived a useful equation for the required onset voltage V_{on} at the capillary tip, which leads to instability of the Taylor cone and formation of the charged jet:

$$V_{on} = \left(\frac{r\gamma\cos\theta}{2\epsilon} \right)^{1/2} \ln(4d/r) \quad 1-2$$

where γ is the surface tension of the solvent, ϵ is the permittivity of vacuum ($8.8 \times 10^{-12} \text{ J}^{-1} \text{ C}^2\text{m}^{-1}$), and θ is the half angle of the Taylor cone (49.3)

The charged droplets formed at the end of the filament jet undergo solvent evaporation while the charge remains constant, which results in an increase in the surface charge density. An increase in surface charge density will eventually lead to an increase of the electrostatic repulsion or coulombic repulsion. When coulombic repulsion of the ions overcomes the surface tension, a droplet with a charge q , is close to the Rayleigh stability limit.⁶⁷ This limit is expressed below and fission occurs at the limit:

$$q^2 = 64 \pi^2 \epsilon \gamma r^3 \quad 1-3$$

Gomez and Tang⁶⁸ observed that fission actually occurs at 80% of the Rayleigh limit, resulting in approximately 20 offspring droplets. The offspring droplets are approximated to account for 2% of the parent droplet's original mass and 15% of its charge. Both the residual parent droplet and its offspring continue the same sequence of solvent evaporation and fission.

Different theories have been proposed to explain the process that ultimately leads to the formation of gas phase ions from these small droplets. Dole and coworkers⁵⁷ described a "charge residue" model which was later renamed by Kebarle and Tang⁶³ as the "single ion in droplet theory" or SIDT. This theory is based on successive Rayleigh fission events finally resulting in the formation of microdroplets containing a single charged species. These small droplets convert to gas phase ions upon evaporation of the last solvent molecules. Iribarne and Thomson^{69,70} proposed an alternative mechanism called "ion evaporation theory" or IET. IET assumes that ions evaporate from small highly charged droplets. The coulomb repulsion between the ion and the droplet surface would push the ions out of the droplet. At a certain stage the droplet does not undergo subsequent fission, but instead emits gas phase ions. After much discussion, no consensus has been achieved on which gas phase ion formation mechanism is correct. But the electrospray continues to be used and improved as a popular ionization method for mass spectrometry.

1.3.2. Nanoelectrospray

Traditionally,^{71,72} the electrospray capillary tip has a diameter of $> 100 \mu\text{m}$ o.d. and the capillary is either fused silica or stainless steel. The liquid was driven by electroosmotic flow (EOF) or mechanical forces such as pumping and the flow rate was in the $\mu\text{l}/\text{min}$ range.

The word "nanoelectrospray" first appeared in the paper published by Wilm and Mann in 1996.⁷³ In their experiment, one end of a Borosilicate glass capillary was pulled to 1-2 μm diameter and the outer surface was vapor deposited with gold. Sample (0.2-2

μl) was injected from the open end and sprayed at ~ 20 nl/min while the electrospray voltage was applied to the gold. At such a low flow rate, small droplets around 200 nm were generated in the electrospray process while 1-2 μm droplets were generated with the conventional electrospray. The liquid flow in the pulled capillary was due to the electrospray process itself, and no solvent pumps were needed. This nanoES was a separate off-line setup for direct spray of a small volume of samples. It was named nanoES because of the low nanoliter per minute flow rate and droplet size in the nanometer range. Later on, in CE-ESMS,⁷⁴ microchip-CE-ESMS^{37,75,76} and LC-ESMS^{77,78} literature, when a sheathless interface was used and the electrospray flow rate was in the low nl/min range it was referred to as nanoelectrospray.

Nanoelectrospray has several advantages: 1) When the sample amount is limited, the low flow extends the analysis time. 1 μl could give 50 min for 20 nl/min and this allows extensive MS/MS analysis of several peptides, while this is impossible for conventional electrospray at $\mu\text{l}/\text{min}$. 2) The low flow rate in nanoelectrospray produces a small droplet size which makes the desolvation and ionization efficiency higher. Wilm and Mann⁷³ found that 1 in 390 analyte ions were detected, while in traditional electrospray only 1 in 20,000 analytes ions were detected. The ionization efficiency in nanoelectrospray could be 1-2 orders of magnitude higher. This higher ionization efficiency also makes the sensitivity higher. 3) Wilm and Mann⁷³ found that nanoelectrospray could be operated over a wide range of solvent composition and pH, and could tolerate some salt contamination. 4) Finally, nanoelectrospray could be coupled on-line with CE, microchip-CE and LC because they usually have a flow rate in the low nl/min range.

1.4. Capillary zone electrophoresis

Electrophoresis was first introduced in 1897⁷⁹ as a technique for the separation of charged molecules based on their different migration speed in the electric field. In the early 1980s, Jorgenson and Lukacs^{80,81} introduced capillary electrophoresis (75 μm i.d.), which is usually called capillary zone electrophoresis (CZE) or high performance capillary zone electrophoresis (HPCE). Characterized by low sample consumption (several nl), high resolution and efficient separation, CE has become more and more popular. A variety of CE instruments have become commercially available in recent years.

Traditionally, CE is performed in a capillary tube with a typical inner diameter of 10-100 μm and total length of 27-100 cm. The majority of CE separations have been performed in fused silica capillaries, due to the excellent electrical and optical properties of the wall material. Both ends of the capillary are immersed in buffer reservoirs that contain electrodes. Sample is injected as a narrow plug either hydrodynamically or electrokinetically. A high voltage, typically in the range of 10-30 kV, is applied to the electrodes for separation. On-column detection is usually used to avoid loss of separation efficiency and for ease in set-up. Capillary electrophoresis can also be performed in the channels of the microchip. In the microchip, less sample is consumed and shorter lengths can be used, leading to faster separation can be achieved.

1.4.1. Electroosmosis and electrophoresis

Fundamentally, two processes are associated with CZE: electroosmotic flow (EOF), and electrophoresis of charged species. EOF of the background electrolyte is generated as

a result of an immobilized charge on the capillary wall. The EOF is usually cathodic due to negative charges of the silanol groups (Si-OH). At pH > 3, the silanol groups are ionized to SiO⁻ and attract the cationic species in the buffer, forming the compact and diffuse layers. Under the applied electric field, the mobile cations in the diffuse layer migrate in the direction of the cathode, carrying hydration water with them. Thus the positively charged ions drag the electrolyte solution along and there is a net flow of solvent towards the cathode. This is the origin of the electroosmotic flow (EOF). The electroosmotic flow affects all species equally, and the mobility is expressed as ⁸²

$$\mu_{eo} = \frac{\epsilon \zeta_{eo}}{4\pi\eta} \quad 1-4$$

where μ_{eo} is the electroosmotic mobility, ϵ and η are the dielectric constant and the viscosity of the solution, respectively, and ζ is the zeta potential at the plane of shear in the double layer where the ions and solvent become mobile.

When an ion is placed in an electric field E , it experiences a force that is proportional to its effective charge, q , and the electric field strength. The translational movement of the ion is opposed by a viscous drag force that is proportional to the particle velocity, v_{ep} , hydrodynamic radius, r , and medium viscosity, η . When the two forces are counterbalanced, the particle moves with a steady state velocity

$$v_{ep} = \mu_{ep} E \quad 1-5$$

where μ_{ep} is the electrophoretic mobility and is described as

$$\mu_{ep} = \frac{q}{6\pi\eta r} \quad 1-6$$

When an electric field is applied to an ion in the buffer solution, electrophoretic and electroosmosis forces act simultaneously on the ion. The observed velocity of an ion is the addition of the electroosmotic and electrophoretic vectors.

$$v_{ob} = \mu_{ob} E = (\mu_{ep} + \mu_{eo}) E \quad 1-7$$

The migration time t of an ion can be expressed by

$$t = \frac{Ll}{(\mu_{eo} + \mu_{ep})V} \quad 1-8$$

where L is the length of the separation capillary and l is length between the injection end to the detector. V is the high voltage applied at the end. For cations, both electrophoretic and electroosmotic mobilities are in the same direction, and so cations migrate first out of the capillary. Neutral molecules experience only electroosmosis, while for anions electroosmosis and electrophoretic mobilities are in the opposite directions and they are the last to be detected. In principle, the separation of solutes depends only on the electrophoresis. The charge/size ratio of analyte species determines the separation as indicated in equation 1-6. The efficiency of any electrophoretic separation can be measured by calculation of the resolution, R . Resolution of two components in CE is defined as

$$R = \frac{\sqrt{N} \Delta v}{4 v_{av}} \quad 1-9$$

where Δv is the difference in component flow velocity and v_{av} is the average velocity of the two components. N is the plate number of one ion species, defined by

$$N = \frac{l^2}{\sigma_{all}^2} \quad 1-10$$

where σ_{all} is the peak variance of a Gaussian peak and l is length between the injection end to the detector. σ_{all} contains all bandbroadening terms. Generally, σ_{all} consists of longitudinal diffusion, σ_{LD} , sample injection, σ_{Inj} , detection, σ_{Det} , Joule heating, σ_{Heat} , and other terms such as wall adsorption. The overall σ_{all}^2 can be expressed as⁸³

$$\sigma_{\text{all}}^2 = \sigma_{\text{LD}}^2 + \sigma_{\text{Inj}}^2 + \sigma_{\text{Det}}^2 + \sigma_{\text{Heat}}^2 + \sigma_{\text{other}}^2 \quad 1-11$$

1.4.2. Channel surface modification

The CE separation performance can be impaired by the adsorption of analytes at the internal surface of the capillary or microchip channels. Proteins and peptides can be easily adsorbed by interactions such as hydrophobic interaction, electrostatic interaction, hydrogen bonding and van der Waals interactions.⁸⁴ To avoid these undesirable interactions, the channel surfaces can be modified with different chemicals to suit a certain buffer or separation efficiency need. Channel surface coating can be classified into dynamic coating and covalent bonded coating.

The dynamic coating method is attractive because of its simplicity. It involves the adsorption of a surface modifier which is either mixed in the running buffer or applied by rinsing the channels using a separate solution prior to the sample analysis. The compounds used for dynamic coating are usually polymers⁸⁵ or surfactants.⁸⁶ The adsorption of charged polymers or surfactants introduce positive⁷⁴ or negative charges on the surface, thus changing the direction or strength of the EOF. Neutral polymers such as poly(vinyl alcohol) (PVA) and hydroxypropylmethyl cellulose⁸⁵ were used to reduce EOF successfully under pH 5, and 1 million plates per meter separation efficiency was achieved for proteins. The problem with dynamic coating is that it deteriorates during

repetitive runs and some buffer additives for coating might decrease the separation efficiency. For electrospray ionization, polymers and surfactants need to be avoided in the buffer.

Covalently bonded coating is also referred to as a permanent coating. It usually includes two layers: a reactive bifunctional intermediate layer and a polymer top layer.⁸⁷ The intermediate layer is formed via the Si-O-Si or Si-C attachment to the channel surface. The subsequent polymer layer is covalently attached to the intermediate layer. Neutral polymers such as Poly(acrylamide),⁸⁸ cationic polymers such as poly(vinylamine),⁸⁹ [3-(methacryloylamino)propyl]trimethylammonium chloride

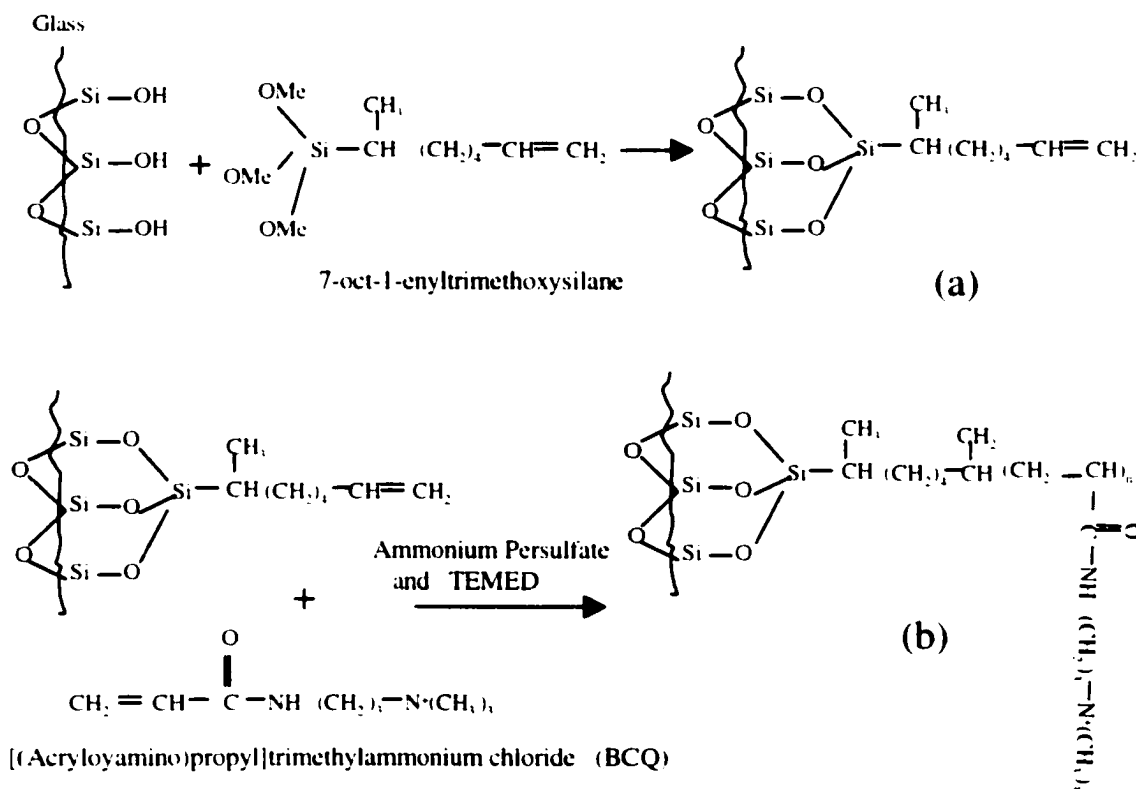


Figure 1-2. Two steps in covalent coating: (a) 7-oct-1-enyltrimethoxysilane reacts with the glass surface, (b) [(Acryloylamino)propyl]trimethylammonium chloride (BCQ) reacts with the silane.

(MAPTAC)⁷⁴ or [(Acryloylamino)propyl]trimethylammonium chloride (BCQ)^{36-37,74} are all used to reduce analyte adsorption and to modify the EOF. The covalently bonded coating process usually has many steps and is time consuming. However the coating generally has a longer lifetime and is stable. The exclusion of coating additives from the running buffer is desirable for CE-MS since the presence of surfactants or polymers in the buffer is detrimental to electrospray. The covalent bonded BCQ coating was used in our microchip-CE-MS experiments. The reaction steps involved in the BCQ coating is given in Figure 1-2. In this coating process, the silanol group on the glass surface first reacts with 7-oct-1-enyltrimethoxysilane and a Si-O-Si bond is formed. The double bond at the end of the attached silane reacts with the BCQ. In this step, ammonium persulfate is the initiator for the polymerization and the N, N, N', N',-tetramethylethylenediamine (TEMED) is the accelerator. After coating, the quarternary amine gives a positive charge on the wall and the electroosmotic flow is reversed. The EOF in uncoated fused silica columns is significantly affected by low pH. However, columns permanently coated could give stable EOF at low pH, but the Si-O-Si bond is prone to hydrolysis in basic conditions.⁸⁴

1.5. Capillary electrophoresis electrospray mass spectrometry interface

The development of a microchip-ESMS interface is actually based on the experience of CE-ESMS. In this section, we will review the CE-ESMS interface. The development of microchip-ESMS interface will be described in Chapter 2.

Since the first coupling of CE-ESMS in 1987 by Olivares et al.⁶⁰ CE-MS has undergone significant developments in instrumentation and application. CE-MS

combines the advantages of both CE and MS which makes it a high separation efficiency and a high sensitivity analysis method. Direct CE-MS coupling requires an interface that does not damage the separation efficiency. Electrospray was chosen because it is easy to set up, sensitive, and versatile enough to be compatible with different CE flow rates. Basically there are three types of ES interfaces: coaxial sheath flow, sheathless and liquid junction.

Figure 1-3a shows the sheath flow interface first developed by Smith et al.⁹⁰ The sheath liquid mixes with the CE separation buffer at the end of the CE capillary tip, providing the electrical contact needed for CE separation and electrospray. The sheath liquid is usually a volatile solvent such as methanol, acetonitrile or isopropanol, modified with some buffer, if needed. In this way, the sheath liquid also aids in the ionization

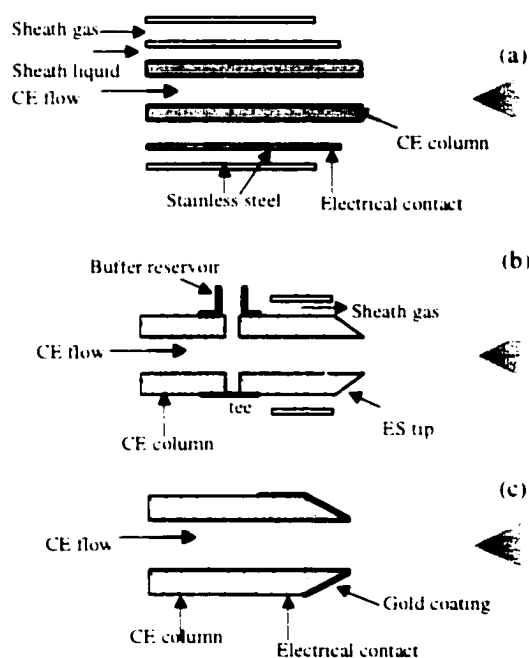


Figure 1-3. Different types of CEME interface: (a) coaxial sheath flow, (b) liquid junction, (c) sheathless. Modified from reference 100.

process and the limitation on CE buffer composition can be relaxed. A third concentric tube may deliver sheath gas (eg. N_2), which can assist in nebulization and create the small droplets required for ES ionization. It can also prevent corona discharge at the electrospray tip. Especially at high liquid flow rate (> 1 ml/min), it is necessary to permit stable electrospray operation.⁹¹ When a sheath gas is used, electrospray is sometimes referred to as ion spray.^{92,93} The sheath

flow interface has been widely used because it is robust and easy to manipulate. The disadvantage is that the sheath liquid dilutes the analytes and introduces background noise,⁹⁴ which lowers the maximum sensitivity obtainable.

A liquid junction interface is shown in Figure 1-3b. It was first developed for CE-MS by Henion and coworkers.⁹⁵ The CE capillary and the electrospray tip are coupled together by a tee which contains the make up liquid. The gap in the tee between the two capillaries is usually 10 to 25 μm . Voltage is applied to the tee to complete the circuit for CE separation and electrospray. Sheath gas can be applied to help nebulization. The disadvantage of this design is that it is cumbersome to align the CE capillary and electrospray tip and that the make up flow could dilute the CE flow. In a comparison of coaxial sheath flow and liquid junction interface, Pleasance et al.⁹⁶ found that the former provided better sensitivity and separation efficiency. Currently, liquid junction is only in limited use.

The third type of interface is the sheathless interface which is shown in Figure 1-3c. The end of the capillary is tapered and the outside surface coated with metal to make electrical contact. The initial setup of a sheathless interface used a blunt end capillary.⁶⁰ Since the onset potential required for stable electrospray decreases with reduced diameter of the electrospray tip, the tapered capillary tip allows 100% aqueous solution to be directly sprayed at lower potential.⁹⁷ The sheathless interface gives good sensitivity, requires low flow rates and eliminates the interference or dilution from the sheath liquid or make up flow. For the metal coating outside the capillary tip, silver was first used, but it is unstable and silver adduct peaks were observed.⁹⁸ Gold coating is more stable than silver and it is now widely used, deposited by sputtering or electroplating.⁹⁹⁻¹⁰¹ The

problem is that the gold at the tip can be gradually “chewed” away in the electrospray process and this makes the life time short. People have been trying to make robust sheathless electrospray tips with simple methods. In one publication, 2 μm gold particles were glued to the capillary tip and the authors claim that it has unlimited lifetime.¹⁰² A soft pencil was used to coat the capillary tip with carbon and the results showed that it could make a stable electrospray, and separation with CEMS was demonstrated.¹⁰³

1.6. Protein identification using mass spectrometry

We have been trying to integrate protein processing steps on a microchip for mass spectrometry analysis. Here we give a basic description of the conventional protein identification method using mass spectrometry. Figure 1-4 illustrates the main processes involved. Protein mixtures extracted from the cells of interest are separated by sodium dodecyl sulfate – polyacrylamide gel electrophoresis (SDS-PAGE). SDS is an anionic surfactant and it is used to denature and impart a strong negative charge on proteins. In 2-D PAGE, proteins first separated by isoelectric focusing according to their pI values and followed by size-based separation via sieving through cross-linked polyacrylamide slab gel. In 1-D gel separation, only separation according to molecular mass is involved. The proteins are then visualized by silver stain or Coomassie blue. SDS-PAGE provides a simple, sensitive and reproducible means to separate proteins.¹⁰⁴ The estimated molecular mass and pI information of the proteins can be derived by comparing with the standard proteins on the 2-D PAGE.

Three methods have been used to generate peptide fragments from the gel-separated proteins:¹⁰⁵ 1) electroelution of the intact proteins followed by chemical or enzymatic

fragmentation in solution, 2) protein spot of interest excised with subsequent in-gel digestion, and 3) electrotransfer onto a membrane and cleavage on the membrane. In-gel digestion is preferred because of its better overall sensitivity, while the other two methods suffer from protein loss during the transfer steps. Protein is usually digested by an enzyme with high sequence specificity, such as trypsin. Trypsin cleaves on the C-terminal side of lysine and arginine residues, but not at Lys-Pro and occasionally not at Arg-Pro. After digestion, the peptide fragments are extracted for further analysis. Traditionally, they are fractionated by RP-HPLC, followed by sequencing. In the past, peptides have been primarily sequenced by automated Edman Sequencing, which currently has a sensitivity in the pico or upper femtomole range.¹⁰⁶ With the advent of mass spectrometric techniques, it has been possible to obtain peptide molecular weights and sequence information by peptide-mass mapping (or fingerprinting) and tandem MS.

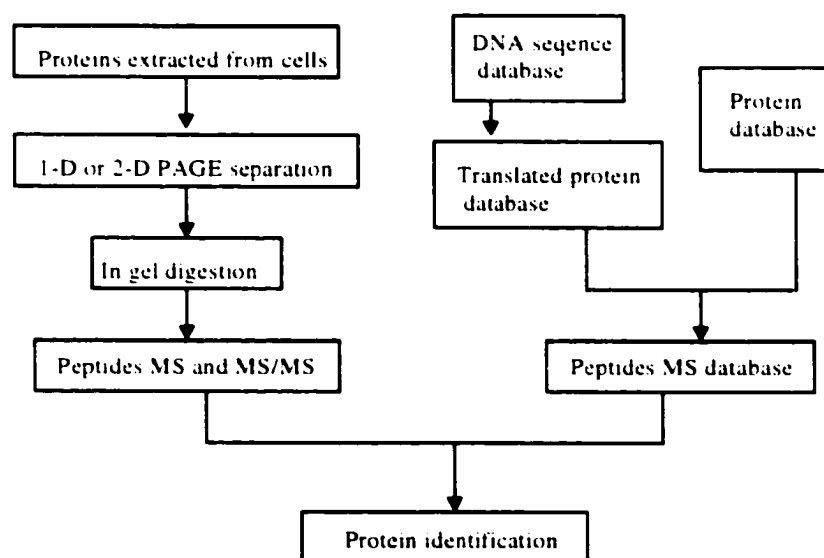


Figure1-4. Flow diagram for the identification of gel-separated proteins by mass spectrum and peptide-mass database searching.

The introduction of electrospray^{60,107} and MALDI¹⁰⁸ in the late 1980s was a breakthrough for MS of proteins, by greatly extending the molecular masses and types of proteins suitable for MS. ES is compatible with on-line separation techniques such as HPLC¹⁰⁹ or CE⁹⁶ and it can also be used for off-line mass measurement of HPLC fractions.^{110,111} MALDI-MS has been used to analyze unfractionated peptide digests¹¹² or HPLC fractions,^{113,114} and it is more easily adapted to high throughput approaches and therefore better suited for large-scale proteomics. Both ionization methods could have low femtomole level sensitivity and they have been widely used for protein identification.^{109,115} On the other hand, the DNA and protein sequence database is growing exponentially. Most of these databases are publicly available via the internet which gives easy access to the databases needed for MS protein identification.¹¹⁶

The most widely used technique of protein identification is peptide mass fingerprinting.^{117,118} The idea underlying MS protein identification is that peptide masses provide a "fingerprint" of a particular protein and that the pattern of masses can be recognized when the protein sequence database is searched. The masses of peptides are obtained from mass spectra of protein digests, using an enzyme having high digestion specificity (e.g. trypsin). The database can also generate the masses of peptides of that individual protein under the assumption that it is cleaved by the same enzyme. The number of matches between masses of the experimentally obtained peptide map and the masses of the peptides from proteins in a database is detected. A score characterizes the results of each comparison. The score could be simply the number of matches, or it is the result of a computation that utilizes the number of matches as well as other criteria. The protein yielding the best score is identified. Using the mass accuracy now available (< 10

ppm) with mass spectrometer such as the Q-TOF or FTMS, in most cases this technique alone is good enough to identify the proteins.¹¹⁹ For unambiguous protein identification, a tandem MS method can be used. Complete or partial amino acid sequences of the peptide obtained by MS/MS in conjunction with peptide mass database searching, is the most discriminating way to identify proteins.^{120,121}

The amino acid sequence in a peptide can be obtained using tandem MS by collision induced dissociation (CID). Tandem MS of a precursor peptide can be achieved using triple quadrupole, quadrupole iontrap and quadrupole-TOF mass spectrometers. The fragmentation spectrum gives the information about the amino acid sequence of the peptide and it is compared with the database to confirm the fingerprinting results. Typically, several peptides possibly from the same protein are sequentially fragmented and each peptide provides an independent database search. This could increase the accuracy of protein identification. Further protein information, such as post translational modification, can also be achieved from the MS/MS spectrum.¹²²

1.7. Microchip Fabrication

Microfabrication is a technology that allows for fabrication of structures smaller than 100 μm . It was originally developed for fabricating electronic devices such as computer chips. Later on, it was used in chemistry, physics and mechanical engineering fields. At present, the typical materials used for a miniaturized chemical system consist of silicon, glass, quartz or plastic, which can be etched or molded with chambers and channels.

Each material has its own advantages and disadvantages. Polymers such as polymethylmethacrylate (PMMA) and polycarbonate (PC) are promising materials for microsystem technology, since they are applicable for mass replication technologies such as injection molding, hot embossing, casting or laser micromachining. Silicon is a semiconductor and the application of high voltages ($> 300\text{V}$) to a silicon microchip is extremely difficult. Quartz is suitable for CE because it is a good electrical insulator and it is transparent to UV light, which is required for absorbance. Other glasses that are less costly than quartz, such as Corning 0211, Pyrex and Borofloat may also be used, although they may have reduced optical qualities. For silicon and glass fabrication, the dominant method is photolithography/wet chemical etching. Wet chemical etching is isotropic. Plasma or dry etching is anisotropic and it can be used for features smaller than $1\ \mu\text{m}$.

In our research, we normally use glass chips and the channels etched on it are typically $10\ \mu\text{m}$ deep and $30\ \mu\text{m}$ wide. The chips are covered with a piece of glass with access holes drilled on it to contain the sample and reagents. A standard one-mask photolithography/wet-chemical-etching microfabrication procedure used in our group¹⁵ for etching a channel into a glass wafer is outlined in Figure 1-5.

The glass substrate (usually 3" or 4" square) is cleaned in piranha ($\text{H}_2\text{SO}_4/\text{H}_2\text{O}_2 = 3/1$) for 10 minutes. After thorough aqueous rinsing and drying, Cr/Au layers are sputtered onto the glass substrate. A solution of photoresist is then spin-coated onto the substrate, followed by soft baking at $110\ ^\circ\text{C}$ for 30 min to improve adhesion. Photoresist consists of a photosensitizer molecule and a polymer, both of which are dissolved in an organic solvent. A mask aligner is used to align the substrate with the photomask and for

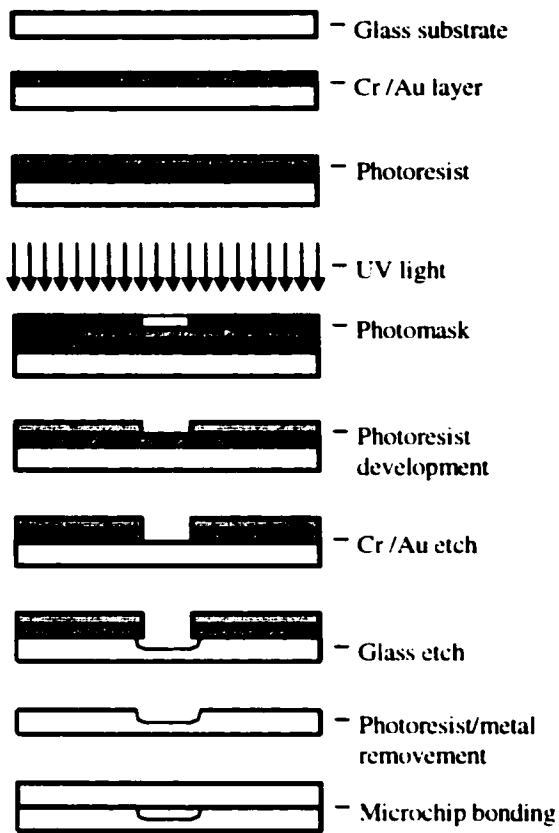


Figure 1-5. The procedure for microchip fabrication using photolithography/wet-chemical etching.

UV exposure. Then the pattern on the photomask is transferred to the photoresist film on the substrate using the mask aligner. The exposed photoresist is removed with photoresist developer. The developed substrate is baked for 30 min at 120°C. Chromium and gold are etched separately with commercial Cr etch and an aqueous Au etch (potassium iodide/iodine) solutions respectively. A mixture of concentrated HF:HNO₃:H₂O (22:14:66) is used for glass channel etching. The etched channel depth can be controlled by the time the substrate spends in the etching solution. The

remaining photoresist and metal layers are removed with acetone and metal etching solutions, respectively.

Access holes to the etched channels were drilled into cover plates. Before bonding, etched substrates and cover plates are thoroughly cleaned by hot piranha and high pressure washing. After aligning the access holes and the etched channels, the two pieces can be cold bonded by slightly applying pressure on the surface to let them contact each other. Permanent bonding can be achieved thermally in a programmable oven.

1.8. Microchip-Electrospray Mass Spectrometry

The content of this thesis focuses on interface development and applications for microchip-CE-ESMS. In the past four years, microchip-ESMS has experienced rapid development and has drawn more and more attention world wide. The first report of coupling microchip to mass spectrometry was from Karger and coworkers³³ in 1997. They used a glass chip with nine $25\ \mu\text{m} \times 60\ \mu\text{m}$ channels to perform electrospray directly from the channel opening on the flat edge of the chip. A syringe pump was used to drive the samples. Mass spectrum of several proteins were demonstrated. With the same set up, they also performed melittin on-chip reservoir digestion followed by ESMS.⁸ This was a breakthrough because they demonstrated the idea of coupling microchip to ESMS. The multichannel approach led to the development of multiplexing and high throughput, and they indicated the potential of integrating enzymatic reactions and protein processing on the microchip device before ESMS detection. At about the same time, the Ramseys¹²³ also demonstrated electrospray from the flat edge of a glass chip and the mass spectrum of tetrabutylammonium iodide was reported. Although it was hard to get stable electrospray from the flat edge of the chip, the idea lead to the further developments in this microchip-ESMS area.

Figeys et al. started to couple a transfer capillary to the chip either at the end of the channel¹²⁴ or from the cover plate perpendicular to the channel with help of a Teflon tube and glue.¹²⁵ The transfer capillary was connected to a liquid junction interface for electrospray. Protein digests were put in different reservoirs, and sequentially infused for electrospray MS and MS/MS by electroosmotic pumping. Microchips with three reservoirs¹²⁴ and nine reservoirs¹²⁵ were demonstrated for this purpose. They also used

the three-reservoir microchip device to deliver a solvent gradient to the coupled capillary, which had C₁₈ sorbent packed inside.¹²⁶ Solvent gradient and solvent flows were generated by computer controlled differential electroosmotic pumping of aqueous and organic solvent. The peptides were loaded off-line onto the sorbent and then the capillary was coupled to the microchip for gradient elution and mass spectrometry analysis.¹²⁶ Figeys et al. showed the possibility of coupling a capillary to the chip. They used the advantage of channel networks in microchip and promoted multiplexing and high throughput potential of the microchip. There is a further need for development to make greater use of microchips than it just being a liquid deliver tool.

After 1998, more research groups presented microchip-ESMS coupling, using different microchip materials and different interface designs. Our group, working with collaborators^{127,36,37} used a low dead volume connection to couple a capillary to the end of the channel of the chip. A one centimeter bare capillary tip, a three centimeter gold coated capillary tip, and a 10-40 cm capillary with sheathflow interface were all used, and separation of standard peptides and tryptic peptides were demonstrated. Karger and coworkers^{38,39} also used a short capillary tip at the end of the channel, in conjunction with liquid junction and a subatmospheric interface to get separation of peptides. The separation step is important for MS detection because it simplifies the mass spectrum and also helps to clean up the sample. This showed another application of microchip-CE-ESMS. Karger and coworkers¹²⁸ also build a multichannel resin device which had a format of a 96-well microtiter plate with 96 fused silica electrospray tips. This was used for high throughput infusion ESMS and they demonstrated analyzing 96 peptides samples in 480 s. Smith and coworkers^{11,12} used polycarbonate to fabricate microchips.

In section 1.2. of this chapter, we talked about their microdialysis ¹¹ and CIEF ¹² microchip-ESMS device and applications. They ¹²⁹ also tried multiple electrospray emitter designs in a polycarbonate substrate. Nine emitters (3×3) of 150 μm diameter were made by laser etching technique. Stable electrospray and good sensitivity was achieved. With the microchip we provided, Henion and coworkers ^{34,35} recently demonstrated drug separations with a micro-ionsprayer coupled at the end of the open chip channel. This expanded the application range of microchip-CE-ESMS to include drug analysis.

Microchip-ESMS demonstrated great potential for sample purification, protein, peptides and drug separation, enzymatic digestion, protein identification, and high throughput with multiplexing. Future work will explore its application to make a multifunctional lab on a chip.

1.9. The outline of this thesis

The Harrison research group have been developing an integrated system to combine protein processing on microchip with MS detection together, a proteomic chip. The first report of microchip connection to mass spectrometer was in 1997. Our group started the project at about the same time. This thesis will present the microchip-MS evolution in our group. The sorrow and happiness with failure and success in this whole process will be described in the following chapters.

Our first effort was to build a reliable interface to couple the microchip and mass spectrometer together. In Chapter 2, first we talk about our initial tests of spraying directly from the edge of the chip at the channel outlet. Based on the low dead volume

chip-capillary coupling technique developed by Cameron Skinner, a gold coated capillary tip was coupled to the microchip channel and served as the electrospray tip. This design gives stable electrospray and has been used in the whole process. Separation of protein and peptides will be demonstrated.

In Chapter 3 we will present a large volume sample stacking method used to preconcentrate samples in the microchip system. Laser induced fluorescence detection and mass spectrometry were all used for this method. Standard peptides were tested and 50-fold improvement on detection limit with bradykinin was achieved. The method was also used for membrane associated proteins from *H. influenzae* strain Rd. This preconcentration method is a useful way to enrich analyte ions with high electrophoretic mobilities in the direction opposite to EOF.

Instead of traditional protein solution phase digestion in a microcentrifuge tube, the proteins were digested directly in the microchip with immobilized trypsin beads. The results will be shown in Chapter 4. Melittin, cytochrome c and bovine serum albumin were used as samples. Two kinds of on-chip digestion methods were used: on-chip reservoir digestion and integrated packed bed digestion. The integrated packed bed appeared to be the fastest digestion method, compared to either reservoir digestion or traditional solution phase digestion. A flow rate of 0.5-1 $\mu\text{l}/\text{min}$ was found adequate for complete consumption of cytochrome c or BSA, corresponding to a digestion time of 3-6 min at room temperature. Five seconds was enough to digest melittin at 60 $\mu\text{l}/\text{min}$. The digests were separated in the microchip channel before mass spectrometry detection. This chip design thus provides a convenient platform for automated sample processing in proteomics applications.

Based on the results in Chapter 4, further development is described in Chapter 5. On-chip solid phase extraction of peptides was investigated and it provided an efficient preconcentration method. A two bed system for protein digestion (immobilized trypsin beads bed) and subsequent peptide concentration (solid phase extraction bed) were constructed. A 200 nM cytochrome could be successfully digested and preconcentrated. This is the first time so many protein processing steps were integrated together on a microchip device before MS detection. This takes us one step closer to our final goal, a proteomic chip.

Chapter 6 will summarize the previous chapters and focus on future work. New ideas and chip designs for further development will be presented.

1.10. References

1. Manz, A.; Graber, M.; Widmer, H. M. *Sensor and Actuators ,B1*, **1990**, 1, 244-248.
2. Wooley, A.T.; Hadley, D.; Landre, P.; deMello, A. J.; Mathies, R.A.; Northrup, M. A. *Anal. Chem.* **1996**, 68, 4081-4086.
3. Chiem N. H.; Harrison, D. J. *Clin. Chem.* **1998**, 44, 591-598.
4. Colyer, C.L.; Magru, S. D.; Harrison, D.J. *J. Chromatogr. A* **1997**, 781, 271-276.
5. Mangru, S. D.; Harrison, D.J. *Electrophoresis* **1998**, 19, 2301-2307.
6. Cohen, C. B.; Chin-Dion, E.; Jeong S.; Nikiforov, T.T. *Anal. Biochem.* **1999**, 273, 89-97.
7. Hadd, A.G.; Raymond, D. E.; Halliwell, J.; Jacobson,S.C.; Ramsey, J. M. *Anal. Chem.* **1997**, 69, 3407-3412.
8. Xue, Q.; Dunayevskiy, Y. M.; Foret, F.; Karger, B. L. *Rapid. Commun. Mass Spectrom.* **1997**, 11, 1253-1256.
9. Ekstrom, S.; Onnerfjord, P.; Nilsson, J.; Bengtsson, M.; Laurell, T.; Varga, G. *Anal. Chem.* **2000**, 72, 286-293.
10. Sanders, G.H.W.; Manz, A. *Trends in Anal. Chem.* **2000**, 19, 364-378.
11. Xu, N.; Lin, Y.; Hofstadler, S.A.; Matson, D.; Call, C.J.; Smith, R.D. *Anal. Chem.* **1998**, 70, 3553-3556.
12. Xiang, F.; Lin, Y.; Wen, J.; Matson, D.W.; Smith R.D. *Anal. Chem.* **1999**, 71, 1486-1490.
13. Harrison, D. J.; Manz, A.; Fan, Z.; Ludi, H.;Widmer, H. M. *Anal. Chem.* **1992**, 64, 1926-1932.
14. Harrison, D. J.; Fluri, K.; Seiler, K.; Fan, Z.; Effenhauser, C.S.; Manz, A. *Science* **1993**, 261, 895-897.
15. Fluri, K.; Fitzpatrick, G.; Chiem, N.; Harrison, D.J. *Anal. Chem.* **1996**, 68, 4285-4290.
16. Jacobson, S.C.; Hengerroder, R.; Koutny, L. B.; Ramsey, J.M. *Anal. Chem.* **1994**, 66, 2369-2375.
17. Raymond, D.E.; Manz, A.; Widmer, H. M. *Anal. Chem.* **1996**, 68, 2515-2522.
18. Effenhauer, C.S.; Paulus, A.; Manz, A.; Widler, H.M. *Anal. Chem.* **1994**, 66, 2949-2953.
19. Moore, A.M.; Jacobson, S.C.; Ramsey, J.M. *Anal. Chem.* **1995**, 67, 4184-4189.
20. Dolnik, V.; Liu, S. R.; Jovanovich, S. *Electrophoresis* **2000**, 21, 41-54.
21. Liang, Z.; Chiem, N.;Ocvik, G.; Tang, T.; Fluri, K.; Harrison, D.J. *Anal. Chem.* **1996**, 68, 1040-1046.
22. Salimi-Moosavi, H.; Jiang, Y.; Lester, L.; McKinnon, G.; Harrison, D. J. *Electrophoresis.* **2000**, 21, 1291-1299.
23. Wooley, A. T.; Lao, K.; Glazer, A. N.; Mathies, R. A. *Anal. Chem.* **1998**, 70, 684-688.

24. Tantra, R.; Manz, A. *Anal. Chem.* **2000**, 72, 2875-2878.
25. Oleschuk, R.; Harrison, D.J. *Trends in Anal. Chem.* **2000**, 19, 379-388.
26. Whitehouse, C.M.; Dreyer, R.N.; Yamashitna, M.; Fenn, J.B. *Anal. Chem.* **1985**, 57, 675-680.
27. Smith, R.D.; Loo, J.A.; Edmonds, C.G.; Barinaga, C.J.; Udseth, H.R. *Anal. Chem.* **1990**, 62, 882-899.
28. Johansson, J.M.; Pavelka, R.; Henion, J.D. *J. Chromatogr.* **1991**, 559, 515-528.
29. Tomlinson, A.J.; Benson, L.M.; Jameson, S.; Johnson, D.H.; Naylor, S. *J. Am. Soc. Mass Spectrom.* **1997**, 8, 15-24.
30. Limbach, P.A.; McCloskey, J.; Crain, P.F. *Nucleic Acids Symposium Series* **1994**, 31, 127-128.
31. Creig, M.J.; Gaus, H.; Griffey, R.H. *Rapid. Commun. Mass Spectrom.* **1996**, 10, 47-50.
32. Apffel, A.; Chakel, J.A.; Fischer, S.; Hancock, W.S. *Anal. Chem.* **1997**, 69, 1320-1325.
33. Xue, Q.; Foret, F.; Dunayevskiy, Y. M.; Zavrachy, P.; McGruer, N. E.; Karger, B. L. *Anal. Chem.* **1997**, 69, 426-430.
34. Deng, Y.; Henion, J.; Li, J.; Thibault, P.; Wang, C.; Harrison, D.J. *Anal. Chem.* **2001**, 73, 639-646.
35. Deng, Y.; Henion, J. *Anal. Chem.* **2001**, 73, 1432-1439.
36. Li, J.; Thibault, P.; Bings, N.; Skinner, C.D.; Wang, C.; Colyer, C.; Harrison, D.J. *Anal. Chem.* **1999**, 71, 3036-3045.
37. Li, J.; Kelly, J.; Chernushevich, I.; Harrison, D.J.; Thibault, P. *Anal. Chem.* **2000**, 72, 599-609.
38. Zhang, B.; Liu, H.; Karger, B. L.; Foret, F. *Anal. Chem.* **1999**, 71, 3258-3264.
39. Zhang, B.; Karger, B. L.; Foret, F. *Anal. Chem.* **2000**, 72, 1015-1022.
40. Oleschuk, R.D.; Shultz-Lockyear, L.L.; Ning, Y.; Harrison, D.J. *Anal. Chem.* **2000**, 72, 585-590.
41. Wooley, A.T.; Mathies, R.A. *Anal. Chem.* **1995**, 67, 3676-3680.
42. Wooley, A.T.; Sensabaugh, G.F.; Mathies, R.A. *Anal. Chem.* **1997**, 69, 2181-2186.
43. Shi, Y.; Simpson, P.C.; Scherer, L.R.; Wexler, D.; Skibola, C.; Smith, M.T.; Mathies, R.A. *Anal. Chem.* **1999**, 71, 5354-5361.
44. Cheng, J.; Shoffner, M.A.; Mitchelson, K. R.; Kricita L. J.; Wilding, P. *J. Chromatogr. A* **1996**, 732, 151-158.
45. Kopp, M.U.; deMello, A.J.; Manz, A. *Science*, **1998**, 280, 1046-1048.
46. Jacobson, S.C.; Ramsey, J.M. *Anal. Chem.* **1996**, 68, 720-723.
47. Hofmann, O.; Che, D.; Cruickshank K.A.; Muller, U.R. *Anal. Chem.* **1999**, 71, 678-689.
48. Mao, Q.; Pawliszyn, J. *Analyst* **1999**, 124, 637-641.

49. Rosser, J. S.; Schwarz, A.; Reymond F.; Girait H. *Electrophoresis* **1999**, 20, 727-731.
50. Wen, J.; Lin, Y.; Xiang, F.; Matson, D.; Udseth, H.R.; Smith, R.D. *Electrophoresis* **2000**, 21, 191-197.
51. Laurell, T.; Nilsson, J.; Varga, G. *J. Chromatogr. B*, **2001**, 752, 217-232.
52. Litbon, E.; Emmer, A.; Roseraade, J. *Anal. Chim. Acta*, **1999**, 401, 11-19.
53. Litbon, E.; Roseraade, J. *J. Chromatogr. B*, **2000**, 745, 137-147.
54. Litbon, E.; Emmer, A.; Roseraade, J. *Electrophoresis*, **2000**, 21, 91-99.
55. Zeleny, J. *Phys. Rev.*, **1914**, 3, 69-75.
56. Zeleny, J. *Phys. Rev.*, **1917**, 10, 1-6.
57. Dole, M.; Mack, L. L.; Hines, R. L.; Mobley, R. C.; Ferguson, L. D.; Alice, M. B. *J. Chem. Phys.*, **1968**, 49, 2240-2249.
58. (1) Yamashita, M.; Fenn J.B. *J. Phys. Chem.* **1984**, 88, 4451-4457.
(2) Yamashita, M.; Fenn J.B. *J. Phys. Chem.* **1984**, 88, 4671-4676.
59. Aleksandrov, M.L.; Gall, L.N.; Krasnov, V.N.; Nikolaev, V.I.; Pavlenko, V.A.; Shkurov, V.A. *Dokl. Akad. Nauk sSSR* **1984**, 277, 379-385.
60. Olivares, J.A.; Nguyen, N.T.; Yonker, C.R.; Smith, R.D. *Anal. Chem.* **1987**, 59, 1230-1232.
61. Fenn, J.B.; Mann, M.; Meng, C.K.; Wong, S.F.; Whitehouse, C.M. *Science* **1989**, 246, 64-71.
62. Loeb, L.B.; Kip, A.F.; Hudson, G.G.; Bennett, W.H. *Phys. Rev.* **1941**, 60, 714-721.
63. Kebarle, P.; Tang, L. *Anal. Chem.* **1993**, 65, 972A-986A.
64. Taylor G.I. *Proc. Roy. Soc. A.*, **1964**, 280, 383-390.
65. Cloupeau, M.; Prunet-Foch, B. *J. Aerosol Sci.* **1994**, 25, 1021-1030.
66. Smith D.P.H. *IEEE Trans. Ind. Appl* **1986**, IA-22, 527-533.
67. Rayleigh, L. *Philos. Mag.* **1882**, 14, 184-192.
68. Gomez, A.; Tang, K. *Phys. Fluids* **1994**, 6, 404-414.
69. Iribarne, J.V.; Thomson, B.A. *J. Chem. Phys.* **1976**, 64, 2287-2294.
70. Thomson, B.A.; Iribarne J.V. *J. Chem. Phys.* **1979**, 71, 4451-4463.
71. Tang, L.; Kebarle, P. *Anal. Chem.* **1991**, 63, 2709-2715.
72. Lee, E.D.; Muck, W.; Henion, J.D. *J. Chromatogr.* **1988**, 458, 313-321.
73. Wilm, M.; Mann, M. *Anal. Chem.* **1996**, 68, 1-8.
74. Bateman, K.P.; White, R.L.; Thibault, P. *Rapid Commun. Mass Spectrom.* **1997**, 11, 307-315.
75. Lazer, I.; Ramsey, R.S.; Sundberg, S.; Ramsey, J.M. *Anal. Chem.* **1999**, 71, 3627-3631.
76. Meng, Z.; Qi, S.; Soper, S.A.; Limbach, P.A. *Anal. Chem.* **2001**, 73, 1286-1291.
77. Hulthe, G.; Petersson, M.A.; Fogelqvist, E. *Anal. Chem.* **1999**, 71, 2915-2921.

78. Alexander, J.N.; Shultz, G.A.; Poli, J.B. *Rapid Commun. Mass Spectrom.* **1998**, 12, 1187-1191.
79. Kohlrausch, F. *Ann. Phys.* **1897**, 62, 209-215.
80. Jorgenson, J.W.; Lukacs, K.D. *Anal. Chem.* **1981**, 53, 1298-1302.
81. Jorgenson, J.W.; Lukacs, K.D. *Science* **1983**, 222, 266-272.
82. Li, S. F. Y. *Capillary electrophoresis principles, practice, and application*, **1993**, Elsevier Science, printed in Netherland.
83. Agilent (HP) *High Performance Capillary Electrophoresis-An Introduction*. 1995. HP, printed in USA.
84. Rodriguez I.; Li, S.F.Y. *Analytica Chimica Acta* **1999**, 383, 1-26.
85. Gilges, M.; Kleemiss, M.H.; Schomburg, G. *Anal. Chem.* **1994**, 66, 2038-2046.
86. Baryla, N. B.; Lucy, C. A. *Anal. Chem.* **2000**, 72, 2280-2284.
87. Horvath, J.; Dolnik, V. *Electrophoresis* **2001**, 22, 644-655.
88. Hjerten, S., *J. Chromatogr.* **1985**, 347, 191-198.
89. Xhiari, M.; Ceriotte, L.; Crini, G.; Morcellet, M. *J. Chromatogr. A* **1999**, 836, 81-91.
90. Smith, R.D.; Olivares, J.A.; Nguyen, N.T.; Udseth, H. R. *Anal. Chem.* **1988**, 60, 436-440.
91. Hopfgartner, G.; Wachs, T.; Bean, K.; Henion, J. *Anal. Chem.* **1993**, 65, 439-446.
92. Bruins, A.P.; Covey, T.R.; Henion, J.D. *Anal. Chem.* **1987**, 59, 2642-2646.
93. Covey, T.R.; Bonner, R.F.; Shushan, B.I.; Henion, J.D. *Rapid Commun. Mass Spectrom.* **1988**, 2, 249-253.
94. Gale, D.C.; Smith, R.D. *Rapid Commun. Mass Spectrom.* **1993**, 7, 1017-1021.
95. Lee, E.D.; Muck, W.; Henion, J.D.; Covey, T.R. *J. Chromatogr.* **1988**, 458, 313-321.
96. Pleasance, S.; Thibault, P.; Kelly, J. *J. Chromatog.*, **1992**, 591, 325-339.
97. Chowdhury, S.K.; Chait, B.T. *Anal. Chem.* **1991**, 63, 1660-1664.
98. Wahl, J. H.; Gale, D.C.; Smith, R.D. *J. Chromatogr. A*, **1994**, 659, 217-222.
99. Wahl, J. H.; Smith, R.D. *J. Cap. Elec.*, **1994**, 1, 62-71.
100. Banks, J. F. *Electrophoresis* **1997**, 18, 2255-2266.
101. Barnidge, D.R.; Nilsson, S.; Markides, K.E.; Eapp, H.; Hjort, K. *Rapid Commun. Mass Spectrom* **1999**, 13, 994-1002.
102. Barnidge, D.R.; Nilsson, S.; Markides, K.E. *Anal. Chem.* **1999**, 71, 4115-4118.
103. Chang, Y.Z.; Her, G.R. *Anal. Chem.* **2000**, 72, 626-630.
104. Aebersold, R.; Leavitt, J. *Electrophoresis* **1990**, 11, 517-527.
105. Patterson, S.D.; Aebersold, R. *Electrophoresis* **1995**, 16, 1791-1814.
106. Andersen J.S.; Svensson B. Rospstorff P. *Nature Biotechnology* **1996**, 14, 449-455.

107. Fenn, J.B.; Mann, M.; Meng, C.K.; Whitehouse, C.M. *Science* **1989**, 246, 64-71.
108. Karas, M.; Hillenkamp, F. *Anal. Chem.* **1988**, 60, 2299-2301.
109. McCormack, A.L.; Schieltz, D.M.; Goode, B.; Yang, S.; Barnes, G.; Drubin, D.; Yates, J.R. *Anal. Chem.* **1997**, 69, 767-776.
110. Lewis, K.C.; Dohmeier, D.M.; Jorgenson, J.W.; Kaufmann, S.L.; Zarrin, F.; Dorman, F.D. *Anal. Chem.* **1994**, 66, 2285-2292.
111. Wilm, M.S.; Mann, M. *Int. J. Mass Spectrom. Ion Processes* **1994**, 136, 167-180.
112. Jensen, O.N.; Podtelejnikov, A.V.; Mann, M. *Anal. Chem.* **1997**, 69, 4741-4750.
113. Udiavar, S.; Apffel, A.; Chakel, J.; Swedberg, S.; Hancock, W. S.; Pungor, Jr. E. *Anal. Chem.* **1998**, 70, 3572-3578.
114. Wall, D.B.; Lubman, D.L.; Flynn, F.J. *Anal. Chem.* **1999**, 71, 3894-3900.
115. Vorm, O.; Roesporff, P.; Mann, M. *Anal. Chem.* **1994**, 66, 3281-3287.
116. <http://prospector.ucsf.edu> (protein prospector)
<http://matrixscience.com> (MASCOT)
<http://www.expasy.ch> (Expasy tools)
<http://mac-mann6.embl-heidelberg.de/> (Peptide Search)
117. Henzel, W.J.; Billeci, T.M.; Stults, J.T.; Wong, S.C.; Grimley, C.; Watanabe, C. *Proc. Natl. Acad. Sci. USA* **1993**, 90, 5011-5015
118. Borchers, C.; Peter, J.F.; Hall, M.; Kunkel, T.A.; Tomer, K.B. *Anal. Chem.* **2000**, 72(6): 1163-1168.
119. Bruce, B.J.; Anderson, G.A.; Wen, J.; Harkewicz, R.; Smith, R.S. *Anal. Chem.* **1999**, 71, 2595-2599.
120. Clauser, K.; Baker, P.; Burlingame, A.L. *Anal. Chem.* **1999**, 71, 2871-2882.
121. Martin, S.E.; Shabanowitz, J.; Hunt, D.F.; Marto, J.A. *Anal. Chem.* **2000**, 72, 4266-4274.
122. Carr, S.A.; Huddleston, M.J.; Bean, M.F. *Protein Sci.* **1993**, 2, 183-196.
123. Ramsey, R. S.; Ramsey, J. M. *Anal. Chem.* **1997**, 69, 1174-1178.
124. Figeys, D.; Ning, Y.; Aebersold, R. *Anal. Chem.* **1997**, 69, 3153-3160.
125. Figeys, D.; Gygi, S. P.; McKinnon, G.; Aebersold, R. *Anal. Chem.* **1998**, 70, 3728-3734.
126. Figeys, D.; Aebersold, R. *Anal. Chem.* **1998**, 70, 3721-3727.
127. Bings, N. H.; Wang, C.; Skinner, C. D.; Colyer, C. L.; Thibault, P.; Harrison, D. J. *Anal. Chem.* **1999**, 71, 3292-3296.
128. Liu, H.; Felten, C.; Xue, Q.; Zhang, B.; Jedrzejewski, P.; Karger, B.L.; Foret, F. *Anal. Chem.* **2000**, 72, 3303-3310.
129. Tang, K.; Lin, Y.; Matson, D. W.; Kim, T.; Smith, R. D. *Anal. Chem.* **2001**, 73, 1658-1663.

Chapter 2

Interface Development for Coupling Microchip Capillary Electrophoresis to Mass Spectrometry Using Electrospray Ionization*

	page
Table of contents	
2.1. Introduction.....	38
2.2. Experimental.....	41
2.2.1. Joint preparation for coupling microchip to capillary tip.....	41
2.2.2. Capillary tip gold coating and chip channel modification with BCQ	44
2.2.3. Device and instrumental for microchip-ESMS detection.....	45
2.3. Results and Discussion.....	50
2.3.1. Electrospray directly from the edge of the chip.....	50
2.3.2. Capillary tip coupled to chip with minimal dead volume connection.....	55
2.3.3. Gold coated capillary tip coupled at channel outlet for microchip-ESMS.....	57
2.4. Conclusions.....	61
2.5. References.....	62

* A portion of this chapter has been published in *Anal. Chem.* **1999**, 71, 3292-3296. by Bings, N.H.; Wang, C.; Skinner, C. D.; Colyer, C.; Thibault, P.; Harrison, D. J.

2.1. Introduction

Microfluidic devices have begun to show their vast potential in the field of analysis,¹⁻¹⁶ but there exists a need to make external fluid connections to these planar devices in order to improve their performance and versatility. The uses for external world-to-chip connections include coupling to conventional capillary electrophoresis (CE) detectors such as photometers or mass spectrometers. Electrospray mass spectrometry (ESMS) has become a powerful tool for protein^{17,18} and drug^{19,20} analysis. The flow rate used and the potential applied for microESMS and nanoESMS are compatible with microchip CE. This situation has led to development of microchip-ESMS,²¹⁻²⁴ in which CE separation on chip is followed by mass spectrometric analysis. A good connection between the microchip and the mass spectrometer is required for such a process, which should give stable electrospray and maintain the separation efficiency established on the chip. The latter requirement demands a minimal dead volume at the microchip-MS interface, which has presented a significant early obstacle to developing microchip-CE-MS techniques.^{25,26}

In the past four years, several groups have reported different microchip-ESMS coupling methods for silicon, glass and plastic chips.²¹⁻³⁴ Basically, these methods can be divided into two categories. One is spraying directly from an exposed channel at the end of the chip and the other is using a capillary attached to the microchip as the electrospray tip. Karger's^{25,26} and Ramsey's²⁷ groups first tried spraying from the channel outlet on the flat edge of glass chips. Liquid tended to spread on the flat surface and the spray was not stable. Although the authors tried to use coatings²⁵, surface derivatization²⁷ or pneumatic

assistance²² to reduce the droplet size and stabilize the spray, this flat-face spray method could not be used as a reliable and efficient method for chip-MS. We also tried several methods to obtain electrospray from the direct opening of the channel, as is described in this chapter. Other researchers have explored the use of monolithic silicon to fabricate electrospray nozzles using deep reactive ion etching. Nozzles with diameters as small as 15 μm were fabricated and stable electrospray was achieved.²⁸ Unfortunately, silicon devices are not capable of sustaining the high electric fields that glass devices exploit for efficient separations. Plastic materials are relatively more easily manipulated. Smith's group reported an integrated IEF device.²⁹ The device, made of polycarbonate, includes a serpentine channel, reservoirs for IEF solutions, inlets for sheath liquid and sheath gas, and a mechanically machined pointed tip for electrospray. A simple mixture of protein standards was separated. Shiea and coworkers³⁰ presented a poly(methylmethacrylate) (PMMA) chip which was mechanically filed and polished to a sharp tip at the end of the channel and obtained a stable electrospray. Eight channels were formed in the chip and it was filed into an octagonal shape to create eight electrospray tips.

To make a sharp end at the channel outlet from a flat glass chip is relatively hard. Glass chip-MS usually involves coupling a short capillary as the electrospray tip. Figeys et al.³¹⁻³³ connected a capillary to the edge or cover plate of a chip with two Teflon sleeves and glue. They did not report the dead volume of the joint, but used the capillary rather than the chip for separation. Zhang and coworkers^{22,23} published two papers showing the separation of peptides or protein digests in the glass microchip. In one case,²² they used wet etching on both glass pieces and created a sleeve in the chip that a transfer capillary was inserted into. The transfer capillary was connected to a liquid

junction followed by a subatmosphere electrospray interface. Their second design was also based on a liquid junction fabricated on the microchip.²³ In both cases, the fabrication was very complex and time consuming, and the subatmospheric electrospray could play an important role in the success of the interface designs. Henion's group³⁴ recently published a paper using a micro-ionsprayer coupled at the end of the open chip channel. The microsyringe was constructed with stainless steel tubes, and included make-up liquid flow and a nebulizing gas supply, with a liquid junction for voltage application. This unit was separated from the chip, and could be re-used by butt-coupling it to the flat edge of a chip. This approach provided a convenient way to couple a chip to a mass spectrometer.

Typical injected sample volumes on a microchip are ~0.2 nl for LIF detection^{1,2} while MS detection needs about 0.5-2 nl to obtain sufficient signal.^{21,35,36} Thus any connectors intended to move sample off the chip after it has been processed on-chip must have extremely low dead volume. In large part, these microchip devices find their greatest utility in separations, so the need for low dead volume connections is significant. To address this need, a method was developed to connect fused silica capillary tips to microfluidic devices with low dead volume connectors that do not impair performance. The coupled capillary tip was coated with gold on the outer surface. The electrospray voltage was applied to the gold tip. This interface gave very stable electrospray and good sensitivity when it was coupled to a mass spectrometer. This chapter explores the characterization of this interface, in which the separation of peptides and protein was demonstrated.

2.2. Experimental

2.2.1. Joint Preparation for Coupling Microchip to Capillary Tip

Figure 2-1 illustrates the process for coupling a capillary tip to a microchip, first developed by Cameron Skinner.³⁷ The chip layout PCRD-2^{2,5} is used here as an example. A detailed description of channel dimensions is shown subsequently. The devices were cleaned and bonded as previously described.² Crystal Bond 509 (CB) (Aremco Products, Valley Cottage, NY) was dyed to aid visualization by mixing one to two drops of black ink from a Staedtler Lumocolor permanent pen in approximately 1-2 ml of melted CB. The device was placed on a hot plate (80 °C) and the CB was put in reservoir L and melted into the end channel shown as the dashed line in Figure 2-1a. The channel segment where the device was to be cut and drilled was filled with CB by applying vacuum on the side channel K (Figure 2-1). The device was cut perpendicular to the main separation channel with a diamond saw and the face was sanded with 220, 600 and 1200 grit silicon carbide abrasive paper. This facilitated locating the end of the separation channel and reduced the risk of the drill catching on the rough surface.

The 200 μm (+0/-8 μm) pointed and supplier-modified flat tipped tungsten carbide drills (Tycom, Mississauga, Ontario) were used for 185 μm OD capillaries (Polymicro Technologies, Inc., Phoenix, AZ). Alternatively, flat tipped drills were prepared in-house by grinding the tip of the drill flat while manually rotating a fine diamond wheel. The tip could also be flattened by gently grinding on silicon carbide abrasive paper. The in-house flattened drill bits appeared to produce better quality holes than the commercially prepared bits.

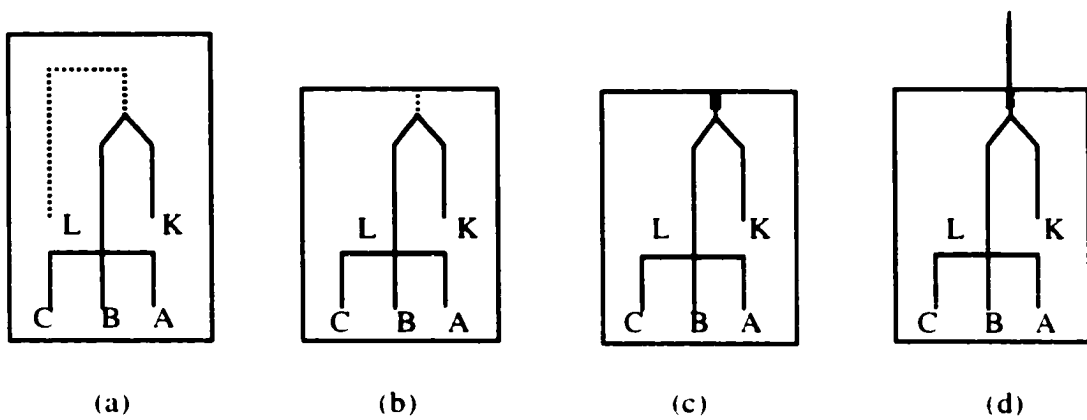


Figure 2-1. The microchip-capillary coupling process. (a) Crystal bond was used to fill the end channel. (b) The end was cut and sanded smooth. (c) A hole was drilled at the channel outlet then crystal bond was removed and the channel was cleaned. (d) A capillary tip was inserted into the hole, a little crystal bond was used to secure it in position.

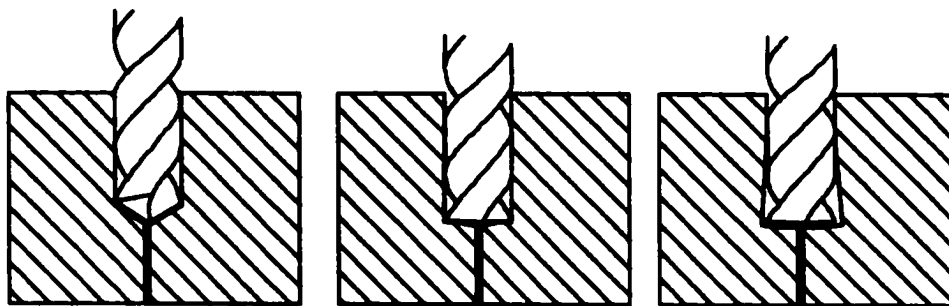


Figure 2-2. Schematic diagram of drilling a flat bottomed hole into glass. The bottom of the hole widens out into a "fishtail" if the flat tipped drill is forced to deepen the hole beyond the depth left by the pointed drill.

The device was clamped vertically to a horizontal XY translation stage (Newport, Irvine, California), in order to position the filled channel directly below the drill bit. Using a 20X jewelers loupe and side illumination, with the drill tip about 0.2-0.5 mm above the surface of the chip, facilitated alignment. The drill (4000 RPM) was lowered until it began removing glass. The chip face was then examined to insure that the hole was centered on the channel. if not, the chip was resanded and a new hole started. A drop of water was used to lubricate and cool the drill bit. The drill was allowed to bore approximately 1-2 drill diameters before it was raised. This process was repeated until a hole of suitable depth (600-800 μm) was obtained. The face of the chip was cleaned with a paper towel to remove the glass powder produced during drilling.

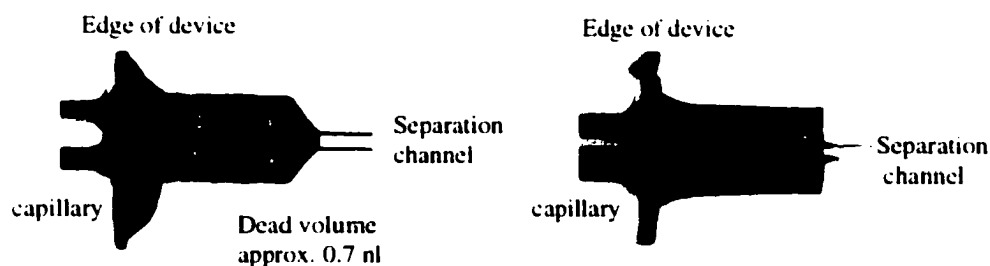


Figure 2-3. The left image is a 185 μm o.d. and 50 μm i.d. capillary inserted into the hole formed by a 200 μm drill. The device is viewed from above. The edge of the chip and the etched channel are marked. Note the 0.7 nL dead volume in the conical area left by the tapered point. The separation channel is 40 μm wide. The right image shows the capillary in the hole produced by the flat tipped 200 μm drill. The dead volume left by the tapered point is absent.

To produce the flat bottomed holes, the pointed drill bit was replaced with the flat tipped drill. A fresh drop of water was placed on the device, the drill was introduced and the bottom of the hole was flattened in one step, as illustrated in Figure 2-2. If the flat tipped drill is forced to drill beyond the end of the hole left by the pointed drill the bottom

of the hole “fishtails”, because the flat face of the drill bit is not capable of removing glass. The cone shaped and flat bottomed holes are shown in Figure 2-3.

Providing there were no air bubbles in the hole, glass debris was removed by inverting the device in a beaker of water and allowing the glass particles to settle out over half to one hour. Alternatively, a capillary (at least 25 μm smaller o.d. than the hole) was used to flush the hole. The chip was then placed on a hot plate and the CB was melted (80°C) and removed via the hole with the aid of vacuum. After cooling, the CB residues were removed with acetone or acetonitrile (Caledon Laboratories Ltd., Georgetown, ON).

The capillary end was sanded flat and square with 600 and 1200 grit silicon carbide paper. Glass particles were then flushed out of the capillary with water. The device was placed on a 10 x 10 cm scrap of glass and the capillary was inserted into the hole (Figure 2-1d). This assembly was heated to the CB melting point (approximately 80 °C). A small amount of CB was applied onto the face of the joint and allowed to wick into the hole until it nearly reached the end of the capillary. The rate of flow was controlled by adjusting the hot plate temperature. The assembly was removed and the CB was frozen quickly with forced air.

2.2.2. Chip Channel Modification with BCQ and Capillary Tip Gold Coating Process

The chip channels were sequentially rinsed with 0.5 M NaOH under 25 psi pressure, then followed by deionized water and methanol for at least 1 hour each. A solution of 7-oct-1-enyltrimethoxysilane (25 μl) and glacial acetic acid (25 μl) in methanol (5 ml) was passed through the microchannels overnight with 20 psi applied. Then the channels were rinsed with methanol and deionized water each for one hour. A 5

ml solution containing 10 μl of TEMED, 70 μl of 15% (w/v) ammonium persulfate and 100 μl of BCQ³⁸ was rinsed overnight. Finally, the chip was flushed with deionized water and stored dry. All solutions were filtered through a 0.22 μm filter (Nylon, Chromatographic Specialties Inc. Brockville, Canada).

The gold coated capillary tip was made at the National Research Council (NRC).^{36,38} Here we give a short description of the process. One end of a piece of fused silica capillary (185 μm o.d. 50 μm i.d.) was tapered to about 10 μm i.d. using a laser puller (Sutter Instruments, Novato, AZ) and cut to approximately 3 cm length. The tapered end of the capillary was first coated with an Inconel alloy using an Edwards 19e thermal evaporation system (Edwards, Wilmington, MA). A layer of gold was subsequently deposited on the metallized tips at a reduced pressure of 9.6×10^{-6} mbar, using the Edwards 19e high-vacuum sputter. The sputtered gold coating was supplemented by electroplating. The gold-plating solution (0.5% gold plating salts in deionized water) was gently stirred at room temperature. A 1 cm section of the capillary tip was immersed in the plating solution and a little silver paint was used to glue the gold tip and electrode together. A constant flow (0.5 $\mu\text{L}/\text{min}$) of filtered deionized water was maintained to prevent blockage. The plating current for a single tip was maintained at 0.2 mA for 45-60 min. The electroplating procedure removed major surface imperfections and produced a capillary with a smooth gold coating. The tips coated with this procedure could be used for at least 3 days.

2.2.3. Device and Instrumental for Microchip-ESMS Detection

The chip layout used for peptide separation with MS detection is shown in Figure 2-4. The device was cut and processed from the PCRD-1 layout.²⁵ Detailed information

about PCRD-1 chip channels is shown in Figure 2-5a. The access reservoirs are identified for reference below. It was fabricated in 600 μm thick, Corning 0211 glass using standard photolithography and wet chemical etching techniques, as described previously.² Channels were etched on one glass plate to a 10 μm depth and 30-35 μm width for the majority of the length, with 250 μm wide segments near the reservoirs (Figure 2.5a). The injector to capillary distance was 4 cm, the double T injector had a 100 μm offset. At the end of the main channel, a flat-bottomed hole (~ 200 μm i.d.) was drilled into the edge of the device and a 3 cm gold coated nano-electrospray capillary tip (10 μm tip) was inserted, and held in place with Crystal Bond (Section 2.2.2). In order to prevent analyte adsorption on the glass walls, the chip channels and the capillary were covalently coated with 7-oct-1-enyltrimethoxysilane, to which BCQ was then cross-linked, as described on Section 2.2.2. This cationic coating gives electroosmotic flow towards the anode (anodal EOF). Small plastic pipette tubes were inserted in the center of septa and used as sample or buffer reservoirs. Then the whole assembly was put in the chip holder and secured in position. A platinum wire was attached to the gold coated capillary tip and maintained in position using a thin coat of silver conductive paint.



Figure 2-4. The microchip layout for ESMS from a PCRD-1 chip (detailed layout information in Figure 2-5). The capillary tip was 3 cm long. Sample was in reservoir X and sample waste was Z. Injection: X (-3.5 kV) to Z (ground), gold capillary tip (ground). Separation: Y (-3.5 kV) to capillary tip (3.2 kV), with push back voltage at X and Z (-2 kV). The power supply relay connection network is shown in Figure 2-7.

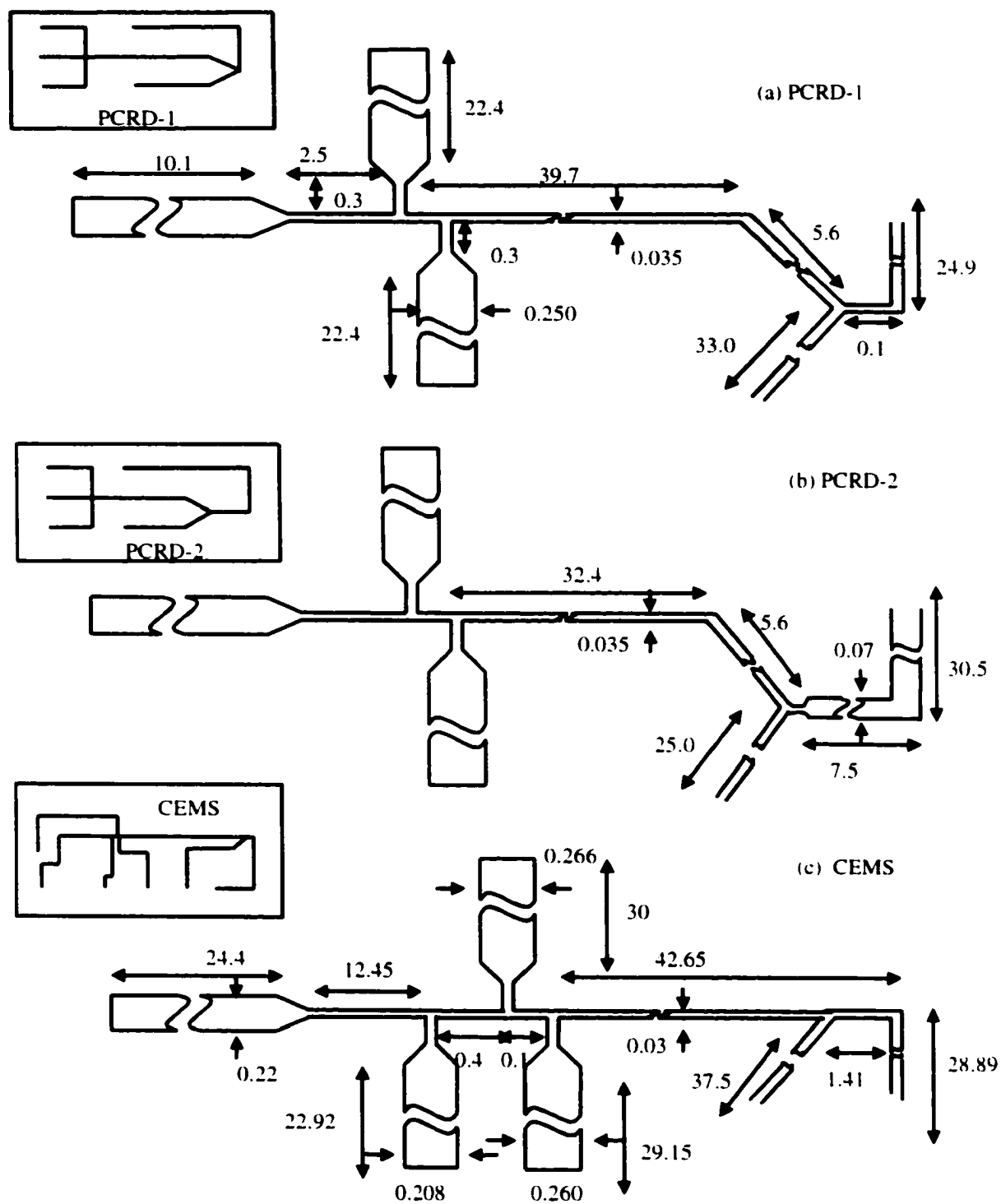


Figure 2-5. Schematic layout of microchip design for (a) PCR-D1, (b) PCR-D2, (c) CEMS. All dimensions are in millimeters. All devices were etched 10 μm deep.

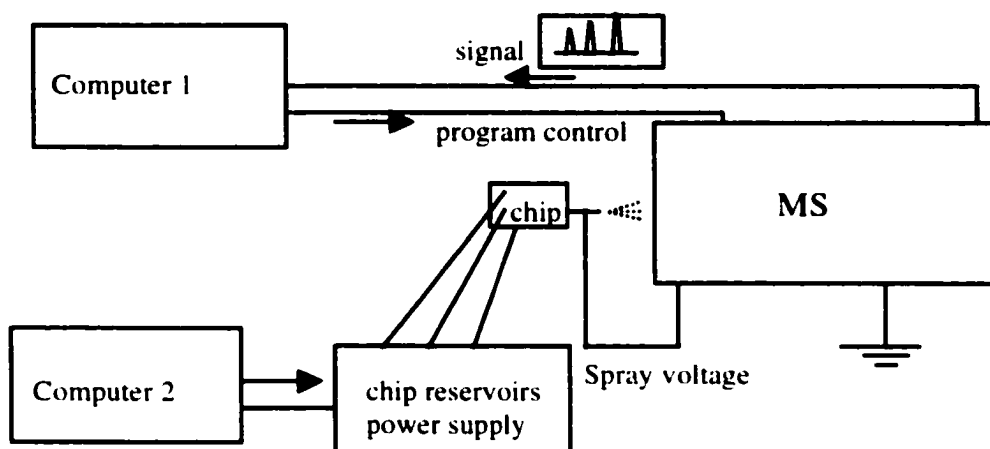


Figure 2-6. Schematic diagram of the instrumental setup for microchip-ESMS. The chip was coupled to a gold coated capillary tip and electrospray voltage was applied to it. Computer 2 was used to control the reservoir voltages. Computer 1 was used to control the mass spectrometer and for data processing.

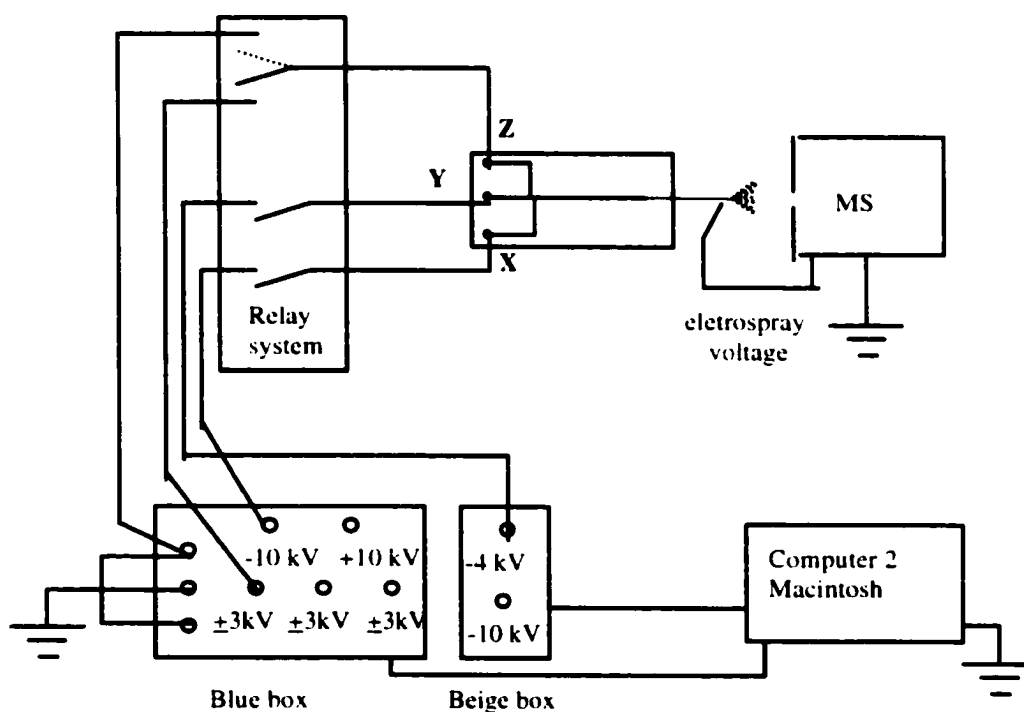


Figure 2-7. Block diagram of the high voltage supply system for reservoirs on chip. A -10 kV supply was connected to sample reservoir X; -4 kV supply to reservoir Y; reservoir Z was connected to ground for injection (dotted line) and a -3 kV supply was connected for separation. Each supply was connected through a relay (actually mounted inside the power supply box). Electrospray voltage was supplied from the mass spectrometer.

Figure 2-6 shows the instrumental set up. In-house written LabView programs (National Instruments, Austin, TX) on computer 2 were used to control the chip reservoir power supplies. Computer 1 was connected to the mass spectrometer for instrument control, data collection and analysis. A PE/Sciex API 150 EX quadrupole mass spectrometer (Perkin-Elmer/Sciex, Concord, ON, Canada) was used for these studies. A schematic showing the high voltage power supply configuration is shown in Figure 2-7. A power supply designed by Larry Coulson and made by the electronics shop at the University of Alberta contained a computer controlled +10 kV, -10 kV, and three manually controlled (+/-) 3 kV power supplies (referred to as the bluebox). To get more power sources, another unit was built which had a -4 kV and a -10 kV supply (referred to as the beige box). The -10 kV supply from the blue box was connected to sample reservoir X. The -4 kV supply from the beige box was connected to reservoir Y. For reservoir Z, ground was connected for injection and a -3 kV supply was connected for separation. The electrospray voltage on the gold tip was supplied by the mass spectrometer. Each power supply was connected to the chip via a computer controlled high voltage relay. The ground line was also connected through a relay.

The position of the electrospray needle was optimized for ion current magnitude and stability while electrokinetically infusing 1 $\mu\text{g/ml}$ of leu-enkephalin (Sigma Chemical Co. St. Louis, MO, USA) from sample waste reservoir Z, with -2 kV on Z (from -10 kV relay in the blue box) and about 3 kV on the needle. Optimal potentials on the needle varied from 2.8 to 3.2 kV. Reservoir Z was then rinsed and filled with separation buffer. Electroosmotic infusion of sample was performed with -2 kV applied at sample reservoir X and the nanoelectrospray tip at 3.1 kV. For separation, a sample

electrokinetic injection was conducted for 18 s by applying -3.5 kV at reservoir X while sample waste reservoir Z and the gold capillary tip were grounded. During separation -3.5 kV was applied to reservoir Y and ~3.2 kV to the nano-electrospray tip. A push back voltage of -2 kV was applied at reservoirs X and Z to prevent sample leakage. The mass spectrometer was scanned over the range m/z 500-1000 at 1 amu per step with a dwell time of 2 ms.

2.3. Results and Discussion

Our microchip-ESMS interface development passed through three stages. At first we tried to spray from the flat edge of the glass chip, with various electrical voltages applied. Cameron Skinner in our group developed a method of coupling a short capillary at the end of the channel with a minimal dead volume connection,³⁷ with the electrospray voltage applied to a reservoir in the chip. Finally we found that using a pulled capillary tip with a gold coating made a good ESMS interface. The latter design gave more flexibility for the voltage setting used on chip, while the electrospray voltage was applied at the gold tip.

2.3.1. Spray Directly From the Edge of the Chip

To couple a microchip to a mass spectrometer our first effort was to try to obtain electrospray directly from the channel outlet at the edge of the chip, following the procedure of Xue et al.^{25,26} This design is attractive because it does not require complex machining and the channel outlet can be exposed by just dicing the chip. In Figure 2-8, all of the chips were diced at the end of the main channel, labeled D. All of the channels were filled with water and the reservoirs were sealed with black tape before dicing, to

prevent glass debris entering the channels. The main channel had a depth of 10 μm and a width of 30 μm . In Figure 2-8a, hydroxy propylmethyl cellulose gel was used to fill the side channel from reservoir E. The gel was put in a pipette tip which was inserted into reservoir E. Pressure (~ 20 psi) was applied to the pipette tip and the gel was pushed to the channel between E and F and stopped right before junction F. All of the reservoirs including E were then filled with running buffer of 50 mM Tris-boric acid buffer (pH 8.5). We hoped that when voltage was applied between reservoir E and sample reservoir A, the sample would be forced to flow through the main channel down stream. This seemed likely because the gel gave a higher resistance to flow between E and F, so that the sample fluid flow should at least partially go to outlet D. At the same time the voltage applied at E could provide the electric field between D and the counter electrode (or mass spectrometer) so as to give electrospray. We found there were problems with this design. First, the gel leaked into the main channel. Second, the sample entered the gel in the side channel EF. When we used FITC as sample and applied voltage to drive it to the end of the channel, we could see the gel became stained with FITC.

For the CEMS device used in Figure 2-8b, a gold line (500 μm wide and 0.24 μm thick) was fabricated on the cover plate. The detailed layout for the CEMS chip is shown in Figure 2-5c. When the cover plate was bonded to the substrate, the gold line crossed and contacted the main channel at point H. When voltage was applied at point G, the voltage at the gold line segment had about the same voltage. The voltage drop between reservoir A and the gold line would drive the sample down the channel. With G about 2000 V above the external counter electrode, this approach should have resulted in electrospray. In this study 50 mM Tris-boric acid buffer was used as the running buffer.

The big problem with this design was that bubble formation from water hydrolysis at the gold line could easily fill the channel with gas, so that solution could not go through.

To avoid bubble formation in the channel, we coated gold on the surrounding area of the channel outlet, as shown in Figure 2-8c and 2-8d. For this case, 50 mM Tris-boric acid buffer (pH 8.5) and 50 mM morpholine (pH 9) were tested as the running buffer. Positive voltages were applied to the gold and even higher potentials to the reservoir, to drive the buffer solution to the gold coated outlet. The counter plate perpendicular to the channel and parallel to the gold coating was grounded. Sprayed droplets could be seen on the counter plate when the distance was about 1.5 mm and the voltage applied to the gold was larger than 1 kV. However, sparks accompanied the droplet formation, occurring between the plated gold and the counter electrode. We tried to use parafilm to cover the surrounding area, but this did not solve the spark problem. The discharge problem meant this design could not be used reliably for microchip-ESMS interface.

Based on the experience that a pointed capillary tip could give stable spray, we also tried to point the end of the chip, as illustrated in Figure 2-8e. The chip was cut and sanded to the shape shown in the figure. It was hard and delicate work locating the ~30 μm channel opening right on the edge of the DH and DI surfaces. Positive high voltage (3-5 kV) was applied at reservoir B to see if the 40 mM ammonium bicarbonate buffer (pH 8.2) could give stable spray to a mass spectrometer, with the curtain plate at 1 kV. However, liquid spreading to the DI and DH surface prevented electrospray. An Immunopen (Calbiochem, LaJolla, CA) was used to coat the area surrounding the channel opening with a hydrophobic coating, but it did not prevent the liquid from spreading.

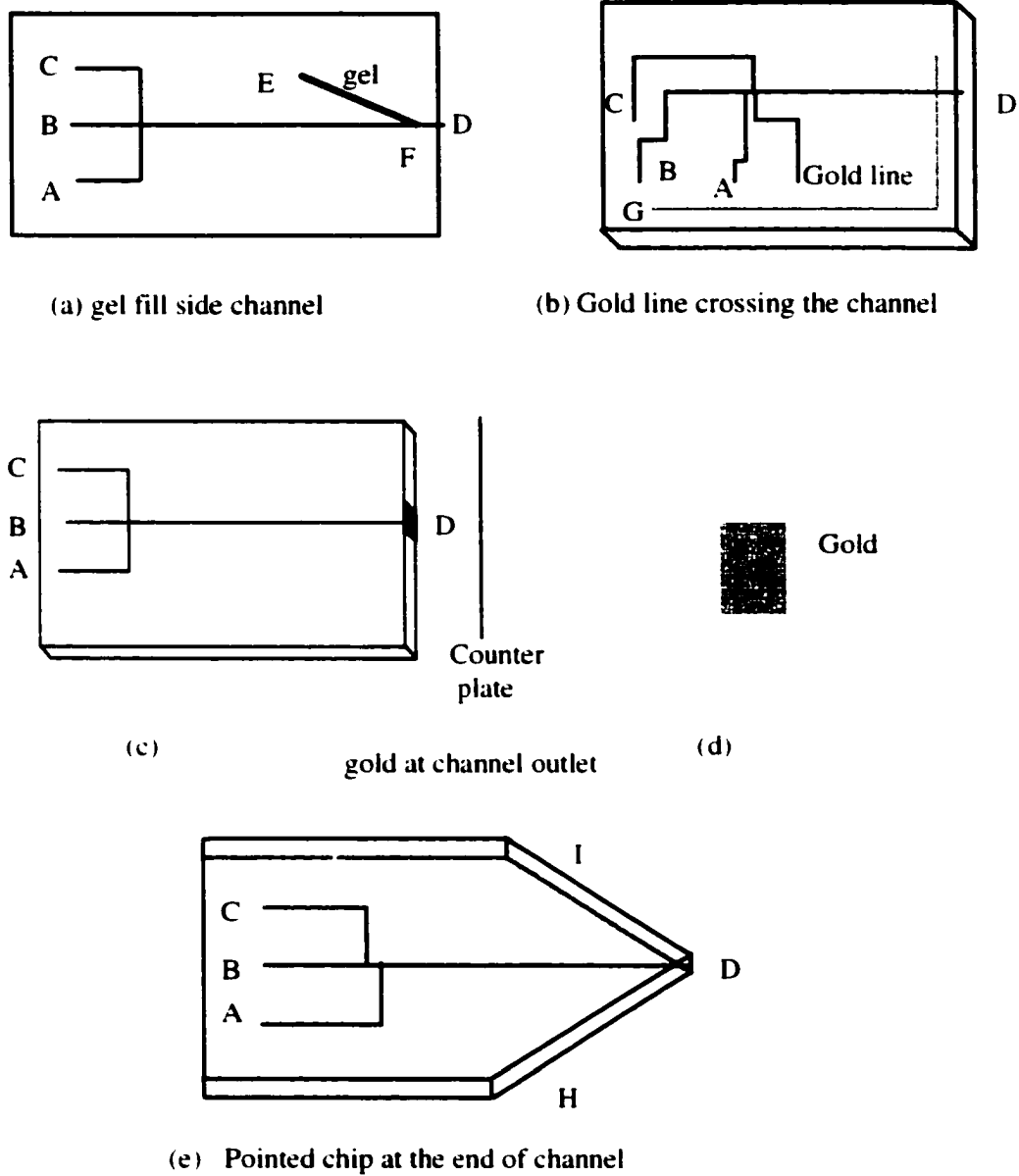


Figure 2-8. Different designs for electro spray directly from the flat edge of the chip: (a) Gel filled the channel between E and F; (b) A gold line crosses the separation channel; (c) and (d) Gold was sputtered at the channel outlet; (e) Pointed chip at the end of the channel.

Just as reported by Ramsey's²⁷ and Karger's^{25,26} groups, we found that large droplets formed and spread over a relatively large area surrounding the exit orifice of a flat-edged chip. A Taylor cone and electrospray was hard to establish at the edge of the microchip. Even if a spray was started, it was not very stable, as evidenced by pulsation of the droplet and Taylor cone. The following equations explain why when the liquid spreads on a flat surface it is hard to obtain stable spray.

The voltage V_{on} applied on the capillary tip required for the onset of ES³⁹ is

$$V_{on} \approx \left(\frac{r\gamma \cos \theta}{2\epsilon} \right)^{1/2} \ln(4d/r) \quad 2-1$$

where γ is the surface tension of the solvent, ϵ is the permittivity of vacuum ($8.8 \times 10^{-12} \text{ J}^{-1}\text{C}^2 \text{ m}^{-1}$), θ is the half angle of the Taylor cone (49.3°), r is the outer radius of the capillary tip, which defines the base of the Taylor cone, and d is the distance between the capillary tip and the counter electrode. When the droplet spreads on the side of the chip, suppose $r = 0.5 \text{ mm}$ and $d = 1.5 \text{ cm}$. Surface tension $\gamma = 0.07275 \text{ Nm}^{-1}$ for water. The calculated onset voltage is 5.55 kV. Even when the distance d is reduced to 0.5 cm, V_{on} is still 4.28 kV. For a pulled capillary tip of $10 \mu\text{m}$, the onset voltage is only 1.42 kV at a d of 1.5 cm. When the size of the droplet increases, the onset voltage for electrospray increases 3-4 times as needed.

When a high voltage is applied to the capillary for electrospray, an electric field exists between the capillary tip and the counter electrode. The magnitude of the electric field E at the capillary tip can be approximated by the following equation.^{40,41}

$$E \approx \frac{2V}{r \ln(4d/r)} \quad 2-2$$

where V is the potential applied to the capillary tip. Suppose $d = 1.5$ cm and $V = 3$ kV, which is the voltage we typically used with a pulled capillary tip, as discussed in the following chapters. When $r = 10$ μm , E equals 68,960 kV/m. While for a spread droplet at $r = 0.5$ mm, E is 2506 kV/m, which is 27.5 times less than at a pulled tip. Even reducing d to 0.5 cm and increasing applied voltage to 5 kV, the electric field for a 0.5 mm droplet size is still 5422 kV/m, which is still 12.7 times less than needed for stable electrospray.

From all of these calculations, we can see that when we spray from the flat edge of the chip, the spreading of the liquid results in much higher onset so it is harder to get the needed electric field for stable electrospray. These calculations suggest why the flat surface design has not been very successful. Based on the information from capillary electrophoresis mass spectrometry interface performance, we moved to couple a short capillary tip at the channel outlet and spray directly from the capillary.

2.3.2. Capillary Tip Coupled to Chip with Minimal Dead Volume Connection

Cameron Skinner, a post-doctor fellow who worked on this project, developed a drilling and coupling method to connect a capillary to the microchip channel.³⁷ This method was a breakthrough for microchip-ESMS. Using laser induced fluorescence detection and FITC labeled amino acids as samples, he demonstrated that it is possible to use a drilling procedure to generate extremely low dead volume couplings between a microfluidic chip and an external capillary. Fused silica capillaries were connected to microfluidic devices by drilling into the edge of the device using 200 μm tungsten carbide drills. The standard pointed drill bits create a hole with a conical shaped bottom that

leads to a geometric dead volume of 0.7 nL at the junction, and significant bandbroadening when used with 0.2 nL sample plugs. The plate numbers obtained on the fused silica capillary connected to the chip were about 16-25% of the predicted numbers. The conical area was removed with a flat tipped drill bit and the bandbroadening was substantially eliminated (on average 98% of the predicted plate numbers were observed). All measurements were made while voltages were applied in the reservoirs and counter plate, and the device was operating with an electrospray from the end of the capillary. The effective dead volume of the flat bottom connection is minimal and allows microfluidic devices to be connected to external detectors like a mass spectrometer.

Based on this interface design, we decided to further develop the capillary to chip interface, rather than attempt to generate an electrospray directly from the edge of the chip. Utilizing an attached capillary, with a tapered tip, provides a small and readily manipulated droplet size, and the length of the attached capillary can be changed to meet changing resolution needs. This design was further tested at Pierre Thibault's lab at the National Research Council with an API 300 mass spectrometer.³⁵ Peptide separation in 3-5 minutes was demonstrated. With a long capillary coupled, such a hybrid device also allowed for the use of a commercial microelectrospray interface, that provided independent control over the electrospray operating parameters.

For the experiments presented here we used a drill press with no measurable vibrations (Model 7010, Servo Products Company, Pasadena, CA). This press produced superior holes, cracking along the hole wall and bottom was not observed. With this tool, the drills remained centered on the channel, even with the larger drills (370 μm).

The choice of capillaries compatible with the 200 μm size of drill was limited to 185 μm o.d. and 50 μm i.d. Unfortunately, the channel cross sectional area was approximately 450 μm^2 whereas the capillary area was 1960 μm^2 or about 4.4 times larger. The 150 μm nominal o.d. drill bits produced holes smaller than the 140-150 μm capillaries available, because of the relatively large negative tolerances on the drills.

The end channel was filled with CB to avoid plugging during cutting and drilling. Crystal Bond was also used to glue the capillary into the device because the joint could be taken apart later with gentle heating. Unfortunately, prolonged exposure of CB to water causes it to soften and expand so that it may plug the joint. Adjustment of the hot plate temperature controlled the flow rate of the glue into the joint and ensured that it only contacted the outside of the capillary. Even though swelling of the CB still occurred, it did not block the joint.

2.3.3. Gold Coated Capillary Tip Coupled at Channel Outlet for Microchip-ESMS

Basically there are three types of capillary electrophoresis-ESMS interface, coaxial sheath flow,⁴²⁻⁴⁵ liquid junction^{46,47} and sheathless.^{38,48,49} For a sheathless interface, a conductive paint like gold and silver is usually used at the capillary tip and the electrospray voltage is applied directly at the tip. The sheathless interface is becoming the most common because it is easy to set up and gives better sensitivity. It eliminates the interference and dilution caused by the sheath solvent or make-up fluid used for sheath flow or liquid junction. A gold coated capillary tip coupled at the end of the channel is also the simplest of interface designs for our microchip-ESMS interfaces. The joint preparation and coupling procedure was discussed above. The capillary tip could be

removed and changed in 20 minutes. This design was first used at Pierre Thibault's lab.²¹ We continued to test and use this interface in our lab after we obtained a mass spectrometer.

To minimize analyte adsorption on bare silica walls, we coated the channels in the chip and the capillary tip with BCQ, a quaternary amine reagent that gives positive charge on the surface. The direction of EOF was reversed, giving what is termed anodal EOF while using 0.1 M formic acid as the running buffer (pH 2.1). For peptide separations, all of the analytes were separated and detected as positive ions. This approach gave better sensitivity than using negative ion separation in basic buffer, followed by positive ion detection, which was required when the tip was not gold coated. The electrospray ionization voltage was applied on the gold tip. The separation electric field was defined by the voltage in reservoir Y of Figure 2-4 and the voltage applied to the gold tip. Separate control of the electrospray and electrophoretic voltages gave the flexibility needed to adjust for stable spray.

To see if the electrospray from the tip was stable, electroinfusion directly from the sample reservoir was tested. -2 kV was applied to sample reservoir X, while the electrospray voltage was around 3 kV. Sample was delivered to the tip using EOF and was then sprayed into the mass spectrometer, without a need of any makeup flow. Figure 2-9a shows the Total Ion Current of a four peptide mixture (10 µg/ml each) in 60 mM formic acid. The mass range was m/z 500-1000. The four peptides were leu-enkephalin (556), angiotensin II (524^{2+}), bradykinin (531^{2+}) and melittin (713^{4+}). We can see that the ion current was very stable, which means that this interface design gave very stable electrospray. Figure 2-9 b shows the mass spectrum at 0.95 min from the total ion

current trace. The four peptide peaks are clearly shown. No make up liquid flow or nebulizer gas was needed, making the interface simple and efficient.

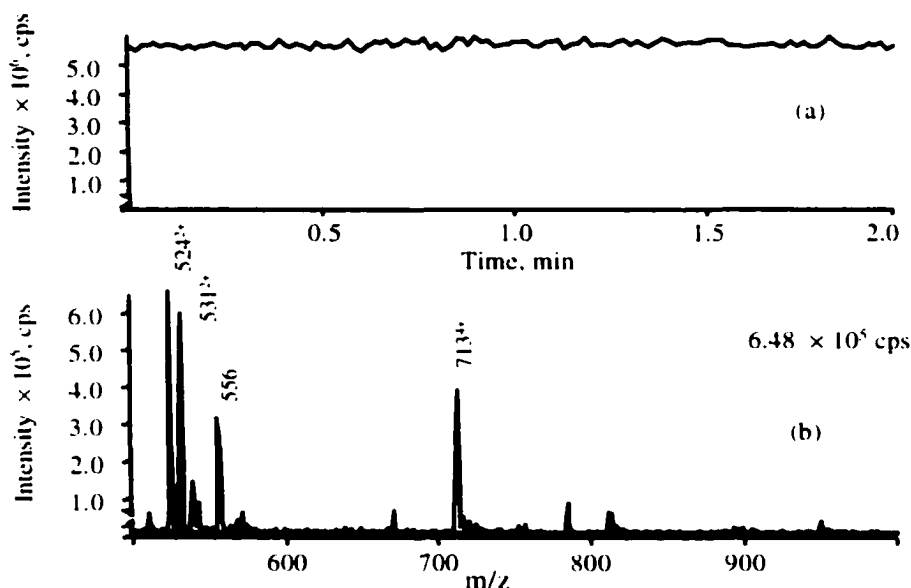


Figure 2-9. (a) Total ion current for electroinfusion of a four peptide mixture (10 $\mu\text{g}/\text{ml}$ each). The chip used was PCRD-1, shown in Figure 2-5. -2 kV was applied to the sample reservoir X while the electrospray voltage was around 3.1 kV. (b) Mass spectrum extracted at 0.95 min, shows leu-enkephalin (556), angiotensin II (524^{2+}), bradykinin (531^{2+}) and melittin (713^{4+}).

Separation of the four peptides is shown in Figure 2-10. Selected ion monitoring was used at four masses, (556 , 524^{2+} , 531^{2+} , 713^{4+}). The total ion electropherogram (TIE) showed three main peaks for leu-enkephalin (556), angiotensin II (524^{2+}) and bradykinin (531^{2+}). Melittin gave too low an intensity to be seen in the TIE, but the extracted or reconstructed ion electropherogram (RIE) clearly shows its separation profile. All of the compounds were separated in 1.5 min. The plate numbers were between 1640 and 3080, which correspond to 23,432 plates/m and 44,004 plates/m for the 7 cm separation channel used here. The plate number was not very high because we used a large injection volume (0.5-2 nl) to obtain good signal intensity. Because melittin is a bigger polypeptide that

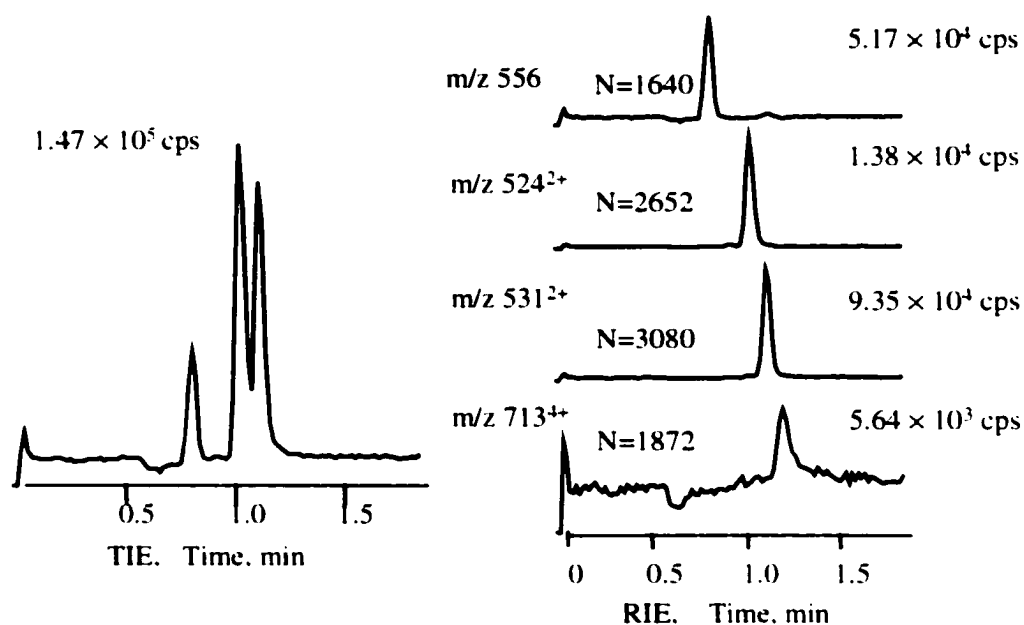


Figure 2-10. TIE and RIE for the separation of four peptides (500 ng/ml) with Selected Ion Monitoring for leu-enkephalin (556), angiotensin II (524²⁺), bradykinin (531²⁺) and melittin (713³⁺). The data was collected in PCRD-1 using the voltage scheme shown in section 2.2.3. Injection time: 20 s. Separation buffer: 100 mM formic acid.

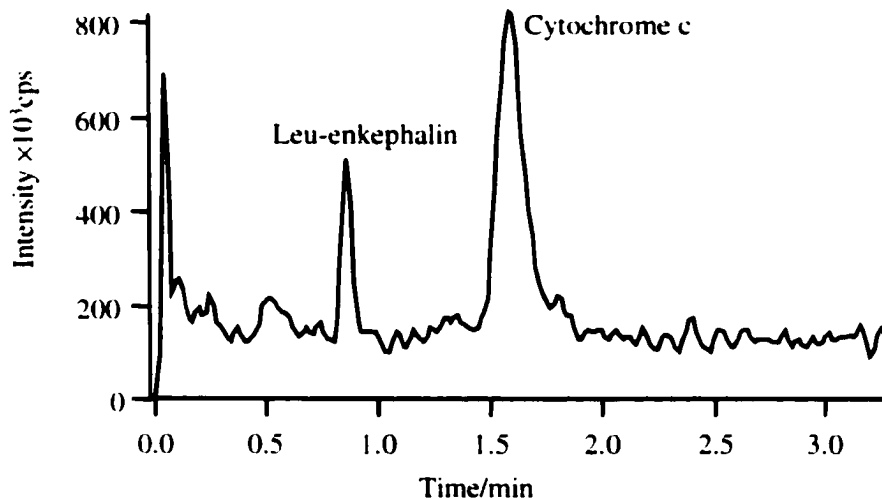


Figure 2-11. Separation of leu-enkephalin and cytochrome c on PCRD-2 chip with ESMS detection. The TIE was collected in the mass range of m/z 500-1000. The capillary tip was 3 cm long. Cytochrome c was 100 $\mu\text{g/ml}$ and leu-enkephalin was 10 $\mu\text{g/ml}$. Buffer: 100 mM formic acid with 10 mM ammonium bicarbonate. Injection: -2.5 kV ~ ground, 28 s. Separation: -2.5 kV ~ 3.1 kV with pushback voltage of -1.5 kV.

may have some tendency to adsorb on channel surfaces, a little tailing was observed. Figure 2-11 shows the separation of leu-enkephalin (10 $\mu\text{g/ml}$) and cytochrome c (100 $\mu\text{g/ml}$, or 8 μM). The protein peak was clearly identified. The two peaks were completely baseline resolved.

2.4. Conclusions

We examined the use of different designs for electrospraying from the edge of the chip. We finally found that coupling a capillary tip at the end provided a good interface for microchip ESMS. Fused silica capillaries were connected to microfluidic devices for capillary electrophoresis by drilling into the edge of the device using 200 μm tungsten carbide drills. The effective dead volume of the flat bottom connection was minimal and allowed microfluidic devices to be connected to a mass spectrometer. The gold coated capillary tip was used for MS detection of a peptide mixture in a BCQ coated chip. Very stable electrospray was observed in the electroinfusion mode and good separation of peptides and proteins was achieved in the CE mode. Compared to other designs used by other research groups for coupling glass chips to a mass spectrometer, the design we have used has several advantages. The fabrication of the coupling hole is not very hard. No liquid junction and make up flow was needed. The straight connection between the chip channel and capillary tip make compound separation achievable within the device instead of just using the chip as a sample feeding device. The capillary tip could be removed and changed in 20 minutes, which makes the chip reusable. The CE separation electric field was defined between reservoir and electrospray voltage, while the electric field for electrospray was defined between the tip and the curtain plate. The gold tip gives the

possibility to apply one more voltage in between and it also gives the flexibility to adjust voltage for stable electrospray and optimum CE separation electric field. This was hard to accomplish with a bare capillary tip and one voltage in a reservoir for both separation and electrospray. For all of the following experiments in this thesis, we used the gold coated capillary tip as our microchip-ESMS interface.

2.5. References

1. Harrison, D. J.; Fluri, K.; Seiler, K.; Fan, Z.; Effenhauser, C. S.; Manz, A. *Science* **1993**, 261, 895-897.
2. Fluri, K.; Fitzpatrick, G.; Chiem N.; Harrison, D. J. *Anal. Chem.* **1996**, 68, 4285-4290.
3. Chiem N. H.; Harrison, D. J. *Clinical Chemistry* **1998**, 44, 591-598.
4. Colyer, C. L.; Magru, S. D.; Harrison, D. J. *J. Chromatogr. A* **1997**, 781, 271-276.
5. Magru, S. D.; Harrison, D. J. *Electrophoresis* **1998**, 19, 2301-2307.
6. Cohen, C. B.; Chin-Dion, E.; Jeong, S.; Nikiforov, T. T. *Anal. Biochem.* **1999**, 273, 89-97.
7. Hadd, A. G.; Raymond, D. E.; Halliwell, J.; Jacobson, S. C.; Ramsey, J. M. *Anal. Chem.* **1997**, 69, 3407-3412.
8. Xue, Q.; Dunayevskiy, Y. M.; Foret, F.; Karger, B. L. *Rapid. Commun. Mass Spectrom.* **1997**, 11, 1253-1256.
9. Ekstrom, S.; Onnerfjord, P.; Nilsson, J.; Bengtsson, M.; Laurell, T.; Varga, G. *Anal. Chem.* **2000**, 72, 286-293.
10. Xu, N.; Lin, Y.; Hofstadler, S. A.; Matson, D.; Call, C. J.; Smith, R. D. *Anal. Chem.* **1998**, 70, 3553-3556.
11. Xiang, F.; Lin, Y.; Wen, J.; Matson, D. W.; Smith, R. D. *Anal. Chem.* **1999**, 71, 1486-1490.
12. Harrison, D. J.; Manz, A.; Fan, Z.; Ludi, H.; Widmer, H. M. *Anal. Chem.* **1992**, 64, 1926-1932.

13. Jacobson, S. C.; Hergerroder, R.; Koutny, L. B.; Ramsey, J. M. *Anal. Chem.* **1994**, 66, 2369.
14. Raymond, D. E.; Manz, A.; Widmer, H. M. *Anal. Chem.* **1996**, 68, 2515-2522.
15. Effenhauer, C. S.; Paulus, A.; Manz, A.; Widler, H.M. *Anal. Chem.* **1994**, 66, 2949-2953.
16. Moore, A. M.; Jacobson, S. C.; Ramsey, J. M. *Anal. Chem.* **1995**, 67, 4184-4189.
17. Whitehouse, C. M.; Dreyer, R. N.; Yamashitna, M.; Fenn, J. B. *Anal. Chem.* **1985**, 57, 675-680.
18. Smith, R. D.; Loo, J. A.; Edmonds, C. G.; Barinaga, C. J.; Udseth, H. R. *Anal. Chem.* **1990**, 62, 882-899.
19. Johansson, J. M.; Pavelka, R.; Henion, J. D. *J. Chromatogr.* **1991**, 559, 515-528.
20. Tomlinson, A. J.; Benson, L. M.; Jameson, S.; Johnson, D. H.; Naylor, S. *J. Am. Soc. Mass Spectrom.* **1997**, 8, 15-24.
21. Li, J.; Kelly, J.; Chernushevich, I.; Harrison, D. J.; Thibault, P. *Anal. Chem.* **2000**, 72, 599-609.
22. Zhang, B.; Liu, H.; Karger, B. L.; Foret, F. *Anal. Chem.* **1999**, 71, 3258-3264.
23. Zhang, B.; Karger, B. L.; Foret, F. *Anal. Chem.* **2000**, 72, 1015-1022.
24. Deng, Y.; Henion, J.; Li, J.; Thibault, P.; Wang, C.; Harrison, D.J. *Anal. Chem.* **2001**, 73, 639-646.
25. Xue, Q.; Foret, F.; Dunayevskiy, Y. M.; Zavracky, P. M.; McGruer, N. E.; Karger, B. L. *Anal. Chem.* **1997**, 69, 426-430.
26. Xue, Q.; Dunayevskiy, Y. M.; Foret, F.; Karger, B. L. *Rapid. Commun. Mass Spectrom.* **1997**, 11, 1253-1256.
27. Ramsey, R. S.; Ramsey, J. M. *Anal. Chem.* **1997**, 69, 1174-1178.
28. Schultz, G. A.; Corso, T. N.; Prosser, S. J.; Zhang, S. *Anal. Chem.* **2000**, 72, 4058-4063.
29. Wen, J.; Lin Y.; Xiang F.; Matson D. W.; Udseth H. R.; Smith R. D. *Electrophoresis*, **2000**, 21, 191-197.
30. Yuan, C.; Shiea, J. *Anal. Chem.* **2001**, 73, 1080-1083.
31. Figeys, D.; Ning, Y.; Aebersold, R. *Anal. Chem.* **1997**, 69, 3153-3160.

32. Figeys, D.; Gygi, S.P.; McKinnon, G.; Aebersold, R. *Anal. Chem.* **1998**, 70, 3728-3734.
33. Figeys, D.; Aebersold, R. *Anal. Chem.* **1998**, 70, 3721-3727.
34. Wachs T.; Henion J. *Anal. Chem.* **2001**, 73, 632-638.
35. Li, J.; Thibault, P.; Bings, N.; Skinner, C. D.; Wang, C.; Colyer, C.; Harrison, D. J. *Anal. Chem.* **1999**, 71, 3036-3045.
36. Li, J.; Wang, C.; Kelly, J.; Harrison, D. J.; Thibault, P. *Electrophoresis* **2000**, 21, 198-210.
37. Bings, N.H.; Wang, C.; Skinner, C. D.; Colyer, C.; Thibault, P.; Harrison, D. J. *Anal. Chem.* **1999**, 71, 3292-3296.
38. Bateman, K. P.; White, R. L.; Thibault, P. *Rapid Commun. Mass Spectrom.* **1997**, 11, 307-315.
39. Smith D.P.H. *IEEE Trans. Ind. Appl* **1986**, IA-22, 527-533.
40. Loeb, L. B.; Kip, A. F.; Hudson, G.G.; Bennett, W. H. *Phys. Rev.* **1941**, 60, 714-721.
41. Kebarle, P.; Tang, L. *Anal. Chem.* **1993**, 65, 972A-986A.
42. Smith, R. D.; Olivares, J. A.; Nguyen, N. T.; Udseth, H. R. *Anal. Chem.* **1988**, 60, 436-440.
43. Hopfgartner, G.; Wachs, T.; Bean, K.; Henion, J. *Anal. Chem.* **1993**, 65, 439-446.
44. Bruins, A. P.; Covey, T. R.; Henion, J. D. *Anal. Chem.* **1987**, 59, 2642-2646.
45. Covey, T. R.; Bonner, R. F.; Shushan, B. I.; Henion, J. D. *Rapid Commun. Mass Spectrom.* **1988**, 2, 249-253.
46. Lee, E. D.; Muck, W.; Henion, J. D.; Covey, T. R. *J. Chromatogr.* **1988**, 458, 313-321.
47. Pleasance, S.; Thibault, P.; Kelly, J. *J. Chromatogr.* **1992**, 591, 325-339.
48. Barnidge, D. R.; Nilsson, S.; Markides, K. E.; Eapp, H.; Hjort, K. *Rapid Commun. Mass Spectrom* **1999**, 13, 994-1002.
49. Barnidge, D. R.; Nilsson, S.; Markides, K. E. *Anal. Chem.* **1999**, 71, 4115-4118.

Chapter 3

Large Volume Sample Stacking to Preconcentrate Samples on a Microchip*

Table of contents	Page
3.1. Introduction.....	66
3.2. Experimental.....	70
3.2.1. Large volume sample stacking on microchip using LIF detection.....	70
3.2.2. Large volume sample stacking on microchip using MS detection.....	72
3.2.3. Preparation of protein digests.....	75
3.3. Results and Discussion.....	76
3.3.1. Large volume sample stacking on microchip using LIF detection.....	77
3.3.2. Large volume sample stacking on microchip using MS detection.....	81
3.4. Conclusions.....	88
3.5. References	89

* A portion of this chapter has been published in *Electrophoresis* **2000**, 21, 198-210. by Li, J.:

Wang, C.; Kelly, J. F.; Harrison, D. J.; Thibault, P.

3.1. Introduction

Capillary electrophoresis (CE) and microchip-capillary electrophoresis have become useful separation techniques for the analysis of small volume samples.¹⁻⁴ But at the same time, the small sample volume and short pathlength limits the concentration detection sensitivity. To overcome this limitation, several approaches have been used. In absorbance detection, the optical pathlength could be increased by designing a Z-⁵ or U-shape ⁶ or by using a multireflection cell.^{7,8} Laser induced fluorescence detection is much more sensitive and widely used for CE and microchip-CE.^{1-3,9} The development of a confocal microscope based detection system reduced the detection limit to 0.3 pM for fluorescein dye.⁹ However, there is a limit to how much the detector sensitivity can be improved. An alternative may be to preconcentrate the sample. Three preconcentration methods have been widely used: isotachopheresis (ITP); solid phase extraction (SPE); and field amplified sample stacking (FASS).

Isotachopheresis dates back to the 1970s.¹⁰ In ITP, the sample plug is sandwiched between leading and trailing buffers that have high and low electrophoretic mobilities respectively. By applying voltages at the end of the capillary, the analytes are separated according to their electrophoretic mobilities and focused according to the concentration of the leading buffer. ITP-CE has been reported for concentrating analytes and it can provide a sharp sample band.¹¹⁻¹⁴ The disadvantage is that several different kinds of buffers need to be introduced into a single capillary.

Solid phase extraction is a powerful preconcentration technique which is widely used for drugs, proteins and peptides.¹⁵⁻²⁰ On-line SPE-CE involves packing of a short plug of extraction phase coated beads, or membrane, which is connected to a CE

capillary. The process includes sample loading onto a reversed phase material such as silica based C_{18} ¹⁵⁻¹⁸ or a polymer phase.^{19,20} followed by washing and organic solvent elution. A large sample volume can be used in this approach. This method has been successfully used on-line for CE and microchip-CE. For example a sample enrichment of 500-fold was achieved by the Harrison research group with a packed bed in a microchip.²¹ This method could preconcentrate hydrophobic analytes, but is not good for hydrophilic samples.

Sample stacking was first introduced to CE by Mikker et al.²² in 1979 and was intensively studied by Chien or Burgi et al.²³⁻²⁷ They proposed a model to explain the

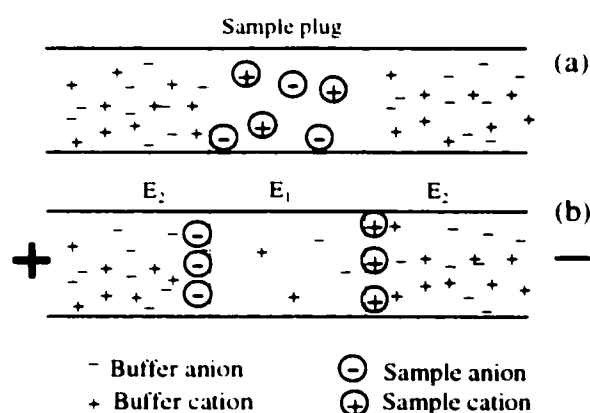


Figure 3-1. Schematic drawing of small volume sample stacking: (a) Sample plug in low conductivity buffer was injected, (b) Analytes were stacked at the sample/buffer boundary. Adapted from reference 26.

sample stacking phenomena. The discussion below is adapted from their detailed review in reference 26.

Sample stacking is achieved by using a lower conductivity sample plug than the running buffer. Usually sample is dissolved in water, or in a lower concentration of the same running buffer. When voltage is applied, the

sample plug experiences a higher electric field relative to the buffer zone, due to its lower conductivity. The field rapidly drives anions to one end and cations to the other end of the sample plug, as is shown in Figure 3-1. The ion velocities decrease when they cross the sample/buffer boundary, and as a result they stack up at the interface. In Figure 3-1, suppose the length of the capillary is L and the sample plug is χL ($0 < \chi < 1$), then the

buffer length is $(1 - \chi) L$. The electric field strengths in sample buffer plug E_1 and in running buffer regions E_2 are given by

$$E_1 = \gamma E_0 / [\gamma\chi + (1-\chi)] \quad 3-1$$

$$E_2 = E_0 / [\gamma\chi + (1-\chi)] \quad 3-2$$

where $\gamma = \rho_1 / \rho_2$, which is the ratio of resistivities of the sample plug and the buffer plug, $E_0 = V / L$, where V is the total voltage applied to the capillary. It is possible to show that $E_1 / E_2 = \gamma$, so the higher the resistivity difference, the higher the electric field difference.

When the analyte ions pass the sample/buffer boundary, the flux of the ions in these two plugs must be conserved

$$C_1 v_{ef1} = C_2 v_{ef2} \quad 3-3$$

where C_1 and v_{ef1} are the concentration of analyte ions and their electrophoretic velocity in the sample plug, and C_2 and v_{ef2} are the concentration of analyte ions and their electrophoretic velocity in the running buffer plug. Because the electrophoretic velocity is simply proportional to the electric field strength, equation 3-3 can be rearranged to

$$C_1 \gamma = C_2 \quad 3-4$$

The analyte ions are concentrated γ times in the running buffer. Because the total moles of the analyte is a constant and the cross section of the capillary is the same everywhere, neglecting diffusion the stacked analyte plug length X_2 can be expressed as

$$X_2 = X_{1mj} / \gamma \quad 3-5$$

where X_{1mj} is the original sample plug length. Theoretically, the greater the conductivity difference between the sample plug and the running buffer, the narrower the resultant peak and the greater the extent of stacking. However, as proposed by Chien et al.²⁶

pressure is generated between the sample plug and the running buffer because of the mismatch of the two electroosmotic flows. The sample plug has a higher electric field and larger ζ potential, so it has a larger localized electroosmotic flow than the running buffer. The pressure introduces parabolic flow and broadens the stacked sample plug. Stacking and broadening compete with each other, creating an optimum length of sample plug and conductivity that can be introduced into the capillary and still give high resolution. Sample stacking has been widely used for CE and microchip-CE to get better sensitivity.

To maintain the stacking results and avoid bandbroadening from EOF mismatching, the sample solvent can be entirely removed by large plug sample stacking accompanied

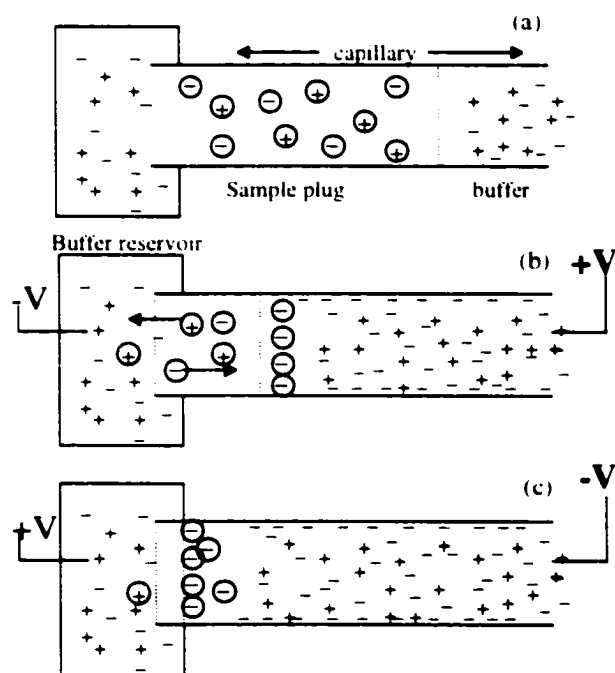


Figure 3-2. Large volume sample stacking with polarity switching: (a) Large plug of low conductivity sample was introduced into the capillary, (b) Sample buffer and cations were driven out of the capillary and anions were stacked, (c) Polarity was switched and the anions were separated. Adapted from reference 26.

by polarity switching.^{26,27} The procedure for this method is shown in Figure 3-2. Sample is introduced to fill the whole or part of the capillary (Figure 3-2a), followed by applying voltage to drive the sample solvent out. The negative ions stack at the back of the sample plug (Figure 3-2b). Since the cations stack at the front of the sample plug (defined as the leading edge during the reversed polarity stacking step), they are swept out of the capillary by normal cathodal EOF (

Figure 3-2c). The anions can then be separated when almost all of the sample solvent is removed by switching the voltage polarity again (Figure 3-2c). The positive ions can be enriched by this method when using a capillary that has a positive charge on the wall, such as induced by an appropriate coating.²⁸ This large volume sample stacking with polarity switching method has been used by others, and 10 to 65 times sensitivity enhancement can be achieved.²⁹⁻³³

In this chapter we present the first report on adapting the large volume sample stacking procedure to a microchip system. We used negative ion sample stacking in an uncoated capillary when using laser induced fluorescence detection, while positive peptides were analyzed in positively coated channels using mass spectrometry detection.

3.2. Experimental

3.2.1. Large Volume Sample Stacking in Microchip Using LIF Detection

A PCRD-2 chip made with Schott Borofloat glass was used for this study (Figure 3-3). The device was fabricated using standard photolithography and wet chemical etching techniques, as described before.³ The fluid channel layout is illustrated in Chapter 2, while the access reservoirs are identified for reference below. Channels were etched on one glass plate to a 10 μm depth and 30 μm width for the majority of the length, with 250 μm wide segments near the reservoirs. The distance from the double T injector to the Y junction was 3.8 cm; the double T injector had a 100 μm offset. Because the chip was not coupled to the MS for detection, it was not cut and no capillary was attached. At the beginning of the experiment the device was flushed with water, 0.1 M NaOH, water and then with the running buffer for 30 min. Morpholine buffer (30 mM, pH 9.5) prepared in

deionized distilled water was used. The FITC labeled arginine, stored at 4 °C, was prepared by mixing 7.63 mM amino acid with 1.52 mM FITC before allowing the mixture to stand overnight at room temperature. A 0.05 μ M FITC labeled arginine solution, diluted with 3 mM morpholine buffer was used as the sample.

Large volume sample stacking preconcentration and detection on the microchip includes three steps: sample loading, reversed direction large volume sample stacking, sample separation and detection, as shown in Figure 3-3. Sample was put in reservoir A

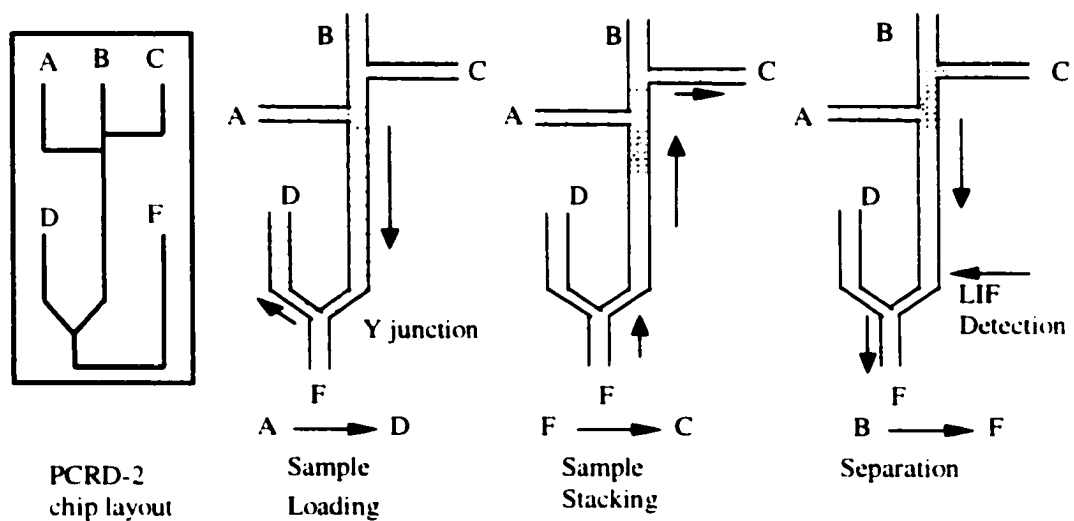


Figure 3-3. Procedures for large volume sample stacking using laser induced fluorescence detection on microchip. Flow direction: sample loading from A to D; sample stacking from F to C; and separation from B to F.

and all of the other reservoirs were filled with running buffer. In the sample loading step, reservoir A was grounded and -2.6 kV was applied at sample waste reservoir D. Sample filled the main channel (3.8 cm) and went to the sample waste D. To prevent sample leakage to the direction of reservoir F, this reservoir was also grounded. The long plug of the sample (10 nl) was then reversed and stacked by running buffer flowing from reservoir F (ground) to the stacking waste reservoir C (-4 kV). -0.8 kV was applied at

reservoir D to block the sample waste flowing back to the main channel. When the end of the stacked sample plug reached the double T injector (~20 s), the flow direction was reversed for separation. The main flow was from reservoir B (5 kV) to reservoir F (ground) with a push back voltage of 2.6 kV on reservoirs A and C. The stacked sample plug migrated in the main channel and was detected 2.5 cm down stream from the double T.

In house written Labview programs (National Instruments, Austin, TX) were used for computer control of the voltage supply and for data collection. A 4 mW argon ion laser beam (488 nm) was focused on the channel of the device. Fluorescence signal was collected with a 25 X (0.35 N.A.) Leitz Fluotar microscope objective. A 530DF30 (Omega Optical, Brattleboro, VT) emission filter and a Hamamatsu PMT were used as the detector. The PMT was connected to the signal amplifier and noise filter (25 Hz) and the signal was collected at a frequency of 50 Hz.

3.2.2. Large Volume Sample Stacking in Microchip Using ESMS Detection

The chip used for ESMS detection was the same design as for LIF detection, a PCR2 chip layout. However it was fabricated in 600 μm thick, Corning 0211 glass. At the end of the main channel, a flat-bottomed hole (~200 μm i.d.) was drilled into the edge of the device and a 3 cm gold coated nano-electrospray capillary tip (50 μm i.d., pulled to 10 μm i.d. tip) was inserted, and held in place with Crystal Bond. In order to prevent analyte adsorption on the glass walls the chip channels and the capillary were covalently coated with 7-oct-1-enyltrimethoxysilane to which BCQ was then cross-linked, as described in Chapter 2. This cationic coating gives electroosmotic flow towards the

anode (anodal EOF). Small plastic pipette tubes were inserted in the center of septa and used as sample or buffer reservoirs. Then the whole assembly was put in the chip holder and secured in position. A platinum wire was attached to the gold coated capillary tip and maintained in position using a thin coating of silver conductive paint.

A 100 mM formic acid buffer was used as the separation electrolyte. Sample was dissolved in water for stacking. All aqueous solutions were filtered through 0.45 μm filters (Millipore, Bedford, MA) before use. For large volume sample stacking, the steps were almost the same as used with the LIF detector described in Figure 3-3. An in house written Labview program was used to control reservoir voltage supply and the main channel current monitoring. During the sample loading period a -2.5 kV potential was applied to the sample reservoir A, while the gold coated capillary tip was maintained at 2.8 kV. This filled the entire separation channel and the capillary tip, and corresponded to a sample volume of approximately 70 nl. After sample loading, the direction of the EOF was reversed by inverting the voltages applied across the separation channel (reservoir C ground and the capillary tip at -3 kV). For this step the capillary tip was immersed in a drop of running buffer sitting on a small piece of glass. This enabled the EOF to evacuate most of the sample buffer to waste channel C. Active removal of excess sample buffer was monitored by recording the slow increase in current (typically 50~60 s). When the current reached 99% of its maximum value, 71 μA , the polarity of the voltage was reverted once again such that the direction of the EOF was towards the gold coated capillary tip (-3 kV at reservoir B and 2.8 kV at the capillary tip). The small piece of glass with a drop of running buffer was removed manually from the capillary tip right before this separation step. To prevent sample leakage from sample waste and sample

reservoirs, a push back voltage (-2 kV) was applied to reservoir A and C during the separation period.

To compare the results from large volume sample stacking effect, we also tried normal double T injection and large volume sample stacking without polarity switching with the same PCRD-2 chip. For the double T sample injection, -2.5 kV was applied at sample reservoir A for 30 s, while reservoir C and the capillary tip were grounded. These potentials caused the injected plug to extend a short distance along the separated column. The separation was performed by applying -3 kV at reservoir B and 2.8 kV at the capillary tip, with a push back voltage of -2 kV at reservoirs A and C. For large volume sample stacking without polarity switching, sample was loaded into the separation channel by applying -2.5 kV to sample reservoir A, while the gold coated capillary tip was maintained at 2.8 kV until all peptide signals were observed in the mass spectrometer. Then running buffer was pumped through side channel D at 50 nl/min for about 1.5 min to fill the capillary tip with running buffer, leaving the channel between the double T and the Y junction filled with sample. This large plug of sample (10 nl) was then run in the separation mode, as described above, and detected by the mass spectrometer.

The mass spectrometry detection was done at the National Research Council (NRC) in Ottawa. I am grateful that Pierre Thibault and Jianjun Li let me use their two mass spectrometers, an API 3000 triple quadrupole and a prototype Qq-TOF MS (now called Q Star) (PE/Sciex, Concord, ON), and that they gave me lots of help in the whole process. The interface conditions were optimized by infusing a 1 µg/ml solution of angiotensin I from the side channel D. This peptide was also used as an internal standard to facilitate

accurate mass measurements. Tandem mass spectra of selected precursor ions were obtained using the Qq-TOF MS instrument at collision energies of 40-60 eV with Ar as the target gas. This Qq-TOF MS was set to a resolution of 10,000.

Accurate peptide masses were determined using internal standardization on the Qq-TOF MS instrument and were transferred into the PeptideSearch program. Peptide masses were searched using database downloaded from the European Bioinformatics Institute website at <ftp://ftp.ebi.ac.uk/pub/databases/peptidesearch>. All searches assumed that masses corresponded to tryptic peptides and that cysteine residues were converted to S-(carbamidomethyl)cysteine. All peptide masses were considered monoisotopic and the maximum deviation between the calculated and the measured masses was set to < 10 ppm.

3.2.3. Preparation of Protein Digests

The protein digest was prepared at NRC by John Kelly. A short description is provided here. *Haemophilus influenzae* R250 cells were grown at 37 °C on chocolate agar plate, scrapped off and lysed by mechanical shearing. A tablet containing a cocktail of protease inhibitors was added to prevent proteolysis. The solution was centrifuged at 3020 × g to remove the large particles such as intact cells. The supernatant was then centrifuged at 100000 × g for 1 h. The pellet was resuspended in PBS buffer, the proteins were precipitated by adding acetone and stored at -20 °C overnight. Approximately 250 µg of *H. influenzae* protein extract was used for isoelectric focusing for 16 h at 2500 V. Then the strip was removed and proteins were separated by SDS-PAGE and visualized by silver staining. The protein bands were excised, reduced/alkylated with iodoacetamide

and digested in-gel with trypsin. The gel pieces were first extracted with 5% acetic acid solution and then with 50% acetonitrile, 5% acetic acid solution (100 μ l each). Then the extracts were combined and evaporated to dryness. 20 μ l water was added to redissolve them for the stacking experiment right before the sample loading.

3.3. Results and Discussion

The purpose of this large volume sample stacking study was to find a way to preconcentrate samples such as tryptic peptides using microchip-CE-ESMS. Generally, proteins are separated by 1-D or 2-D gel and the bands are detected by silver staining at a level of 1-10 ng loading, corresponding to 10-500 fmoles of the original proteins. However, the practical limit of identification by microchip-CE-ESMS system was found to be slightly higher, reflecting not only the inherent losses attributed to incomplete digestion and sample transfer but also the relatively low volume of sample loading available on the microchip device (typically 0.5-2 nl). Sample preconcentration is needed for such small amounts of protein digests. Large volume sample stacking is easy to perform and could be done by switching voltages in the reservoirs to change the direction of EOF. We first evaluated large volume sample stacking using laser induced fluorescence detection. The advantage of this was we could see the sample plug, in order to get a clear idea of how the sample behaved. Based on these results, large volume sample stacking for peptide preconcentration was tested with ESMS detection.

3.3.1. Large Volume Sample Stacking on Microchip Using LIF Detection

In microchip capillary electrophoresis, it is convenient to control the direction of liquid flow in the channels using EOF by manipulating the voltage applied to the reservoirs. Large volume sample stacking can be easily achieved in a microchip system by switching the sample flow direction. The original sample buffer can be eliminated by directing it towards a waste reservoir. In the sample loading step, sample goes from sample reservoir A to the side channel D. It was observed under the microscope that in 20 s the main channel could be filled with sample. To make sure there was no sample discrimination caused by different electrophoretic mobility, a little longer sample loading time was used (> 90 s). Sample in diluted concentration buffer (10 times less) filled the channel between the double T and the Y junction, which is about 10 nl in volume and 3.8 cm in length. In all of the experiments here, EOF is used to load the sample plug. Sample could not be filled using pump or vacuum because of the network of the channels. Sample pumping drives the sample to all of the channels. Vacuum not only draws sample but also buffer to fill the main channel, which dilutes the sample and changes the sample buffer condition.

When voltage was applied to switch the flow direction from reservoir F to sample waste reservoir C, the sample plug was sandwiched between the two high concentration buffer plugs (reservoir F to Y junction and double T to reservoir C). The sample was dissolved in low concentration buffer. Because of the low conductivity of the sample plug, a larger electric field was developed in the sample plug zone compared to the buffer zones. The electrophoretic velocity of the negatively charged sample ions increased because of the higher electric field, moving faster in the direction of reservoir F. When

ions reached the junction between the sample plug and the buffer plug, their electrophoretic velocity decreased because the buffer plug had a lower electric field. The sample accumulated at the end of the sample plug. Figure 3-4 shows the sample concentration change during the stacking process. A laser spot was located at the double

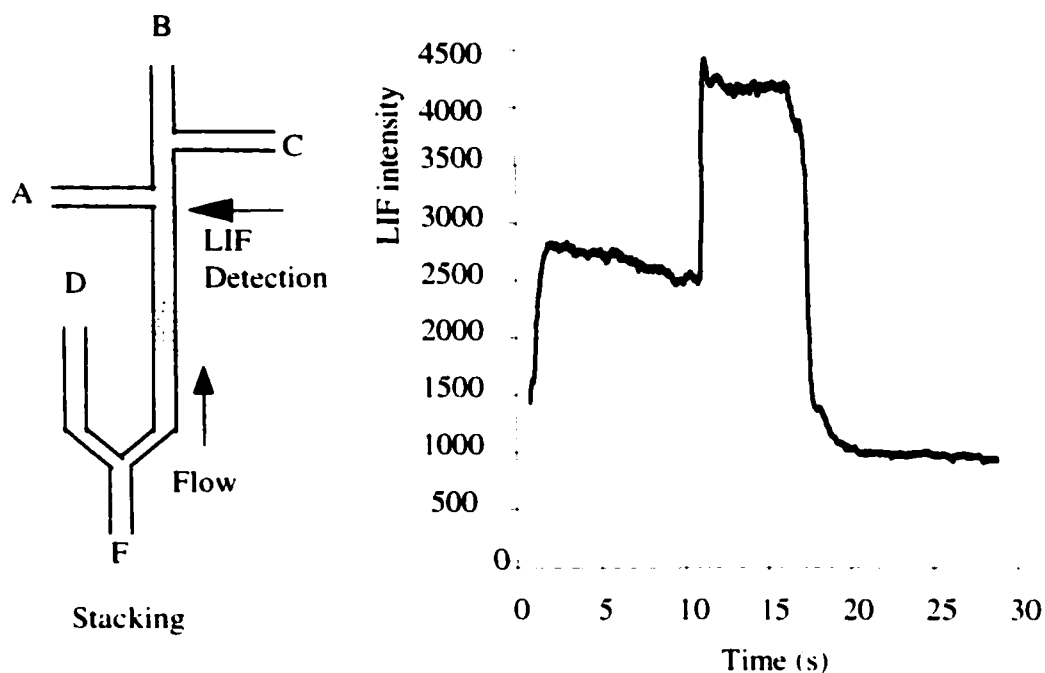


Figure 3-4. Laser induced fluorescence detection in the sample stacking step to trace the stacking profile. Sample: 0.05 μ M FITC labeled arginine in 3 mM morpholine, running buffer: 30 mM morpholine.

T and detection was started at the same time the voltages were switched for stacking. The sample plug completely passed the detector in about 18 s. During the first 12 s, the intensity was around 2700, decreasing slightly with time. Then the sample intensity rapidly increased to about 4200 and was constant for the following 6 s. The signal intensity then dropped to the level of running buffer (900). This stacking profile tells us that the sample was accumulated towards the back of the plug.

Instead of a sharply stacked peak at the sample/buffer boundary, the sample formed a broad plug. According to Chien and Burgi's explanation for large volume sample stacking with polarity switching,²⁶ one relies on the principle of field enhancement inside the sample plug, such that the analyte electrophoretic velocity in the sample buffer v_{efl} is big enough to overcome the average EOF of the solutions in the channel v_{eo} . These two velocities have different directions. When the value of v_{efl} is bigger, the analyte ions stack better. They also proposed that the maximum length of the sample plug that could be injected without loss of analytes is

$$\chi_{\text{max}} = -v_{\text{efl}} / v_{\text{eo}} \quad 3-6$$

In our experiment, the 6 s wide sample plug may suggest that the electrophoretic velocity of the analyte used is not large enough, or that the sample plug was too long.

When the end of the concentrated plug came to the double T, voltages in the reservoirs were changed for sample separation. Figure 3-5a shows the separation profile after performing the large volume sample stacking with polarity switching. Figure 3-5b presents the normal double T injection for the same sample. Because the sample was dissolved in 3 mM morpholine and the running buffer was 30 mM morpholine, Figure 5b actually is the stacked results of the 100 μm double T sample plug. Comparing these two figures, Figure 3-5a has much higher intensity (~ 4 times) and about 24 times larger peak area, confirming that large volume sample stacking significantly enriches the analyte. The migration time was also changed, which is common for large volume sample stacking results. The different amounts of sample buffer involved in these two injection procedures may result in a different net EOF in the separation channel.

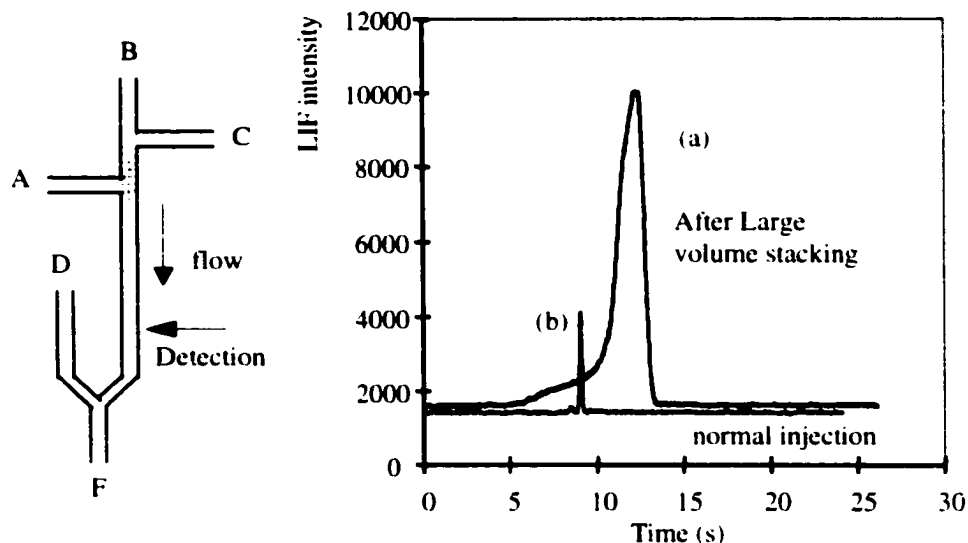


Figure 3-5. Comparison of separation profile between large volume sample stacking and normal double T injection with stacking. PMT voltage: 450 V, Sample: 0.05 μ M FITC labeled arginine in 3 mM morpholine, running buffer: 30 mM morpholine. (a) Separation profile after large volume sample stacking with polarity switching. (b) Normal separation profile with double T injection and small volume stacking. Injection: 30 s, A (-2 kV) to C (ground), B and F ground. Separation: B (5 kV) to F (ground), push back voltage at A and C (2.6 kV).

Regarding band broadening due to large volume sample stacking, there are no clear explanations in the literature. Based on the results in Figure 3-4, it is most likely that the relative velocity difference between sample ions and the buffer were not large enough to produce a sharply stacked peak. Also, at this stage in developing the procedure we used timing to judge when to switch the voltages. Possibly, the separation step was started before complete stacking was achieved. In the future, the following steps could be added to increase resolution: when the stacked sample reaches the double T one can let the stacked plug completely enter the waste channel C, then change the EOF direction and let the sample flow from C to A. As the stacked sample plug passed the double T again, the voltage would then be switched to separation mode. In this way a small plug of stacked sample could be injected. However, the timing of so many steps might prove challenging.

3.3.2. Large Volume Sample Stacking on Microchip Using Mass Spectrometry Detection

Our target was to preconcentrate peptides for ESMS, so it was decided to perform further development of the stacking procedure using a microchip-ESMS device. Optimization of the focusing conditions used in large volume sample stacking method was first conducted in selected ion monitoring (SIM) mode using an API 3000 triple quadrupole mass spectrometer. The procedure was described in section 3.2.2. of the experimental section. The conventional definition of limit of detection (LOD) is the concentration corresponding to a signal of 3σ , where σ is standard deviation of the noise. This definition usually provides an impractically low estimation in mass spectrometry. In this chapter, the LOD is defined by

$$Y / C = 3X / (\text{LOD}) \quad 3-7$$

where Y is the peak height above the average baseline, C is the concentration corresponding to peak height Y , and X is maximum peak to peak excursion observed in the baseline in a region near the peak. The value of X is approximately 5σ ³⁴ so that Equation 3-7 corresponds approximately to the value of the limit of quantitation (10σ).³⁵

A mixture of five standard peptides was analyzed using the normal double T injection and separation procedure. The concentration of the peptides is 10 ng/ml each (bradykinin at 30 ng/ml). For the peptides dissolved in 100 mM formic acid running buffer, the results are shown in the first column of Figure 3-6. In the separation shown in the second column of Figure 3-6, the peptides were dissolved in water, in which small volume sample stacking occurred due to the use of water for the sample zone and 100 mM formic acid for the running buffer. An estimated sample loading of 0.5-2 nl was injected. As indicated from the TIE and RIE profiles of the different peptide ions, 10

ng/ml was close to the practical limit of detection for most of the analytes. The small volume sample stacking procedure gave better LOD than the double T injection without stacking, as is shown by comparing the first and second columns in Figure 3-6 and Table 3-1. For example, a six times enhancement for bradykinin was achieved.

Table 3-1 Comparison of LOD with and without sample stacking

Peptides	m/z	LOD ^(a) without stacking	LOD ^(b) with double T stacking	LOD ^(c) with large volume sample stacking
Leuenkaphalin	556	8.2 nM	7.6 nM	3.9 nM
LHRH	592	17 nM	6.9 nM	0.79 nM
Somatostatin	820	24 nM	6.7 nM	0.89 nM
Angiotensin	524	19 nM	15 nM	1.6 nM
Bradykinin	531	17 nM	2.8 nM	0.34 nM

a) Double T injection, sample in 100 mM formic acid. b) Double T injection, sample in water. c) large volume sample stacking with polarity stacking, sample in water.

Improvement of sample loading and signal detectability was achieved by filling the separation channel using a prolonged electrokinetic injection, as indicated by the electropherograms presented in the third column of Figure 3-6. In this particular experiment, the injection volume was determined by the plug between the double T and the Y junction, corresponding to about 10 nl. This unusually large sample loading resulted in significant peak broadening and concurrent loss in separation efficiency. Again, sample stacking would have occurred due to the mismatch between sample buffer and running buffer.

In order to increase the amount of sample introduced to the chip while simultaneously maintaining good resolution, proper removal of the sample buffer is required prior to zone electrophoresis. Such a procedure was achieved by monitoring the electrophoretic current and by carefully controlling the direction and magnitude of the EOF during the stacking period. Proper focusing of analyte bands with concurrent

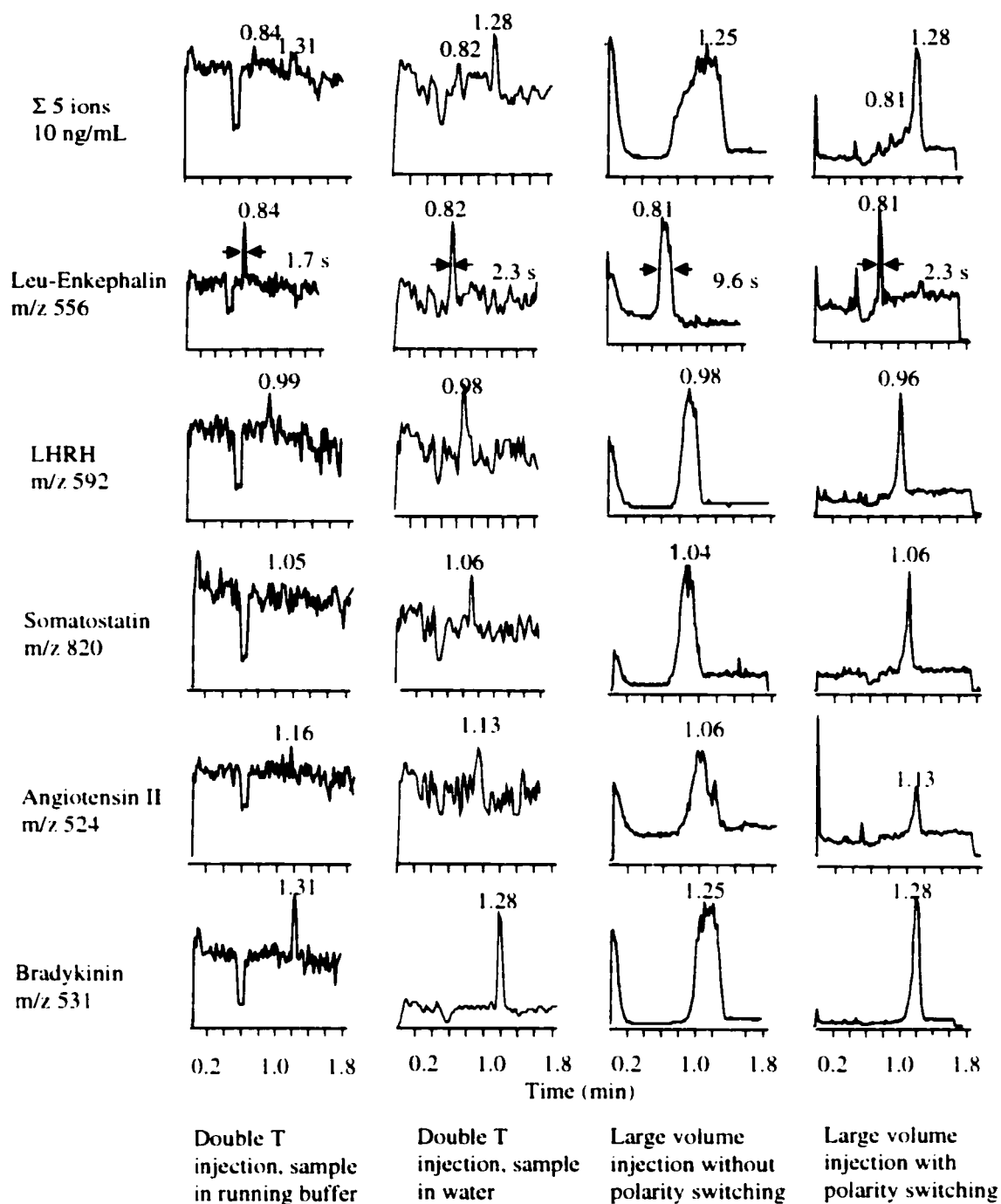


Figure 3-6. API 3000 triple quadrupole analysis of 10 ng/ml peptide standards (bradykinin: 30 ng/ml) using various injection methods on microchip. The TIE and RIE profiles for selected multiply protonated ions are presented in the first, second, third and fourth columns for experiments conducted using a normal double T injection (sample in running buffer, and then in water respectively), a 10 nl sample large volume injection without polarity switching, and a 70 nl large volume sample stacking with polarity switching respectively. Running buffer was 100 mM formic acid. Voltage application was described in the experimental section 3.2.2.

removal of sample buffer involved three distinct steps: electrokinetic sample loading, band stacking with polarity reversal, and separation of analytes under zone electrophoresis. Sample injection was performed by applying a voltage between reservoir A and the capillary tip, such that the sample filled the entire separation channel. This large sample plug, dissolved in water, was then focused into a narrow band using a running buffer of 100 mM formic acid. During the stacking period (approximately 1 min. duration) the direction of EOF was reversed (compared to sample injection and separation flow direction), and the flow was directed into reservoir C, eliminating the sample buffer. During the stacking period the current slowly increased to 71 μ A, as the low conductivity buffer was removed from the separation channel. When the current reached about 99% of its maximum value, the zone electrophoresis separation was initiated by applying a voltage between reservoir B and the capillary tip, such that the EOF was directed towards the mass spectrometer.

The application of this sample stacking procedure is illustrated in the right column in Figure 3-6, for 10 ng/ml each of peptide standards (30 ng/ml of bradykinin). In contrast to the large sample injection with no stacking (Figure 3-6, the third column), the removal of sample buffer enabled proper focusing and separation of the analyte band, resulting in narrower peak widths. For example, a 2.3 s peak width was observed for leu-enkephalin using sample stacking whereas a value of 9.6 s was obtained without stacking. The band sharpening resulting from sample stacking provided peak width comparable to those obtained with a 0.5-2 nl sample injection (1.7 s for leu-enkephalin). The improvement in sensitivity was investigated using serial dilution ranging from 0.1 to 1000 ng/ml of each peptide in SIM mode. The results are summarized in Table 3-1. The

concentration limit of detection values observed for the different peptides ranged from 0.34 to 3.9 nM, and represented a 2 to 50 fold improvement in sensitivity compared to the conventional double T injection. More significant improvements in sensitivity were noted for peptides of higher mobility such as bradykinin (50-fold). In contrast, leu-enkephalin, which migrates almost at the EOF rate, shows lower enhancement (2 times), presumably due to partial removal of the analyte band during the stacking period.

A separate study using a solid phase extraction method was done by J. Li and P. Thibault.¹⁸ A single layer of C₁₈ membrane was inserted between the PTFE tube and a transfer capillary. A hole (200 µm diameter) aligned with the separation channel was drilled in the cover plate of the chip. We prepared the chip device at the University of Alberta. The transfer capillary was inserted into the hole and held in place with Crystal Bond. The peptides were preconcentrated in the membrane and eluted to the chip channel for separation. The separation efficiencies and peptide recoveries obtainable with this preconcentration procedure are typically lower than that with sample stacking due to the relatively large plug of elution buffer used (25 nl). Li and Thibault showed that bradykinin was poorly retained on the C₁₈ membrane and an estimated concentration limit of detection (LOD) of only 19 nM was observed. Adsorptive preconcentration favored the enrichment of only hydrophobic peptides, whereas sample stacking provided significant enhancement for peptides with high electrophoretic mobilities. Stacking thus provides an efficient preconcentration method for hydrophilic peptides with high electrophoretic mobilities.

The application of sample stacking for the analysis of trace level tryptic peptides was evaluated for in-gel digestion of proteins excised from a 2-D gel separation. An

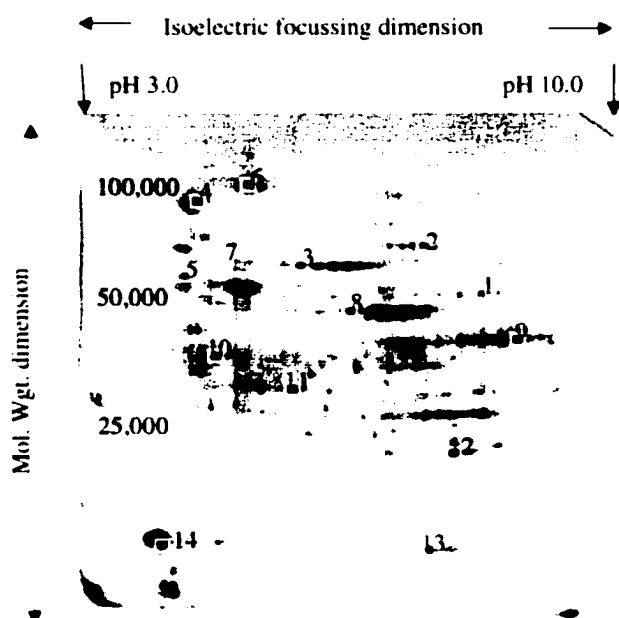


*Figure 3-7. 2-D gel electrophoresis separation of a 200 μ g membrane protein from *H. influenzae* Rd strain. Silver staining was used for band visualization. Sample was provided by John F. Kelly.*

example of this is presented in Figure 3-7 for membrane associated proteins of *H. influenzae* strain Rd. For bands estimated to be present at a level less than 500 fmoles, enhancement of sample loading was required for proper spot identification. The analysis of tryptic peptides from in gel digestion of spot #14 is shown in Figure 3-8. In this particular analysis, the peptides extracted from spot #14 were dissolved in 20 μ l

distilled water, and only 10 μ l of this solution was loaded in the sample reservoir. The electrokinetic injection proceeded until the sample started emerging from the capillary tip, and then stacking and separation was performed as described above. The TIE of the corresponding analysis (Figure 3-8a) enabled the identification of a number of components including the doubly protonated peptides at m/z 651.85 (Figure 3-8b and 3-8c) and m/z 578.81 (Figure 3-8e and 3-8f). From a single injection, the potential precursor ions were identified and selected for sequencing analysis. In a subsequent microchip CE/MS/MS experiment, the product ion spectra of the doubly protonated peptides m/z 651.85 (Figure 3-8d) and m/z 578.81 (Figure 3-8g) were obtained and enabled the identification of partial amino acid sequences. These sequence segments plus the accurate

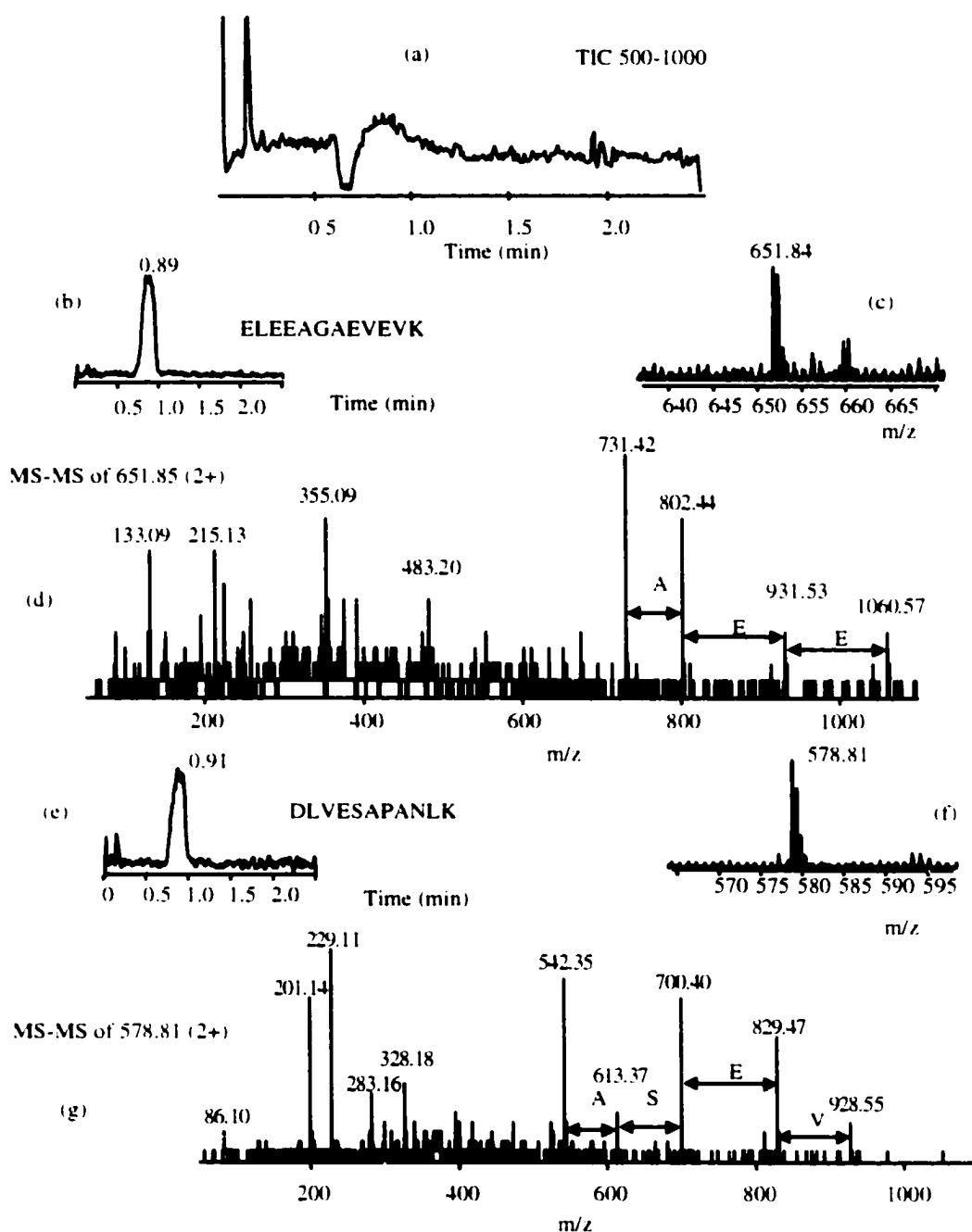


Figure 3-8. Microchip-CE/Qq-TOF-MS analysis of tryptic peptides from spot 14 of Figure 3-7 using large volume sample stacking. (a) TIC (m/z 550-1200) (b) RIE of fragment at m/z 651.84. (c) mass spectrum of fragment at m/z 651.84. (d) MS/MS product ion of m/z 651.84. (e) RIE of fragment at m/z 578.81. (f) mass spectrum of fragment at m/z 578.81. (g) MS/MS product ion of m/z 578.81. Thanks goes to Jianjun Li for his help with these experiments.

molecular masses of these two peptides were sufficient to uniquely identify this protein as 50s Ribosomal protein.

3.4. Conclusions

Sample stacking with polarity switching was performed on a microchip to preconcentrate samples. Laser induced fluorescence detection was tested with FITC labeled amino acid and mass spectrometry detection was used for peptide standards and tryptic digest. This preconcentration method was a useful way to enrich analyte ions with high electrophoretic mobilities in the direction opposite to EOF. For applications requiring higher sensitivity, such as those arising from 2-D gel electrophoresis, a sample stacking procedure enabling higher sample loading (10 nl to 70 nl) was developed. This method provided concentration detection limits of 0.3-4 nM for different peptide standards, thus providing up to a 50-fold enhancement in detection limits compared to those the conventional double T injection could achieve. This sample stacking procedure could be implemented in an automated fashion on a microchip in the future.

3.5. References

1. Jorgenson J. W.; Lukacs K. D. *Anal. Chem.* **1981**, 53, 1298-1302.
2. Harrison, D. J.; Fluri, K.; Seiler, K.; Fan, Z.; Effenhauser, C. S.; Manz, A. *Science* **1993**, 261, 895-897.
3. Fluri, K.; Fitzpatrick, G.; Chiem N.; Harrison, D. J. *Anal. Chem.* **1996**, 68, 4285-4290.
4. Jacobson, S. C.; Ramsey, J. M. *Electrophoresis* **1995**, 16, 481-486.
5. Moring, S. E.; Reel, R. T.; Van Soest, R. E. *Anal. Chem.* **1993**, 65, 3454-3459.
6. Liang, Z.; Chiem, N.; Ocvik, G.; Tang, T.; Fluri, K.; Harrison, D. J. *Anal. Chem.* **1996**, 68, 1040-1046.
7. Albin, M.; Grossman, P. D.; Moring, S. E., *Anal. Chem.* **1993**, 65 489A-497A.
8. Salimi-Moosavi, H.; Jiang, Y.; Lester, L.; McKinnon, G.; Harrison, D. J. *Electrophoresis* **2000**, 21, 1291-1299.
9. Ocvik G.; Tang T.; Harrison D.J. *Analyst* **1998**, 123, 1429-1434.
10. Martin, A.; Everaerts, F. *Proc. Roy. Soc. London A* **1970**, 316, 493-514.
11. Stegehuis, D. S.; Tjaden, U. R.; van der Greef, T. *J. Chromatogr.* **1992**, 591, 341.
12. Foret, F.; Karger, B. L. *Electrophoresis* **1993**, 14, 417-428.
13. Jandik, P.; Jones, W. R. *J. Chromatogr.* **1991**, 546, 431-443.
14. Larsson, M.; Lutz, E. S. M. *Electrophoresis* **2000**, 21, 2859-2865.
15. Naylor, S.; Benson, L.M.; Tomlinson, A. J. *J. Chromatogr. A* **1996**, 735, 415-438.
16. Tomlinson, A. J.; Benson, L. M.; Jameson, S.; Johnson, D. H.; Naylor, S. *J. Am. Soc. Mass. Specrom.* **1997**, 8, 15-24.
17. Bonneil, E.; Waldron, K. C. *J. Chromatogr. B* **1999**, 736, 273-287.
18. Li, J.; Wang, C.; Kelly, J. F.; Harrison, D. J.; Thibault, P. *Electrophoresis* **2000**, 21, 198-210.

19. Tong, W.; Link, A.; Eng, J. K.; Yate, J. R. *Anal. Chem.* **1999**, 71, 2270-2278.
20. Herring, C. J.; Qin, J. *Rapid Commun. Mass Spectrom.* **1999**, 13, 1-7.
21. Oleschuk, R. D.; Shultz-Lockyear, L. L.; Ning, Y. B.; Harrision, D. J. *Anal. Chem.* **2000**, 72, 585-590.
22. Mikker, F. E. P.; Everaerts, F. M.; Verkeggen, E. M. *J. Chromatogr.* **1979**, 169, 1-10.
23. Burgi, D. S.; Chien, R. L. *J. Microcol. Sep.* **1991**, 3, 199-202.
24. Chien, R. L.; Helmer, J. C. *Anal. Chem.* **1991**, 63, 1353-1361.
25. Burgi, D. S.; Chien, R. L. *Anal. Chem.* **1991**, 63, 2042-2047.
26. Chien, R. L.; Helmer, J. C. *Anal. Chem.* **1992**, 64, 489A-496A.
27. Chien, R. L.; Helmer, J. C. *Anal. Chem.* **1992**, 64, 1046-1050.
28. Smyth, W. F.; Harland, G. B.; McClean, S.; McGrath, G.; Oxspring, D. *J. Chromatogr. A* **1997**, 772, 161-169.
29. McGrath, G.; Smyth, W. F. *J. Chromatogr. B* **1996**, 681, 125-131.
30. Alberta, M.; Debusschere, L.; Demesmay, C.; Rocca, J. L. *J. Chromatogr. A* **1997**, 757, 281-289.
31. Harland, G. B.; McGrath, G.; McClean, S.; Smyth, W. F. *Anal. Commun.* **1997**, 34, 9-11.
32. He, Y.; Lee, H. K. *Anal. Chem.* **1999**, 71, 995-1001.
33. Lichtenberg, J.; Verpoorte, E.; deRooij, N. F. *Electrophoresis* **2001**, 22, 258-271.
34. Ingle, J. D.; Crouch, S.R. Page 136, *Spectrochemical Analysis*, 1988, Prentice-Hall Inc., Printed in USA.
35. Skoog, D.A.; Leary, J.J. Page 8, *Principles of Instrumental Analysis* 1992, Saunders College Publishing, printed in USA.

Chapter 4

Integration of Immobilized Trypsin Bead Beds for Protein Digestion Within a Microfluidic Chip Incorporating Capillary Electrophoresis Separations and an Electrospray Mass Spectrometry Interface*

Table of content	Page
4.1. Introduction.....	92
4.2. Experimental.....	94
4.2.1. Chemicals and materials.....	94
4.2.2. Microchip device.....	95
4.2.3. Off-chip digestion in microcentrifuge tube.....	97
4.2.4. Digestion with immobilized trypsin within the chip reservoir.....	98
4.2.5. Integrated packed bed for on-chip digestion with immobilized trypsin.....	98
4.2.6. Microchip-CE/nanoESMS.....	100
4.3. Results and discussion.....	101
4.3.1. Digestion with immobilized trypsin within the chip reservoir.....	101
4.3.2. Integrated packed bed for on-chip digestion with immobilized trypsin.....	104
4.3.3. Sample carry over evaluation.....	113
4.4. Conclusions.....	116
4.5. References.....	117

* A portion of this chapter has been published in *Rapid Commun. Mass Spectrom.* **2000**, *14*, 1377-1383. by Wang, C.; Oleschuk, R.; Ouchen, F.; Li, J.; Thibault, P.; Harrison, D. J.

4.1. Introduction

Microfluidic systems may present a powerful new means to automate protein sample preparation for electrospray ionization mass spectroscopy (ESMS). Since the introduction of microchip electrospray devices in 1997 the development of these devices has grown explosively.¹⁻¹⁶ Several groups have proposed that protein sample preparation could benefit significantly from the miniaturization and automation capabilities that microfluidics may provide.^{1,3,6,9,12,14-16} The increasing demand for sophisticated and rapid protein analysis, driven by the emerging field of proteomics,¹⁷⁻²⁰ means such improvements are greatly needed. However, there is a need for further development of on-chip, protein processing elements before highly integrated sample processing systems become a reality. We present here the first report of a microfluidic-ESMS interfaced device in which integrated tryptic digestion, separation and electrospray of proteins is performed. These results move such devices a step closer to automated sample processing.

Protein digestion is a key element of protein identification by ESMS.^{21,22} The rate of digestion can be limited by the enzyme or substrate concentration,²³ so that enhanced digestion rates may be obtained by confining the reactions to smaller volumes at elevated concentrations. The nl- μ l volumes within microfluidic devices²⁴⁻²⁶ offer a means to work with small volume samples in confined reaction zones, in order to enhance digestion rates. Xue et al³ reported that protein could be digested in the well of a microchip in a homogeneous solution of trypsin. The sample was then infused into the MS by syringe pump, through a flow channel in the device. The kinetics of the digestion process was readily followed, but this relatively simple system represents only the first step in creating protein processing devices. A separation step was not demonstrated, yet with complex

proteins, or protein mixtures, subsequent separation of the digest before ESMS allows for much easier analysis and protein identification.^{5,9,10} Additionally, homogeneous digestion creates a number of trypsin autolysis products that may interfere with the ESMS analysis, particularly when high concentrations of trypsin are used to enhance the speed of digestion. The use of trypsin immobilized on a solid support may be preferable.^{23,27-29} Immobilized trypsin can offer less trypsin autolysis products, potentially higher enzyme stability, much faster digestion because the amount of trypsin used can be higher without leading to autodigestion, and a better route to automation with continuous flow through the use of a packed reactor bed. The integration of an immobilized trypsin digestion bed with subsequent separation and ESMS is thus an important step forward for chip-based sample processing.

In this chapter we describe the use of trypsin-loaded beads, either packed within the sample inlet reservoir or in an integrated packed bed (about 2.5 μ l volume) in a microfluidic chip, for the on-board digestion of peptides and proteins. Integrated within the same device was a double-T injector,³⁰ a capillary electrophoresis (CE) separation channel^{24,25} and an ESMS interface.^{12,13} The speed and extent of digestion was compared when using bead digestion off-chip in a microcentrifuge tube versus on-chip in the reservoir, or on-chip in a packed bed with a syringe pump to deliver the sample. Practical use of these devices requires that they are readily cleaned to prevent sample carryover, and the procedures required to allow repetitive use were determined. By avoiding external sample handling steps during digestion and afterwards, sample losses, contamination and undesired oxidation were avoided.

4.2. Experimental

4.2.1. Chemicals and Materials

Cytochrome c, bovine serum albumin (BSA), N, N, N', N',-tetramethylethylenediamine (TEMED), ammonium bicarbonate and the polypeptide, melittin, were obtained from Sigma Chemical Co. (St. Louis, MO, USA). Formic acid and HPLC grade methanol were from Aldrich Chem. Co. Inc. (Milwaukee, WI, USA). [(Acryloylamino)propyl]trimethylammonium chloride (BCQ) was obtained from Chemische Fabrik Stockhausen (Krefeld, Germany), 7-oct-1-enyltrimethoxysilane was from United Chem. Tech. Inc. (Bristol, PA, USA). TPCK treated trypsin, immobilized on 40-60 μm diameter, 4% crosslinked, agarose beads, 200-250 units per ml of bead volume, were from Pierce (Rockford, IL, USA). About 2 ml of beads were suspended in a total slurry volume of 4 ml (aqueous slurry containing 50% glycerol, 0.05% sodium azide). Fused silica capillary (50 μm i.d. and 185 μm o.d.) was from Polymicro Technologies (Phoenix, AZ, USA) and Teflon tubing (180 μm i.d. and 1.4 mm o.d.) was from LC Packing (San Francisco, CA, USA).

Proteins were dissolved in digestion buffer, 20 mM ammonium bicarbonate, pH 8.1, before use. A running buffer of 10 mM ammonium bicarbonate, 100 mM formic acid was used. Solutions were prepared with Ultrapure water (Millipore Canada, Mississauga, ON) and filtered through 0.2 μm Nylon syringe filters (Chromatographic Specialties Inc. Brockville, Canada). Diluted bead suspensions (gel) were prepared by agitating the initial suspension, withdrawing 20 μL , then washing the gel 3 times with bicarbonate digestion buffer using centrifugation to remove the supernatant. The gel was then suspended in 100

μl of digestion buffer to create suspension 1. Suspension 2 was prepared using 30 μl of the initial suspension, followed by washing and diluting in 20 μl of digestion buffer.

4.2.2. *Microchip Devices*

The microfluidic devices for on-chip reservoir digestion shown in Figure 4-1 were fabricated in 600 μm thick, Corning 0211 glass (Corning Glass Works, NY, USA) using standard photolithography and wet chemical etching techniques, as described before.^{31,32} On-chip reservoir digestion was performed in this device. The fluid channel layout is illustrated in Figure 4-1, where the access reservoirs are identified for reference below. Channels were etched on one glass plate to a 10 μm depth and 30 μm width for the majority of the length, with 250 μm wide segments near the reservoirs. Channel lengths were essentially the same as PCRD-2, described in Figure 2-5b;³² the injector to capillary distance was 45 mm, the double T injector had a 100 μm offset, and the additional channel attached to reservoir D was 24 mm long from the junction. Figure 4-2 shows the device used for integrated packed bed digestion. The bottom etched substrate is similar to that in Figure 4-1, except that a large volume channel, 800 μm wide, 150 μm deep and 15 mm long was etched into the cover plate. Access holes were drilled into the cover plate, and it was bonded to the other plate at 592° for 6 h, after rigorous high pressure rinsing and cleaning of the two plates.³² For both of the devices, at the end of the main channel, a flat-bottomed hole (~200 μm i.d.) was drilled into the edge of the device and a gold coated nano-electrospray capillary tip was inserted, and held in place with Crystal Bond (Aremco Products, Valley Cottage, NY).⁸ The exit end of the 3 cm long nanoelectrospray emitter tip (185 μm o.d., 50 μm i.d.) was tapered to 10 μm i.d. using a capillary puller

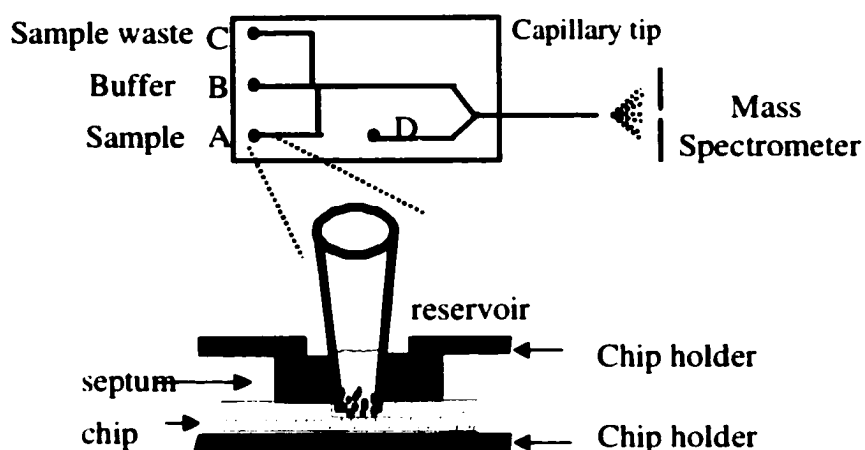


Figure 4-1. Schematic representation of the on chip reservoir digestion device. The top shows the chip layout and the bottom shows how the reservoir is fixed in the position and digestion is performed inside.

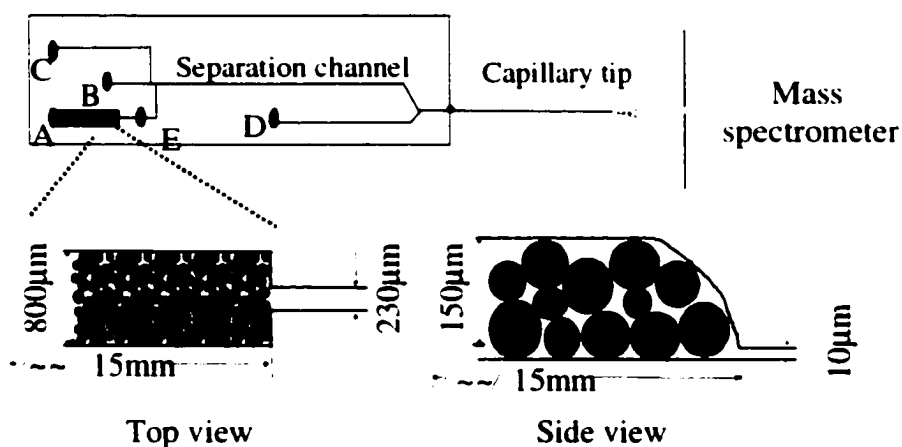


Figure 4-2. Schematic representation of the integrated enzyme reaction bed and capillary electrophoresis chip. Top and side views show a blow up of the packed trypsin bead bed. The other channels on the chip are 230 μm wide and 10 μm deep near each fluid reservoir, then narrow to 30 μm wide and 10 μm deep for the majority of their length.

(Sutter Instruments, Phoenix, AZ).⁹ In order to prevent analyte adsorption on the glass walls the chip channels and the capillary were covalently coated with 7-oct-1-enyltrimethoxysilane to which BCQ was then cross-linked, as described previously.¹² This polycationic coating gives electroosmotic flow towards the anode (anodal EOF).

The chips were mounted in a Plexiglass holder. Small pipet tips, serving as solution reservoirs, were inserted through the center of septum mounted over the access holes in the chip for all reservoirs except A in Figure 4-2. The top plate of the holder was then compressed onto the septa in order to tightly seal the septa and pipet tips into the access reservoirs. For reservoir A in Figure 4-2, Teflon tubing (~180 μm i.d.) was inserted into the center of a septum over the access hole and used to seal a capillary transfer line. This capillary was coupled to a syringe pump via a low dead volume Valco Connector (SPE, Concord, ON, Canada), which was used to deliver buffer or protein solution from a syringe pump (Harvard Apparatus, Quebec, Canada) into the digestion bed. The dead volume of the coupling and transfer line was about 600-800 nl. As a result, the syringe in the pump could be filled with just 1 μl more than was needed for the digestion volume. Syringe and transfer line could be exchanged in less than 30 s.

4.2.3. *Melittin Off-Chip Digestion*

An off chip digestion was performed to allow a comparison with the results of the on-chip digestion. Melittin was digested off-chip in a microcentrifuge tube by mixing 1.8 μl (20 μl of suspension 1) of beads with 10 μg of melittin in 80 μl of bicarbonate buffer. The solution was vortexed at room temperature for fixed periods of time during digestion, then 15 μl of digest supernatant was removed and mixed with 15 μl of 200 mM formic acid.

Samples were then loaded in reservoir A in Figure 4-1 and delivered by electrokinetic infusion or electrophoretic separation for ESMS, as described below.

4.2.4. Digestion With Immobilized Trypsin Within the Chip Reservoir

On-chip reservoir digestion was performed in the device shown in Figure 4-1. To empty reservoir A was added 1.3 μ l of beads (3 μ l of suspension 2) and 0.3 μ g of melittin in 3 μ l of digestion buffer. Alternately, up to 3 μ l of initial bead solution was mixed with 3 μ l of 32 μ M cytochrome c. A thin gel-loading pipet tip was used to stir the mixture occasionally. The beads stayed in the reservoir without entering the channels due to their large diameter of 40-60 μ m. After several minutes, 6 μ l of 200 mM formic acid was added to the reservoir to stop the digestion. Sample injection was then performed by applying -2.5 kV at reservoir A with C grounded. Because of leakage effects at the intersection causing sample entry into the separation channel,^{9,31,33} the volume of sample injected varied with the injection time. The separation buffer was 100 mM formic acid, 10 mM ammonium bicarbonate, pH 2.5, to match the diluted mixture in reservoir A. Reservoirs B, C and D were filled with separation buffer. During separation, -2.5 kV was applied at reservoir at B and ~3 kV at the nano-electrospray tip. Push back voltages of -1.4 kV were applied at reservoirs C and A to prevent sample leakage during separation.⁹

4.2.5. Integrated Packed Bed for On-chip Digestion With Immobilized Trypsin

Trypsin-loaded beads were packed in the fat channel between reservoirs A and E, as indicated in Figure 4-2. About 20 μ l of the commercial bead suspension was washed with digestion buffer as before, then 100 μ l of digestion buffer was used to resuspend them.

Before placing the chip in the holder the bead suspension was loaded into reservoir A and vacuum was applied at reservoir E to pack the bed using the diluted suspension. The packing process proceeded smoothly, usually taking 5-10 minutes, requiring about 2.5 μl of beads to fill the 15 mm long, large channel and part of the reservoir A.

A syringe pump was used to deliver all solutions through the bed. Before any digestion, the bed was washed with 5 μl digestion buffer. Protein solution in 20 mM ammonium bicarbonate was pumped through the capillary transfer line into the packed bed and then into reservoir E. Reservoir E was initially empty and open to atmospheric pressure, so that the digest accumulated in reservoir E and was not transferred into the separation channels during digestion. First 2 μl of protein solution was delivered at 10 $\mu\text{l}/\text{min}$ to displace buffer from the bed. Then reservoir E was emptied by pipet and a specified volume of digested protein solution was pumped from A to E. Then an equal volume of 200 mM formic acid was added to reservoir E and mixed with the digest using the end of a pipet tip. For electroinfusion experiments the sample was introduced to the mass spectrometer by applying -2 kV to reservoir E and about 3 kV to the electrospray tip. This step also served to rinse the sample and separation channel; rinsing was judged to be complete when the total ion current of the MS stabilized. Buffer was then run from reservoir B for 2 min to flush the separation channel, with -2.5 kV on reservoir B and 3 kV on the electrospray tip. A sample electrokinetic injection was conducted for 25 s by applying -2.5 kV at reservoir E while sample waste, reservoir C, was grounded. During separation -2.5 kV was applied to reservoir B and -3 kV to the nano-electrospray tip. A push back voltage of -1.1 kV was applied at reservoirs C and E to prevent sample leakage. The digestion bed was then flushed with digestion buffer for 4 min at 25 $\mu\text{l}/\text{min}$.

and the rinse buffer was removed from reservoir E. The cycle above was then re-initiated for the next sample.

At the end of each day the bead bed was unloaded by applying vacuum at reservoir A with reservoir E filled with water. Pressure was applied to reservoir E to dislodge persistent beads if necessary. After bead removal the fat channel was flushed with water for 5 min., then the remaining channels were flushed with water for 10 min. A single chip could be used for many weeks. Individual electrospray tips could be used for ~ 36 h of continuous use before exchanging them for a fresh tip.

4.2.6. Microchip-CE-nanoESMS

A PE/Sciex API 150 EX quadrupole mass spectrometer (Perkin-Elmer/Sciex, Concord, ON, Canada) was used for these studies. The position of the electrospray tip was optimized for ion current magnitude and stability using a 3D translation stage while electrokinetically infusing 5 µg/ml of leu-enkephalin from reservoir D, with -1 kV on D and about 3 kV on the tip. Optimal potentials on the tip varied from 2.8 to 3.2 kV. Reservoir D was then rinsed and filled with separation buffer. Electroosmotic infusion of sample was performed with -2 kV applied at sample reservoir E and the nanoelectrospray tip between 2.8–3.2 kV. The separations were performed as stated above. Unlike previous reports^{12,13} no internal standard was introduced from the side channel attached to D. The mass spectrometer was scanned over the range m/z 550-1000 at 0.5 amu per step with dwell time of 1 ms. Peptide masses were compared to the results from a database search of the MS-Digest at <http://prospector.ucsf.edu>. A tolerance of ± 0.5 Da/z was set on peptide molecular mass and all values agreed within ± 0.5 . Search parameters were

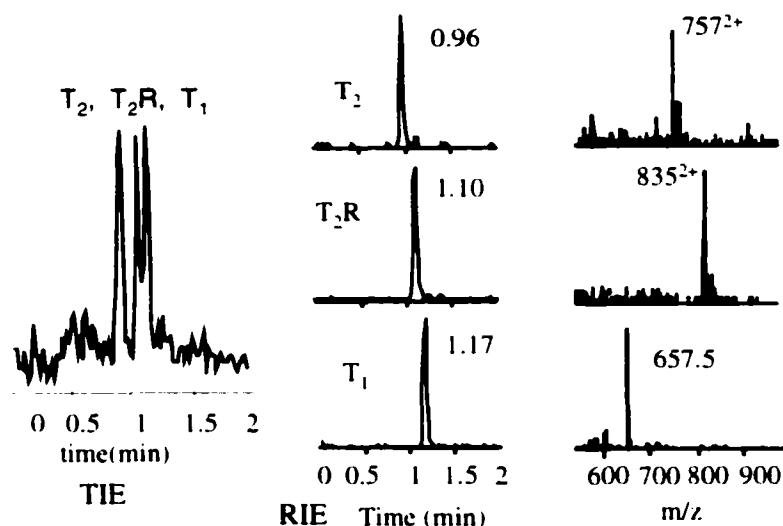


Figure 4-3. Total ion electropherogram (TIE) for 50 $\mu\text{g/ml}$ melittin digested with beads loaded into reservoir A (see Figure 4-1) for a 3 min "in-reservoir" digestion, to which an equal volume of 200 mM formic acid was added before separation and ESMS. Also shown are the reconstructed ion electropherograms (RIE) and the corresponding mass spectra for the three main melittin digestion products identified in Table 4-1.

sedimentation on the distribution of the beads. Three components were observed, the T₁ and T₂ peptide products of digestion and a T₂R intermediate digestion component, as identified in Table 4-1. After 3 min of digestion, no intact melittin was observed. The extracted mass electropherograms and the mass spectra of the three components show good signal to noise ratio and clearly identify the peptide fragments. The ratio of T₁, T₂ and T₂R peaks in the total ion electropherogram (TIE) was equivalent to that obtained after 10 min of off-chip digestion, as discussed below. Importantly, no peaks were seen for the autolysis products of trypsin.

Studies of melittin digestion as a function of time were performed with off-chip digestion in "vortexed" microcentrifuge tubes (shown in Figure 4-4). Subsequent separation and ESMS of off-chip digests using 0.18 μl beads/ μg of melittin in 100 μl (0.036 units/ μg melittin) showed complete consumption of melittin within about 7 min.

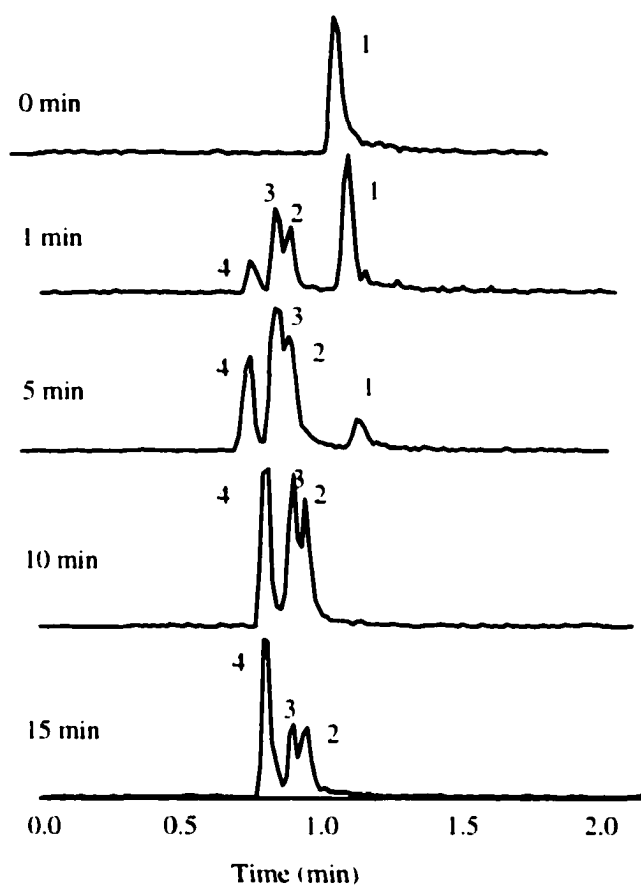


Figure 4-4. Separation profile of off-line melittin digest at different digestion times. Melittin was digested off-chip in a microcentrifuge tube by mixing 1.8 μl (20 μl of suspension 1) of beads with 10 μg of melittin in 80 μl of bicarbonate buffer. The solution was vortexed at room temperature for fixed periods of time during digestion, then 15 μl of digest supernatant was removed and mixed with 15 μl of 200 mM formic acid. 1. Melittin (712.5^{4+}) 2. T_1 (657.5) 3. T_2R (835^{2+}) 4. T_2 (757^{2+}).

while steady state for the T_1 component occurred in 7-10 min. The T_2 fragment was dominant over the T_2R precursor after 15 min. Reducing the volume of beads used by a factor of 2 increased the time of disappearance of melittin to about 12 min., indicating the kinetics were enzyme limited. The 3 min required to consume melittin within the trypsin-bead filled reservoir, demonstrates it is possible to obtain high trypsin to protein ratios in the reservoirs in order to speed up the reaction. A similar "in-reservoir" digestion was attempted with cytochrome c. Frequent stirring of the bead bed did not result in rapid digestion of this protein, nor did increasing the volume of beads used by 10-20 times. After 5 min of digestion, over 50% of the protein remained undigested, so this method was not pursued further. We concluded that the mass transport rate of protein in the reservoir was insufficient for rapid digestion of the more complex protein compared to melittin, even with stirring of the bed.

4.3.2. Integrated Packed Bed for On-chip Digestion with Immobilized Trypsin

Formation of a large diameter channel in the cover plate of the device before bonding afforded a bed into which the 40-60 μm diam. trypsin coated beads could be packed. The bed was readily packed by loading 2.5 μl of beads in a dilute suspension into reservoir A and then applying a vacuum at reservoir E. Preliminary tests were again performed with 20 $\mu\text{g/ml}$ melittin. Pumping melittin through the integrated digestion bed into reservoir E resulted in extremely rapid digestion of the peptide. Delivery of 5 μl of digest at 60 $\mu\text{l/min}$ required only 5 s and produced the same product distribution as seen after 15 min of off-chip digestion, as shown in Figure 4-5b and 4-5c. We can see that at 5 min. off chip digestion, there were still a significant amount of melittin present, indicated by the peak

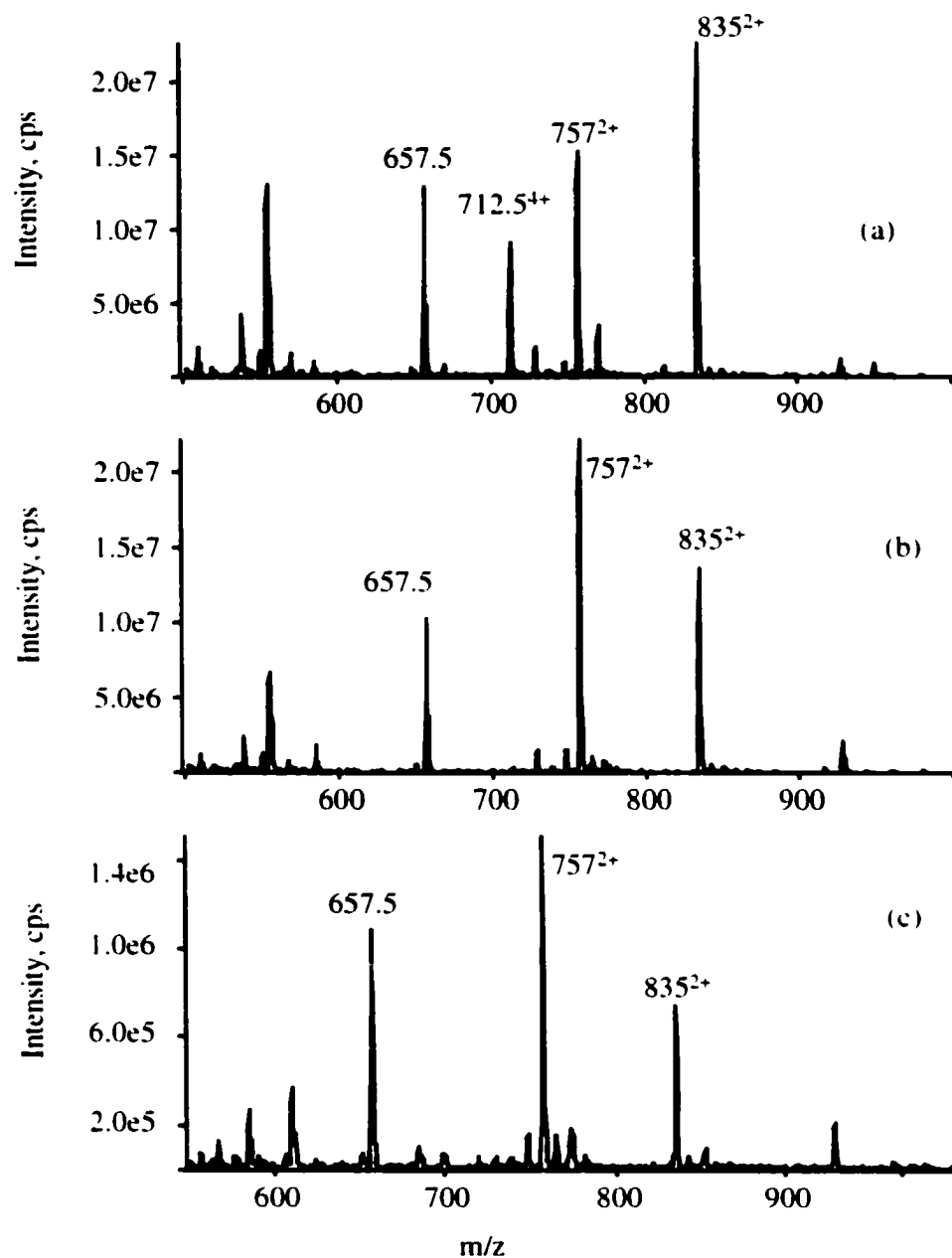


Figure 4-5. Comparison of electroinfusion melittin digestion profile with off-line digestion and in-chip packed bed digestion. Off-chip digestion of 100 $\mu\text{g/ml}$ melittin using immobilized trypsin beads is shown for (a) 5 min and (b) 15 min. These two mass spectrum are the sum of 30 scans. Digestion of 20 $\mu\text{g/ml}$ melittin in an on-chip packed bed is shown in (c) for a flowrate of 60 $\mu\text{l/min}$ as a sum of 50 scans. 1. Melittin (712.5^{4+}) 2. T_1 (657.5) 3. T_2R (835^{2+}) 4. T_2 (757^{2+}).

at m/z 712.5 shown in Figure 4-5a. The dramatically improved digestion speed presumably results from the higher bead to peptide ratio (25 μl beads/ μg melittin, or 5 units/ μg melittin) and from the efficient mass transport that is achieved within the pumped reactor bed.²³

Figure 4-6 illustrates the total ion electropherogram for digestion of 16 μM cytochrome c as a function of flow rate in the reactor bed. A constant 3 μl of solution

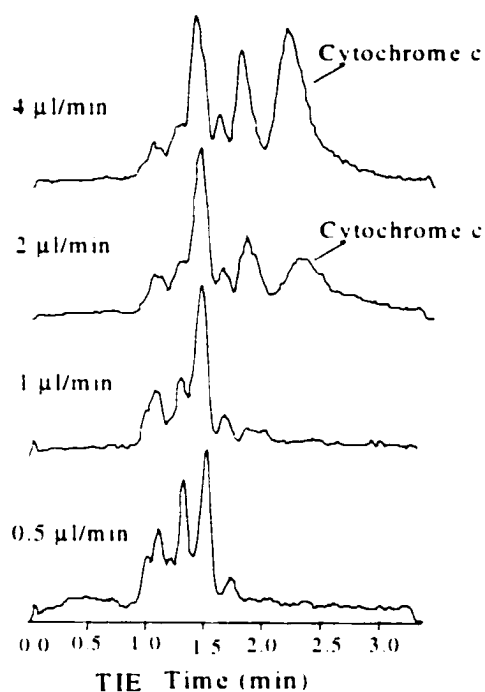


Figure 4-6. Total ion electropherogram for digestion of 16 μM cytochrome c within the packed bead bed, using four different flow rates to pump protein across the trypsin bed from reservoir A to E. Three μL was delivered in each run, to which 3 μL of 200 mM formic acid was then added before separation and ESMS.

was delivered at each flow rate, so the digestion time increased with the inverse of pump rate, requiring 6 min for the slowest pump rate. Separation of the digest was completed within 3 min, and reasonable resolution of the components was seen. While intact cytochrome c represented a significant fraction of the protein present at fast flow rates, the native protein was fully consumed at flow rates of 1 and 0.5 $\mu\text{l}/\text{min}$, or 3 and 6 min of digestion, respectively. For a 3 min. digestion and separation, the detection limit for cytochrome c in the initial

digestion buffer was in the range of 2 μM . Figure 4-7 shows the extracted ion electropherogram of 12 peptide fragments from the last total ion electropherogram in Figure 4-6. All of the peaks were clearly identified with high signal to noise ratio. Figure

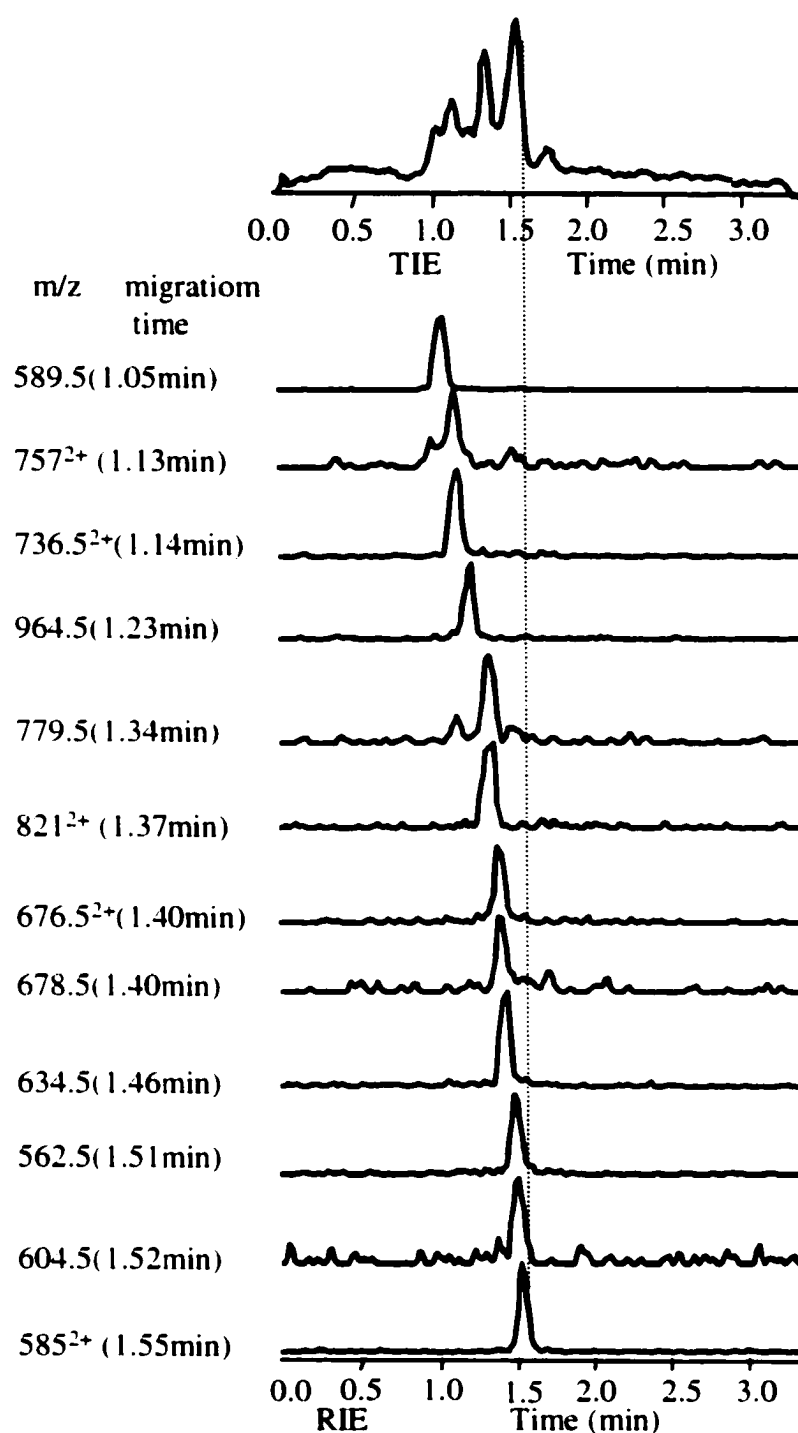


Figure 4-7. Total ion electropherogram (TIE) and reconstructed ion electropherogram (RIE) for digestion of 16 μM cytochrome *c* within the immobilized trypsin bed. Protein was pumped across the trypsin bed at 0.5 $\mu\text{l}/\text{min}$ from reservoir A to E. 3 μl was delivered in each run, to which 3 μl of 200 mM formic acid was then added before separation and ESMS. The dot line was added to guide the eye and show the position of the peaks.

4-8 shows the mass spectrum for a 45 s infusion of 1 μM cytochrome c digested at 1 $\mu\text{l}/\text{min}$, which means the whole digestion took 3 min. Summing 50 mass scans gave a digested cytochrome c detection limit below 1 μM . Peptide fragments, listed in Table 4-1, were assigned on the basis of the Protein Prospector, MS Digest database. The sequence coverage for this digestion was about 96%. In the range of 550-1000 m/z , no more than two missed cleavages were present in any of the observed fragments. At no time were any autolysis products of trypsin observed. However, several peaks arising from the buffer were observed, as indicated in Figure 4-8.

About 1 μl of additional solution was required due to the dead volume of the capillary transfer line and 2 μl (a conservatively high value) was used to remove buffer from the bed, so that the total volume of protein solution used was 6 μl . With an estimated detection limit of 2 μM for separations of the cytochrome c digest, this

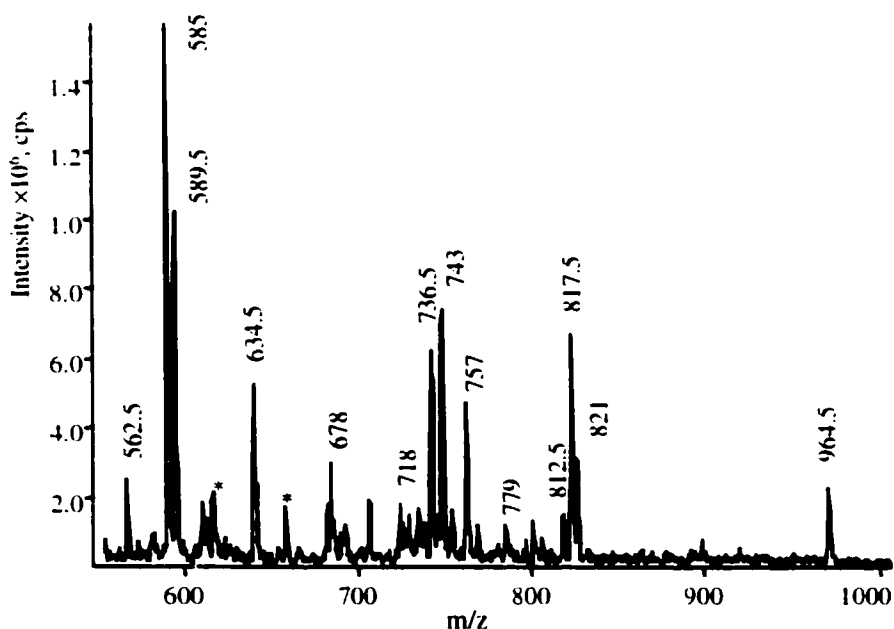


Figure 4-8. Electrokinetically driven infusion of 1 μM cytochrome c for 45 s, following 3 min digestion of 3 μl of protein solution on the packed trypsin bed. The trace shows the sum of 50 scans over 45 s. Masses are identified in Table 4-1. Several buffer peaks are indicated with a star.

corresponds to 12 picomoles of protein required. Given a migration time of 90 s and a 70 nl volume in the separation channel and capillary, a 45 s infusion would utilize just 35 nl of sample (35 fmoles at 1 μ M) in the MS. A previous estimate of the double T injection volume of about 2 nl¹³ means about 4 fmoles at 2 μ M are introduced into the MS when a separation is performed.

We compared digestion speed on-chip with that done off-chip using various conditions. Cytochrome c digestion was done using the traditional aqueous solution phase procedure, and with 20% methanol. To 300 μ l 10 μ g/ml cytochrome c in 20 mM ammonium bicarbonate trypsin was added at room temperature with a 1:1 ratio (weight). At certain intervals, 20 μ l of digest was removed and mixed with 20 μ l of 200 mM formic acid and 40 μ l methanol for conventional ionspray, using the interface that came with the API 150 EX Sciex mass spectrometer. Figure 4-9 shows that even with a cytochrome c/trypsin weight ratio of 1:1 there was still a relatively large amount of protein left after 3 and 25 minutes of digestion. Evaluating the cytochrome c peak at m/z 884 in Figure 4-9c shows the undigested protein accounted for 55.7% of original Figure 5-9a amount after 25 min. of digestion. It was reported³⁵ that methanol was mixed with the digestion buffer for rapid protein digestion, so we added 20% methanol to the 20 mM ammonium bicarbonate buffer and performed the same procedure as above. The results show that more cytochrome c was digested, but about 23 % of original cytochrome c remained undigested after 25 min. Thus, on-chip digestion is more rapid than the conventional procedure.

Bovine serum albumin is a higher molecular weight protein containing several disulfide bonds, and frequently it is glycosylated,²⁸ making it a more difficult target for

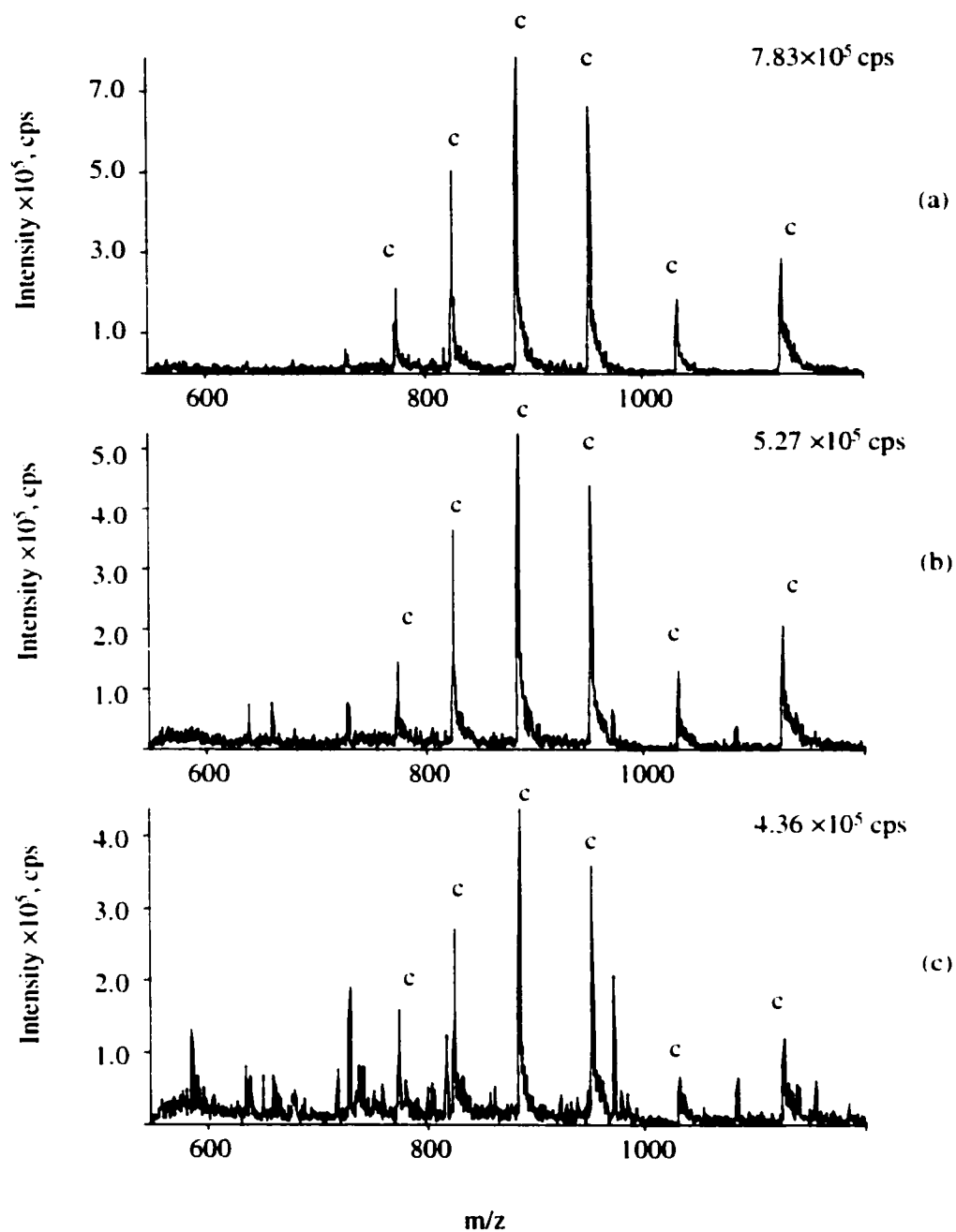


Figure 4-9. Cytochrome *c* 10 $\mu\text{g/ml}$ in solution digestion at room temperature. Protein/Trypsin mass ratio was 1:1, digestion buffer was 20 mM ammonium bicarbonate. The digest was stopped by adding 200 mM formic acid and ionsprayed with 50% methanol. (a) undigested (b) 3 min. digestion (c) 25 min digestion. All mass spectrum are sum of 30 scans. All of the undigested cytochrome *c* peaks are labeled by *c*.

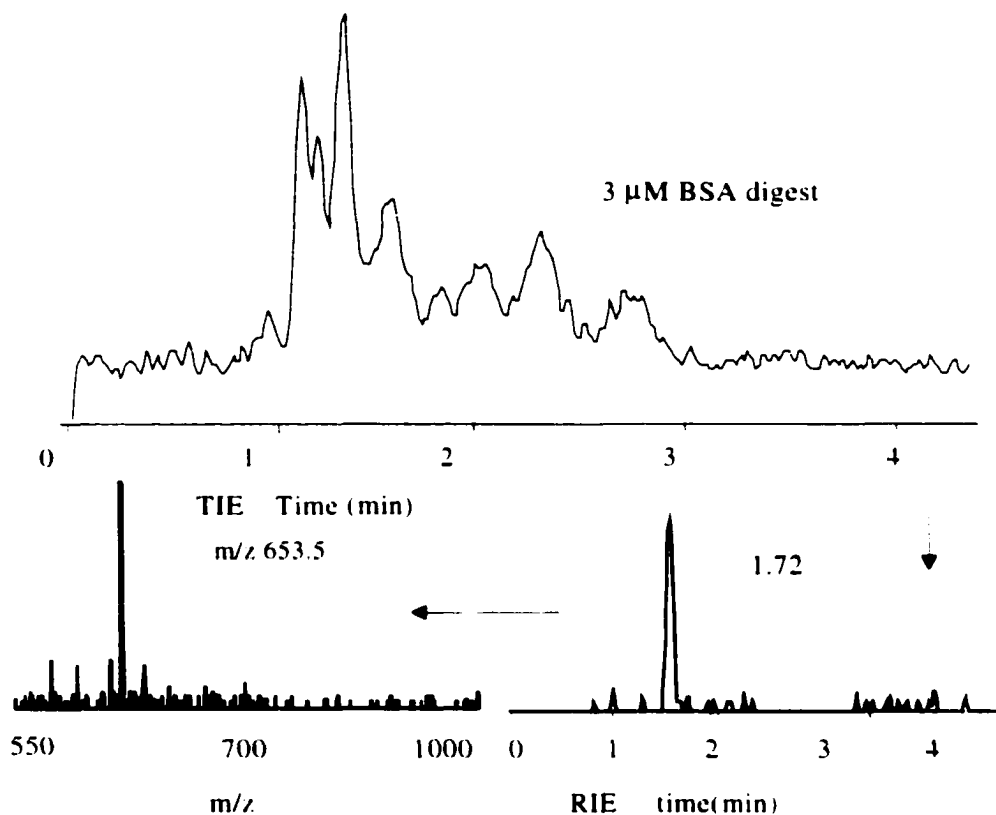


Figure 4-10. Total ion electropherogram for 6 μ M bovine serum albumin (BSA) mixed with dithiothreitol, digested on-chip in the trypsin bed for 3 min at 0.5 μ l/min. The product was diluted 2-fold with formic acid prior to separation and ESMS. Also shown is a single, representative extracted ion electropherogram and the corresponding mass spectrum.

on-chip digestion. By using a premixed solution of 6 μ M BSA and dithiothreitol (DTT) the disulfide linkages were cleaved immediately prior to digestion. This solution was then pumped through the digestion bed. At a flow rate of 0.5 μ l/min for 6 min no undigested BSA was observed in the total ion electropherogram. Figure 4-10 shows the TIE for the digestion of BSA, along with the reconstructed ion electropherogram (RIE) for m/z 653.5 and its corresponding mass spectrum. A mass spectrum obtained using sample infusion, without separation, is shown in Figure 4-11, for which 43 masses were identified with the known peptide fragments of BSA. Table 4-2 lists the observed masses and indicates the

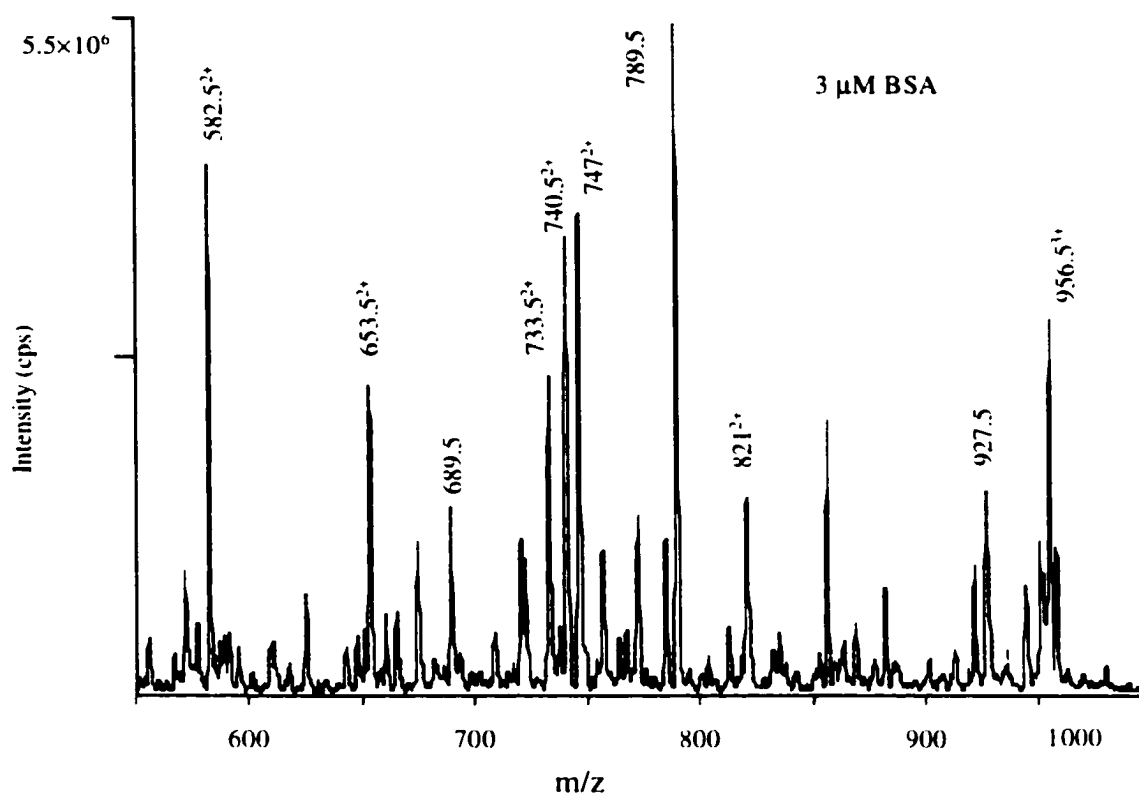


Figure 4-11. Electrokinetically driven infusion of 3 μM BSA after 3 min digestion at 0.5 μl/min on the packed trypsin bed and addition of 3 μl of 200 mM formic acid. The trace shows the sum of 50 scans over 45 s. Peaks were identified using the Protein Prospector MS database and are listed in Table 4-2. Only a few are indicated here, for improved clarity.

numbers of cleavages missed in each partially digested fragment. The sequence coverage in the scanning range of m/z 550-1000 was 71%, comparable to 70-80% reported²⁸ when subsequent iodoacetamide is used to alkylate cysteine residues and about 45% reported without alkylation.³⁶ The minimal sample handling involved between the digestion and the ESMS step likely accounts for the improved recovery, illustrating an advantage of integrated sample processing on chip. For the infusion shown in Figure 4-11, there were 15 fragments with a single missed cleavage, 4 with two missed cleavages, and 5 with 3 missed cleavages out of 43 identified fragments, indicating the extent of digestion.

4.3.3. *Sample Carryover Evaluation*

The trypsin bead bed was quite robust, allowing continuous use of the bed for at least 10 hours with no perceptible change in the digestion profiles for replicate analyses. In addition, the beads were readily removed and replaced, making the device reusable for many weeks or months when exchanging electrospray tips every 3-4 days. However, in any reusable device the issue of sample carryover must be examined. We have evaluated the volume of buffer required to flush cytochrome c digestion products from the reactor bed and the separation channel.

Figure 4-8 shows that a very strong peak at m/z 585 is present in a digested cytochrome c sample. To load the chip, a 3 μM sample of cytochrome c was digested at 1 $\mu\text{l}/\text{min}$ for 3 min, and then infused into the ESMS interface. Various volumes and flow rates were then evaluated for their ability to wash the reactor bed, reintroducing the cytochrome c to the bed between each trial. The rinse solution was removed from reservoir E, and 5 μl of digestion buffer was delivered through the reactor bed by syringe pump into reservoir E, to which 5 μl of 200 mM formic acid was then delivered by pipet. This buffer solution was then infused for ESMS. The top trace in Figure 4-12 shows the sum of 50 mass spectra typically obtained for a 45 s infusion of buffer that had passed through a well cleaned or a fresh reactor bed. The lower trace in Figure 4-12 shows the result of flushing a cytochrome c loaded bed with 50 μl of digestion buffer. The expanded spectra show there is a small peak at m/z 585 after 50 μl of washing buffer, which is similar in magnitude to the less abundant peaks in the buffer background. At a wash volume of 15 μl a considerable 585 peak remained, while washing with 125 μl did not

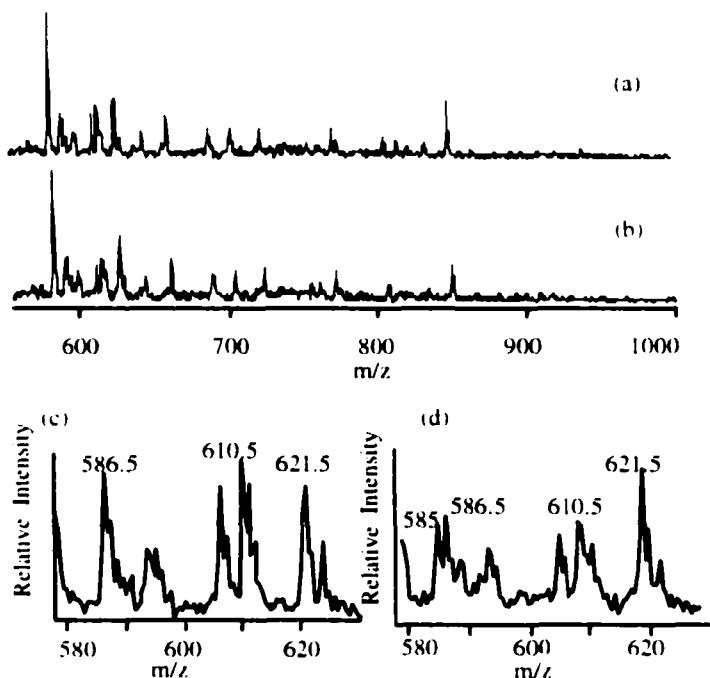


Figure 4-12. Mass spectrum of infusion for 45 s (sum of 50 scans) for (a) digestion buffer passed through a fresh trypsin bead bed, (b) digestion buffer after washing a cytochrome c sample from the bead bed with 50 μ l of buffer at 25 μ l/min, (c) expansion of a region of (a), d) expansion of a region in (b).

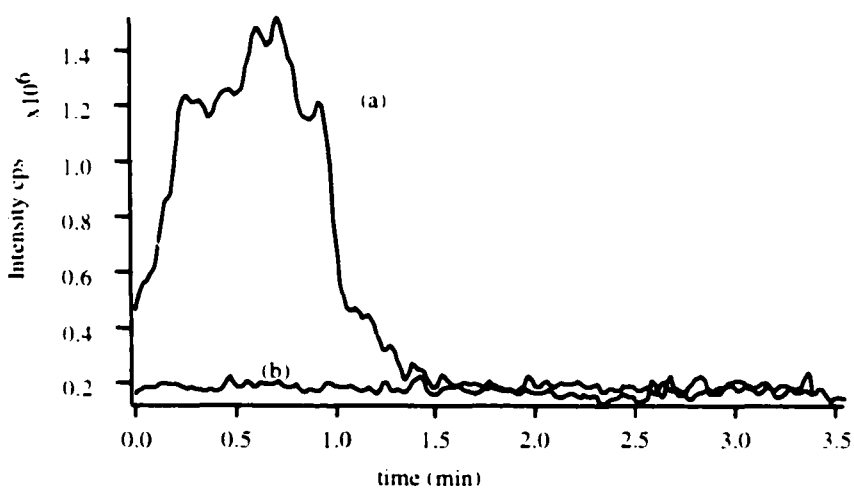


Figure 4-13. Total ion electropherogram (TIE) showing (a) the flushing of 3 μ M cytochrome c digest from the sample and separation channels with running buffer in reservoir E and -2 kV applied to E (see Figure 4-1), and 3 kV on the electrospray tip; (b) the TIE for digestion buffer after passing through a fresh trypsin bead bed, using the same voltage scheme as in (a).

change the 585 peak significantly from those observed with a 50 μ l wash. Varying the flow rate and flush times indicated that the important parameter for cleaning the bed was the total volume used and not the pumping rate. This allows the use of a high flow rate for rapid cleaning.

The sample loading and separation channels located between reservoir E and the electrospray tip must also be flushed of the digestion products. For this purpose buffer that had been passed through the bead bed was directed from reservoir E by application of -2 kV at E and 3.1 kV at the electrospray tip. Figure 4-13 shows the TIE for the removal of cytochrome c digest from the separation channel using this procedure, contrasting the results at the end of the flush with the results for delivering digestion buffer in a clean chip. About 1.5 min was required to clean the channels.

The total time required for performing an infusion and cleaning the reactor bed and the separation channel is about 8 min when using a 25 μ l/min flow rate (bed wash) and the applied potentials described above (channel flush). When combined with a 0.5 - 1 μ l/min flow rate during protein digestion (3 - 6 min digestion time), this corresponds to a total of 11 - 14 min between samples for infusion experiments. An additional 1 - 2 min may be required if a separation is to be performed. Further efforts to optimize the cleaning time by increasing flush rates would significantly improve the time required per analysis with the device. The syringe and capillary transfer line could be exchanged within 30 s, leading to rapid switching of samples.

4.4. Conclusions

A microfluidic device is described in which an electrospray interface to a mass spectrometer (ESMS) is integrated with a capillary electrophoresis channel, an injector and a protein digestion bed on one substrate. The packed bed substantially increases the protein processing capability of the microchip unit. The enhanced speed of melittin digestion in an integrated trypsin bed illustrates a major advantage of creating a packed bed, as opposed to an in-reservoir digestion design. Both melittin and cytochrome c were digested much more rapidly on-chip than off-chip. The kinetic limitations associated with the rapid digestion of low picomole levels of substrate were minimized using an integrated digestion bed with hydrodynamic flow to provide an increased ratio of trypsin to sample. This chip design thus provides a convenient platform for automated sample processing in proteomics applications. A subtle feature of the bed design involves the role of the receiving reservoir E, into which digested protein is pumped. Open to atmosphere, reservoir E acts as a decoupler, separating the hydraulic pressure stage and μl volumes associated with the bed from the nl volume, electrokinetically pumped separation and ESMS stage. The packed trypsin bed digester should provide a useful element for on-chip protein processing. Ultimately, multiple packed beds may be integrated with a single ESMS manifold in order to increase sample throughput. The immobilized trypsin bed may also be coupled to a solid phase extraction bed for analysis of more dilute protein, as will be discussed in the next chapter.

4.5. References

1. Xue, Q.; Foret, F.; Dunayevskiy, Y.M.; Zavracky, P.M.; McGruer, N.E.; Karger, B.L. *Anal. Chem.* **1997**, 69, 426-430.
2. Ramsey, R.S.; Ramsey, J.M. *Anal. Chem.* **1997**, 69, 1174-1178.
3. Xue, Q.; Foret, F.; Dunayevskiy, Y.M.; Karger, B.L. *Rapid Commu. Mass Spectrom.* **1997**, 11, 1253-1256.
4. Figeys, D.; Ning, Y.; Aebersold, R. *Anal. Chem.* **1997**, 69, 3153-3160.
5. Figeys, D.; Gygi, S.P.; McKinnon, G.; Aebersold, R. *Anal. Chem.* **1998**, 70, 3728-3734.
6. Figeys, D.; Aebersold, R. *Anal. Chem* **1998**, 70, 3721-3727.
7. Figeys D, Lock, C, Taylor L, Aebersold R. *Rapid Commu. Mass Spectrom.* **1998**, 12, 1435-1444.
8. Bings, N.H.; Wang, C.; Skinner, C.D.; Colyer, C.; Thibault, P.; Harrison, D.J. *Anal. Chem.* **1999**, 71, 3292-3296.
9. Li, J.; Thibault, P.; Bings, N.; Skinner, C.D.; Wang, C.; Colyer, C.; Harrison, D.J. *Anal. Chem.* **1999**, 71, 3036-3045.
10. Zhang B.; Liu H.; Karger B. L.; Foret, F. *Anal. Chem.* **1999**, 71, 3258-3264
11. Lazar, I.M.; Ramsey, R.S.; Sundberg, S.; Ramsey, J.M. *Anal. Chem.* **1999**, 71, 3627-3631.
12. Li, J.; Wang, C.; Kelly, J.; Harrison, D.J.; Thibault, P. *Electrophoresis* **2000**, 21, 198-210.
13. Li, J.; Kelly, J.; Chernushevich, I.; Harrison, D.J.; Thibault, P. *Anal. Chem.* **2000**, 72, 599-609.
14. Xiang, F.; Lin, Y.; Wen, J.; Matson, D.W.; Smith R.D. *Anal. Chem.* **1999**, 71, 1486-1490.
15. Wen, J.; Lin Y.; Xiang F.; Matson D. W.; Udseth H. R.; Smith R. D. *Electrophoresis* **2000**, 21, 191-197.
16. Oleschuk, R.; Harrison, D.J. *Trends Anal. Chem.* **2000**, 19, 379-388.
17. Walsh, B.J.; Molloy, M.P.; Williams, K.L. *Electrophoresis* **1998**, 19, 1883-1890.
18. Oliver, N.A.; Greenberg, B.D.; Wallace, D.C. *J. Biol. Chem.* **1983**, 258, 5834.

19. Yates, J.R.; Speicher, S.; Griffin, P.R.; Hunkapillar, T. *Anal. Biochem.* **1993**, 214, 397-408.
20. Mann, M.; Hojrup, P.; Roepstorff, P. *Biol. Mass Spectrom.* **1993**, 22, 338.
21. Shevchenko, A.; Wilm, M.; Vorm, O.; Mann, M. *Anal. Chem.* **1996**, 68, 850-858.
22. Patterson, S.D.; Aebersold, R. *Electrophoresis* **1995**, 16, 1791-1814
23. Blackburn, R.K.; Anderegg, R.J. *J. Am. Soc. Mass Spectrum.* **1997**, 8, 483-494.
24. Harrison, D.J.; Manz, A.; Fan, Z.; Ludi, H.; Widmer, H.M. *Anal. Chem.* **1992**, 64, 1926-1932.
25. Harrison, D. J.; Fluri, K.; Seiler, K.; Fan, Z.; Effenhauser, C.S.; Manz, A. *Science* **1993**, 261, 895-897
26. Hadd, A.G.; Raymond, D.E.; Halliwell, J.W.; Jacobson, S.C.; Ramsey, J.M. *Anal. Chem.* **1997**, 69, 3407-3412.
27. Voyksner, R.D.; Chen, D.C.; Swaisgood, H.E. *Anal. Biochem.* **1990**, 188, 72-81.
28. Gobom, J.; Nordhoff, E.; Ekman, R.; Roepstorff, P. *International Journal of Mass Spectrometry and Ion Processes* **1997**, 169/170, 153-163.
29. Davis, M.T.; Lee, T.D.; Ronk, M.; Hefta, S.A. *Anal. Biochem.* **1995**, 224, 235-244.
30. Effenhauser, C.S.; Manz, A.; Widmer, H.M. *Anal. Chem.* **1993**, 65, 2637.
31. Fan, Z.H.; Harrison, D.J. *Anal. Chem.* **1994**, 66, 177-184.
32. Fluri, K.; Fitzpatrick, G.; Chiem, N.; Harrison, D.J. *Anal. Chem.* **1996**, 68, 4285-4290.
33. Shultz-Lockyear, L.L.; Colyer, C.L.; Fan, Z.H.; Roy, K.I.; Harrison, D.J. *Electrophoresis* **1999**, 20, 529-538.
34. Mirgorodskaya, E.P.; Mirgorodskaa, O. A.; Dobretsov, S.V.; Schevchenko, A.A.; Dodonov, A.F.; Kozlovskiy, V.I.; Raznikov, V.V. *Anal. Chem.* **1995**, 67, 2864-2869.
35. Lazar, I. M.; Ramsey, R. S.; Ramsey, J. M. *Anal. Chem.* **2001**, 73, 1733-1739.
36. Whittall, R.M.; Keller, B.O.; Li, L. *Anal. Chem.* **1998**, 70, 5344-5347.

Table 4-1. Peptide Sequences Identified for Trypsin Digests^(a)

Melittin	
m/z	Peptide sequence ^(b)
657.5 (T ₁)	GIGAVLK
757 ²⁺ (T ₂)	VLTTGLPALISWIK
835 ²⁺ (T ₂ R)	VLTTGLPALISWIKR
Cytochrome c	
m/z	Peptide sequence ^(b)
562.5	KATNE
585 ²⁺	TGPNLHGLFGR
589.5 ²⁺	Acetyl-GDVEK
604.5	GITWK
634.5	IFVQK
676.5 ²⁺	TEREDLIAYLK
678	YIPGTK
733	GDVEK GK
718 ²⁺	HKTGPNLHGLFGRO
736.5 ²⁺	TGQAPGFTYTDANK
740 ²⁺	KTEREDLIAYLK
743 ³⁺	GITWKEETLM(ox) EYLENPKK
748 ²⁺	EETLMEYLENPK
762.5	KIFVQK
779.5	MIFAGIK
757 ²⁺	EETLM(ox)EYLENPK
795.5	M(ox)IFAGIK
800 ²⁺	KTGQAPGFTYTDANK
812.5 ²⁺	EETLMEYLENPKK
817.5 ²⁺	CAQCHTVEK (Heme)
821 ²⁺	EETLM(ox)EYLENPKK
964.5	EDLIAYLK

a) The peptide sequences were obtained from <http://prospector.ucsf.edu>

b) Underscores indicate missed cleavages

Table 4-2 BSA peaks and the corresponding sequences

m/z from experiment	m/z in database	Sequence ^{a)}	Number of Missed cleavages
556 ⁴⁺	556.15 ⁴⁺	505 - 523	1
567.5	567.66	410 - 413	1
572.0	572.36	195 - 198	1
577.5 ²⁺	577.70 ²⁺	233 - 242	1
582.5 ³⁺	582.67 ³⁺	42 - 51	
618 ³⁺	618.5 ³⁺	505 - 520	
625.5 ²⁺	625.70 ²⁺	11 - 20	1
642.5 ³⁺	642.75 ³⁺	337 - 347	
648 ²⁺	648.26 ²⁺	222 - 232	1
653.5 ³⁺	653.76 ²⁺	378 - 388	
660.5	660.35	466 - 471	
665.5	665.33	181 - 185	met-ox
674.5 ²⁺	674.64	174 - 185	met-ox 1
689.5	689.37	212 - 217	
708.5 ²⁺	708.82 ²⁺	545 - 556	
708.5 ¹⁺	708.49 ¹⁺	545 - 563	met-ox 1
721 ²⁺	720.82 ²⁺	336 - 347	1
733.5 ²⁺	733.84 ²⁺	432 - 444	1
738 ⁴⁺	737.87 ⁴⁺	160 - 185	2
740.5 ²⁺	740.86 ²⁺	397 - 409	
746.5 ²⁺	746.38 ²⁺	205 - 217	2
757 ²⁺	756.88 ²⁺	414 - 427	
767.5 ¹⁺	767.19 ¹⁺	378 - 396	1
785 ²⁺	784.87 ²⁺	323 - 335	
789.5	789.47	233 - 239	
804 ²⁺	804.44 ²⁺	181 - 194	met-ox 2
813 ¹⁺	812.95 ¹⁺	21 - 41	
818.5	818.90	538 - 544	
821	820.97 ²⁺	413 - 427	1
832.5 ¹⁺	832.61 ¹⁺	42 - 64	1
835 ²⁺	834.99 ²⁺	445 - 458	
856 ⁴⁺	856.23 ⁴⁺	475 - 504	2
869 ⁴⁺	869.26 ⁴⁺	133 - 159	3
881.5 ⁴⁺	881.52 ⁴⁺	397 - 427	3
901.5 ¹⁺	901.72 ¹⁺	436 - 458	1
913.5 ²⁺	913.06 ²⁺	484 - 499	
922.5	922.49	225 - 232	
927.5	927.49	137 - 143	
945.5 ²⁺	945.58 ³⁺	145 - 159	
951.5 ²⁺	951.10 ³⁺	397 - 412	1
953.5 ⁴⁺	953.57 ⁴⁺	240 - 273	3
959 ⁴⁺	958.80 ⁴⁺	82 - 114	3
981 ³⁺	980.81 ³⁺	500 - 524	3

a). The numbers listed are the starting and end numbers of the peptide in the amino acid sequence of BSA.

Chapter 5

Design of a Proteomics Chip: Integration of Protein Digestion, Preconcentration, Capillary Electrophoresis and a Nanoelectrospray Mass Spectrometry Interface Within a Microfluidic Chip

Table of contents	Page
5.1. Introduction.....	122
5.2. Experimental.....	125
5.2.1. Chemicals and Materials.....	125
5.2.2. Microchip Device.....	126
5.2.3 On-Chip Digestion Using Immobilized Trypsin Bead Bed.....	128
5.2.4. Solid Phase Extraction within The Microchip.....	128
5.2.5. Integrated Packed Beds for On-Chip Digestion and Solid Phase Extraction.....	129
5.2.6. Integrated Protein Preconcentration Followed by Trypsin Digestion.....	130
5.2.7 Microchip-CE-nESMS.....	131
5.3. Results and Discussion.....	131
5.3.1. Waters Oasis HLB Beads.....	132
5.3.2. Solid Phase Extraction within the Microchip.....	134
5.3.3. Integrated Packed Beds for On-Chip Digestion and Solid Phase Extraction.....	139
5.3.4. Protein on Beads Preconcentration Followed by Trypsin Digestion within the Microchip.....	144
5.4. Conclusions.....	147
5.5. References	148

5.1. Introduction

The field of proteomics is drawing more and more attention since the completion of the human genome project. Mass spectrometry in conjunction with database searching has become a major tool for protein identification in proteomic analysis.^{1,2} Microfluidic systems may present a powerful new means to automate protein sample preparation for electrospray ionization mass spectroscopy (ESMS).³⁻⁹ Microchips could not only be used as fast CE separation devices, but could also provide a unique compact platform for complex sample processing. Several groups have shown that protein sample preparation could benefit significantly from the miniaturization and automation capabilities that microfluidics can provide. Desalting,⁴ tryptic digestion,^{5,6} sample stacking,⁸ and the IEF process⁹ can be conveniently performed on a microchip before mass spectrometric analysis. We present here the first report of a microfluidic-ESMS interfaced device in which integrated tryptic digestion, solid phase extraction, separation and electrospray ionization is performed. These results move such devices a step closer to an automated proteomic chip.

The analysis of submicromolar protein concentration by ESMS is still challenging for several reasons. Protein loss due to adsorption to surfaces becomes critical when handling submicromolar samples. One needs to limit the number of steps involving lyophilization and transfer of samples. Another reason is that when the protein concentration is low, the digestion speed is greatly reduced. To avoid long digestion times, a high concentration of enzyme needs to be used, but enzyme autolysis becomes a problem at high enzyme-to-protein ratio. For low concentration peptide detection, high sensitivity ionization and mass spectrometer need to be used. To solve these problems,

we need to rapidly digest the dilute protein with less enzyme autodigestion and preconcentrate the sample before analysis. Immobilized trypsin could speed up the protein digestion with high enzyme-to-protein ratio, while giving fewer enzyme autodigestion fragments. Several reports¹⁰⁻¹³ showed that protein digestion could be done in minutes using immobilized enzyme instead of hours or overnight in the solution phase. With short digestion times, protein adsorption to the surface was also reduced. Following digestion, the peptide fragments could be desalted and preconcentrated on a reversed phase sorbent prior to mass spectrometric analysis. Using this technique, impressive results^{12,13} were shown for submicromolar proteins. An alternative approach is to preconcentrate the protein on the solid phase extraction beads followed by enzymatic digestion. When protein is accumulated on the beads, the digestion kinetics could be increased. The digested peptide fragments are also enriched on the beads, which could increase the detection limit of dilute proteins. Doucette et al.¹⁴ showed that proteins could be preconcentrated on POROS R2 beads and washed to remove contaminants. Aguilar et al.¹⁵ also demonstrated that proteins could be digested while bound to C₄ and C₁₈ sorbents. They used high concentrations of proteins to study the binding domains of proteins on the reversed phase sorbent.

Solid phase extraction (SPE) began to be widely used for CE sample preparation since the beginning of 1990s.¹⁶⁻³⁰ Off-line sample pretreatment using SPE usually involves a large volume of sample and takes more time and more steps. Therefore on-line SPE is usually chosen for sample cleanup and enrichment with capillary electrophoresis. On-line SPE-CE was first introduced by Guzman et al.¹⁶ and was further developed by Tomlinson and coworkers¹⁷⁻²¹ for drug metabolites analysis. Now it is also widely used

for peptides and proteins.²²⁻³⁰ On-line SPE-CE involves packing a short column of reversed phase beads or membrane at the sample injection end of the capillary. The reversed phase beads are usually silica C₁₈ beads^{22,24,27-30} or polymer beads,^{23,25} and the membrane is impregnated with suitable stationary phase.²¹ Sample is loaded onto the stationary phase and followed by washing, elution with organic solvent and separation in the CE column. The advantages of SPE are that it can tolerate intensive washing to remove salts or other contaminants, and that large volume sample adsorbed can be eluted with small volume to achieve good preconcentration. Peptide preconcentration of 1000 fold was reported.²⁸ Some problems encountered in the on-line SPE-CE are backpressure generated by tight packing,²⁶ peak broadening,²² and the need of frits to hold beads in position.²⁵ People have been trying to solve these problems by making low resistance packing using glass wool,²⁵ and solvent gradient elution of adsorbed samples.²³

Moving solid phase extraction to microchip for protein digest analysis has not been extensively explored. Figeys et al.³¹ used a microchip device to deliver solvent gradient to a coupled capillary which had C₁₈ sorbent packed inside. The peptides were loaded off-line to the sorbent and then the capillary was coupled to the microchip for gradient elution and mass spectrometric analysis. Li et al.⁸ also tried to couple solid phase extraction to a microchip. The C₁₈ membrane was inserted in the capillary which was connected to the microchip through a hole drilled on the cover plate above the separation channel. The preconcentrated peptides were eluted to the microchip channel for separation. In these two designs, the solid phase extraction bed was outside the microchip and the extra capillary was needed to hold the sorbent. To increase the integration and the

performance, and for future automation, it is desirable to have solid phase extraction bed in the microchip device.

In this chapter we describe the use of an immobilized trypsin bed for fast protein digestion and a solid phase extraction bed for protein or peptide preconcentration in a 2 cm × 6 cm chip. Integrated within the same device was a double-T injector, a capillary electrophoresis (CE) separation channel and an ESMS interface. We used two methods. The first method used a two bed system. Protein was digested in the immobilized trypsin bed followed by preconcentration in the solid phase extraction bed. Then the peptides were eluted for CE-MS analysis. The second method used only a solid phase extraction bed. Protein was concentrated in the bed, followed by digestion with a trypsin solution. Submicromolar cytochrome c was used as the analyte, and the results were compared to digestion without preconcentration.

5.2. Experimental

5.2.1. Chemicals and Materials

The immobilized TPCK treated trypsin beads were from Pierce (Rockford, IL, USA). Oasis HLB solid phase extraction beads were a gift from Waters Limited (Mississauga ON, Canada). POROS R2 (50 μm diameter) beads were from Applied Biosystem (Boston, MA, USA). Cytochrome c, bovine serum albumin (BSA), N, N, N', N'-tetramethylethylenediamine (TEMED), and ammonium bicarbonate were obtained from Sigma Chemical Co. (St. Louis, MO, USA) and were used as received. Formic acid and HPLC grade methanol were from Aldrich Chemical Company Inc. (Milwaukee, WI, USA). [(Acryloylamino)propyl]trimethylammonium chloride (BCQ) was from Chemische

Fabrik Stockhausen (Krefeld, Germany). 7-oct-1-enyltrimethoxysilane was from United Chemical Technologies Inc. (Bristol, PA, USA). Fused silica capillary was from Polymicro Technologies (Phoenix, AZ, USA) and Teflon tubing was obtained from LC Packing (San Francisco, CA, USA).

All of the proteins were prepared in 20 mM ammonium bicarbonate right before use. The separation buffer was a mixture of 10 mM ammonium bicarbonate and 100 mM formic acid, which was prepared in ultrapure water (Millipore Canada, Mississauga, ON) and filtered through a 0.22 μm Nylon syringe filters (Chromatographic Specialties Inc. Brockville, Canada).

5.2.2. *Microchip Device*

The microfluidic device shown in Figure 5-1 was fabricated in 600 μm thick Corning 0211 glass (Corning Glass Works, NY, USA) using standard photolithography and wet chemical etching techniques, as described before. The fluid channel layout is illustrated in Figure 5-1, where the access reservoirs are identified for reference below. Channels were etched on one glass plate to a 10 μm depth and 30 μm width for the majority of the length, with 230 μm wide segments near the reservoirs. Channel lengths were essentially the same as PCRD-2, described previously: the injector to capillary distance was 45 mm, the double T injector had a 100 μm offset, and the channel connected to reservoir D was 24 mm long, measured from the junction. Two large volume channels, 11 mm and 4 mm long, with a width of 800 μm and depth of 150 μm , were etched into the cover plate, after which access holes were drilled in the cover plate. The cover plate was bonded to the other etched plate, after rigorous high pressure rinsing

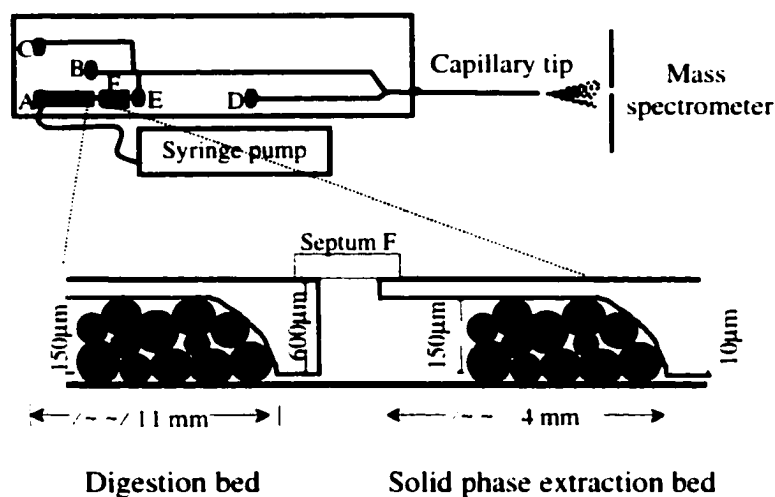


Figure 5-1. Schematic representation of the integrated immobilized trypsin digestion bed, solid phase extraction preconcentration bed and capillary electrophoresis mass spectrometry chip. The bottom shows a blow up of the two bed system. The other channels on the chip are 230 μm wide and 10 μm deep near each fluid reservoir, then narrow to 30 μm wide and 10 μm deep for the majority of their length.

and cleaning. At the end of the main channel, a flat-bottomed hole ($\sim 200 \mu\text{m}$ i.d.) was drilled into the edge of the device and a gold coated nano-electrospray capillary tip was inserted, and held in place with Crystal Bond (Aremco Products, Valley Cottage, NY). The exit end of the 3 cm long nanoelectrospray emitter ($185 \mu\text{m}$ o.d., $50 \mu\text{m}$ i.d.) was tapered to a $10 \mu\text{m}$ i.d. using a capillary puller (Sutter Instruments, Phoenix, AZ). In order to prevent analyte adsorption on the glass walls, the chip channels and the capillary were covalently coated with 7-oct-1-enyltrimethoxysilane to which BCQ was then cross-linked, as described previously.^{3,6,8} This cationic coating gives electroosmotic flow towards the anode (anodal EOF).

The chip was mounted in a Plexiglass holder, described previously.^{3,6,8} Small pipet tips, serving as solution reservoirs, were inserted through the center of a septum, mounted over the access holes in the chip, for all reservoirs except A. The top plate of the holder

was then compressed onto the septa in order to tightly seal the septa and pipet tips into the access reservoirs. For reservoir A, Teflon tubing (~180 μm i.d.) was inserted into the center of a septa over the access hole and used to seal a capillary transfer line. This capillary was used to deliver buffer or protein solution from a syringe pump into the digestion bed or solid phase extraction bed.

5.2.3. On-Chip Digestion Using Immobilized Trypsin Bead Bed

This method was described in detail in Chapter 4. Trypsin-loaded beads were packed in the fat channel between reservoirs A and F, as indicated in Figure 5-1. The bead suspension was loaded into reservoir A and vacuum was applied at reservoir F to pack the bed. Reservoir F was capped after packing. All of the other steps were the same as described in Chapter 4.

5.2.4. Solid Phase Extraction within the Microchip

Oasis HLB solid phase extraction beads were taken from an extraction cartridge. The beads are a copolymeric reversed-phase sorbent, with a diameter of about 60 μm . They were packed in the second fat channel between reservoirs F and E, as indicated in Figure 5-1. Dry beads were conditioned with methanol and equilibrated with water. The bead suspension in water was put in reservoir F. Vacuum was applied at reservoir E and the beads were packed into the bed. The packing process usually took 3-5 minutes, requiring about 0.4 μl (~ 0.15 mg) of solid phase extraction beads for the 4 mm long bed.

After the beads were packed, a septum was used to cover reservoir F and the chip was placed in a chip holder. A syringe pump (Harvard Apparatus, Quebec, Canada) was

used to deliver the solution to the bed through a capillary transfer line inserted in reservoir A. Protein digest in 20 mM ammonium bicarbonate was pumped through the capillary transfer line into the packed bed at a flow rate of 3-4 $\mu\text{l}/\text{min}$. The peptide fragments were adsorbed to the beads while the solvent accumulated in reservoir E and was removed. Reservoir E was initially empty and open to atmospheric pressure, so that the solvent accumulated in reservoir E and was not transferred into the separation channels during this process. After a specified volume of protein digest solution was delivered, the bed was washed by passing 10 μl of 20 mM ammonium bicarbonate at 3 $\mu\text{l}/\text{min}$ and the waste was removed from reservoir E. The adsorbed digests were eluted into reservoir E using 9 μl of methanol at a flow rate of 3 $\mu\text{l}/\text{min}$. Vacuum was applied just above reservoir E to speed up methanol evaporation. When all methanol evaporated, 6 μl of separation buffer was placed in reservoir E to dissolve the peptide fragments and the sample was ready for analysis.

5.2.5. Integrated Packed Beds for On-Chip Digestion and Solid Phase Extraction

Immobilized trypsin beads were packed first in the fat channel between reservoirs A and F. The solid phase extraction bed was packed as described above. After the two beds were packed, a septum was used to cover reservoir F and the chip was placed in a chip holder. The two-bed system is schematically shown in Figure 5-1. Before digestion, the beds were washed with 5 μl 20 mM ammonium bicarbonate digestion buffer. Protein solution in 20 mM ammonium bicarbonate was pumped through the capillary transfer line connected to reservoir A into the packed beds and then into reservoir E. Protein solution was digested as it passed the immobilized trypsin bed. To get full protein

digestion the flow rate used was 0.5 $\mu\text{l}/\text{min}$. The digested fragments were adsorbed to the solid phase extraction beads while the solvent accumulated in reservoir E and was removed. After a specified volume of protein solution was delivered, reservoir E was emptied. The bed was washed by passing 10 μl 20 mM ammonium bicarbonate at 3 $\mu\text{l}/\text{min}$. The adsorbed digests were eluted into reservoir E using 9 μl of methanol at a flow rate of 3 $\mu\text{l}/\text{min}$. Vacuum was used above the reservoir to speed up methanol evaporation. When all methanol evaporated, 6 μl of separation buffer was added to reservoir E to dissolve the peptide fragments. The sample was ready for capillary electrophoresis and electrospray mass spectrometry.

5.2.6. Integrated Protein Preconcentration Followed by Trypsin Digestion

The solid phase extraction bed was packed as described before. To saturate the bed with cytochrome c and prevent trypsin adsorption in the digestion step, only about 2 mm of the bed was packed between F and E in Figure 5-1. Protein solution was pumped through the bed at 1.5 $\mu\text{l}/\text{min}$. After a certain volume passed, the bed was washed with 10 μl of 20 mM ammonium bicarbonate at 3 $\mu\text{l}/\text{min}$. The adsorbed protein was then digested by a 100 ng/ μl trypsin solution passed through the bed at 0.5 $\mu\text{l}/\text{min}$ for one hour. Then the bed was washed with 10 μl of 20 mM ammonium bicarbonate to flush away unused trypsin at 3 $\mu\text{l}/\text{min}$. Reservoir E was emptied and the digested cytochrome c fragments were eluted from the beads using 9 μl of methanol at a flow rate of 3 $\mu\text{l}/\text{min}$. Vacuum was applied above reservoir E to speed up methanol evaporation. When all methanol evaporated, 6 μl of separation buffer was added to reservoir E to dissolve the peptide fragments.

5.2.7. *Microchip-CE-nESMS*

A PE/Sciex API 150 EX quadrupole mass spectrometer (Perkin-Elmer/Sciex, Concord, ON, Canada) was used for these studies. The position of the electrospray needle was optimized for ion current magnitude and stability while electrokinetically infusing 1 µg/ml of leu-enkephalin from reservoir D, with -1 kV on D and about 3 kV on the needle. Optimal potentials on the needle varied from 2.8 to 3.2 kV. Reservoir D was then rinsed and filled with separation buffer. Electroosmotic infusion of sample was performed with -2 kV applied at sample reservoir E and the nanoelectrospray tip between 2.8 - 3.2 kV. Electrokinetic sample injection was conducted for 25 s by applying -2.5 kV at reservoir E while sample waste, reservoir C, and the gold coated capillary tip were grounded. During separation -2.5 kV was applied to reservoir B and ~3 kV to the nanoelectrospray tip. A push back voltage of -1.1 kV was applied at reservoirs C and E to prevent sample leakage. The mass spectrometer was scanned over the range m/z 550-1000 at 0.5 amu per step with dwell time of 1 ms. Peptide masses were compared with the results from a database search of the MS-Digest at <http://prospector.ucsf.edu>. Search parameters were selected assuming all masses were for tryptic peptides, cysteines were unmodified and that methionine oxidation might have occurred.

5.3. Results and Discussion

Our purpose is to develop a method to integrate protein digestion and preconcentration on-chip for mass spectrometric analysis. Protein digestion with immobilized trypsin bead bed was presented in Chapter 4. Before we integrated the two

processes together, the performance of the solid phase extraction method was tested using cytochrome c peptides and standard peptides. Then digestion by immobilized trypsin with pre-concentration by solid phase extraction (SPE) beads were performed sequentially on-chip for dilute cytochrome c solutions. We also pre-concentrated cytochrome c on SPE beads, followed by passing trypsin solution over the bed to digest the adsorbed protein.

5.3.1. Waters Oasis HLB Beads

For peptide pre-concentration by solid phase extraction method, POROS R2 beads have been popular.^{12-14,23,25} Waters Oasis HLB beads are also available for this purpose. These are a polymeric reversed phase sorbent, made from a macroporous copolymer [poly(divinylbenzene-co-N-vinylpyrrolidone)]. The manufacturer claims that they exhibit both hydrophilic and lipophilic retention characteristics. Using cytochrome c as a model protein, we compared the pre-concentration using R2 or HLB beads. An 8 μ M cytochrome c solution was digested at 37 °C overnight in 20 mM ammonium bicarbonate, with a protein enzyme ratio of 20:1. Then 180 μ l of the digest was added to 0.5 mg of HLB beads, pre-washed with methanol. The mixture was vortexed for 15 min and centrifuged. A 20 μ l supernatant sample was collected and mixed with 20 μ l of 200 mM formic acid and 20 μ l of methanol for subsequent electrospray with a conventional Sciex API 150 interface. The peptide fragments on the beads were eluted with 45 μ l methanol and 5 μ l of 200 mM formic acid. The same experiment was done using 0.5 mg of R2 beads.

Figure 5-2 shows the comparison of the supernatant from these two types of beads. For R2 beads (shown in Figure 5-2a), the signal observed for cytochrome c fragments remaining in the solution was much higher than for HLB beads (shown in Figure 5-2b).

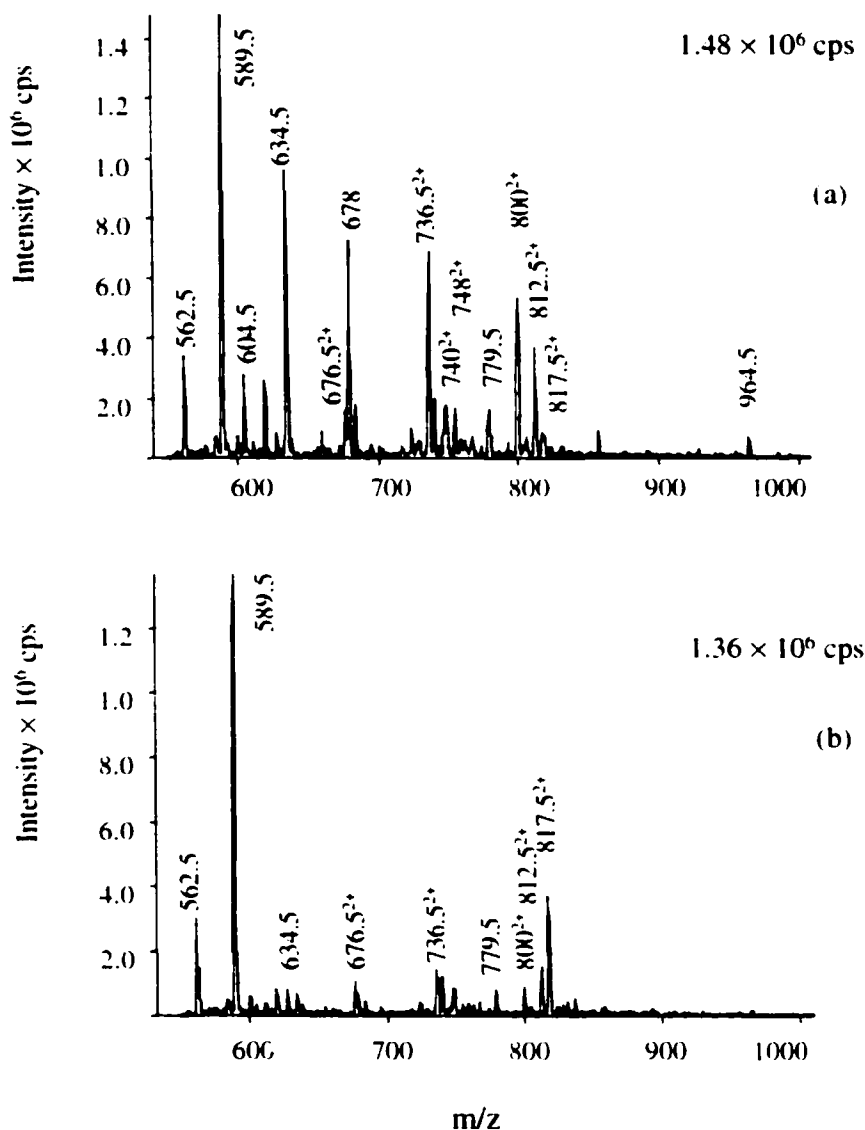


Figure 5-2. Comparison of adsorption effect for (a) POROS R2 beads, and (b) Oasis HLB beads. 180 μ l of 8 μ M cytochrome c digest was added to 0.5 mg of beads and vortexed for 15 min. Then 20 μ l of supernatant was collected and 20 μ l of 200 mM formic acid and methanol each were added for electrospray with traditional Sciex API 150 EX interface. The peptide mass to charge ratio is above the peaks. For discussion see text.

HLB beads left only three fragments with an intensity higher than 2.0×10^5 cps. The fragments at m/z of 562.5 and 589.5 are relatively hydrophilic and were not adsorbed well on the reversed phase beads. We also compared the mass spectrum of the elutes from these two types of beads: corresponding to the results from the supernatant mass spectrum, fragments at m/z 604, 634.5, 676.5²⁺, 678, 800²⁺, 812.5²⁺, 964.5 were better pre-concentrated with HLB beads. For the following experiments, we used HLB beads for pre-concentration of peptides. They are spherical and could be easily packed and unpacked in the fat channel of the chip. With a diameter of about 60 μm , they remain trapped in the bed due to the 10 μm depth of the exit channel. From this study, we also learned that for strongly retained peptides, such as m/z 585 and 964.5, the adsorption capacity of 0.5 mg of the HLB bead is at least as high as 18 μg cytochrome c digest, because the mass spectrum from this supernatant did not show high intensity for these hydrophobic peptide components of cytochrome c, as shown in Figure 5-2b.

5.3.2. Solid Phase Extraction within the Microchip

For solid phase extraction with the microchip, a set of standard peptides were tested first. A mixture of three peptides, leu-enkephalin, angiotension II and LHRH, 0.25 $\mu\text{g}/\text{ml}$ each in a separation buffer of 10 mM ammonium bicarbonate and 100 mM formic acid, was electroinfused from reservoir E. The mass spectrum is shown in Figure 5-3b. When 50 μl of the peptide mixture (0.5 $\mu\text{g}/\text{ml}$ each) was passed through the bed, then eluted with 9 μl of methanol, dried in the reservoir and finally redissolved in 10 μl of the same separation buffer for electroinfusion, and the mass spectrum shown in Figure 5-3a was obtained. Theoretically, the intensity of the corresponding peptide peaks in Figure 5-3a

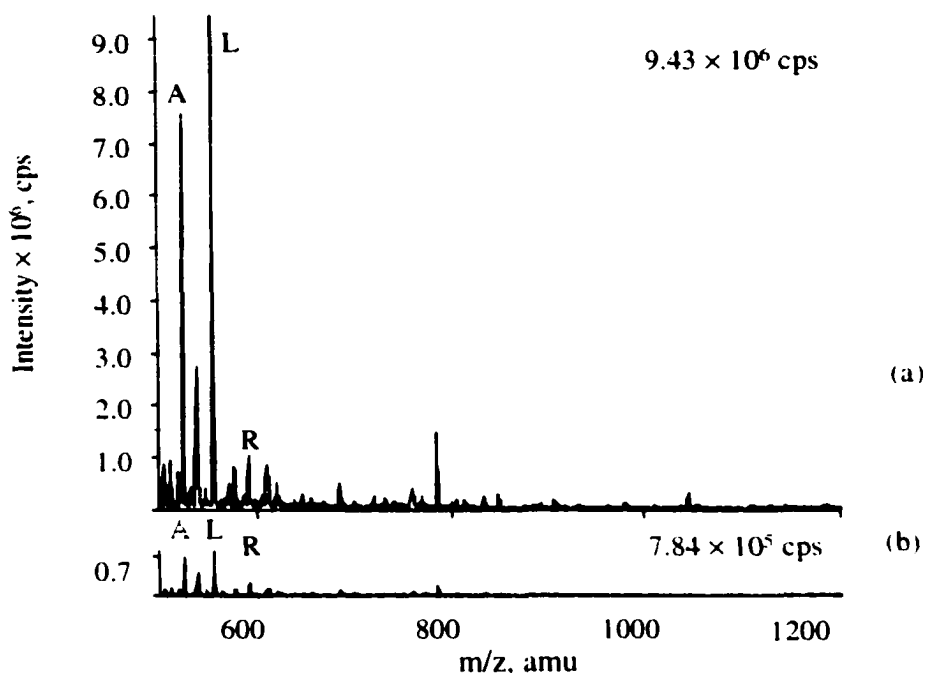


Figure 5-3. Comparison of mass spectrum for three peptides mixture with and without SPE. A: angiotension, L: leu-enkaphalin, R: LHRH (a) 50 μ l of peptide mixture (0.5 μ g/ml) passed through the SPE bed, eluted with methanol, dried and finally dissolved in 10 μ l separation buffer. (b) 0.25 μ g/ml each peptides in separation buffer. The samples were electroinfused from the reservoir E (-2 kV) to the electrospray tip (3 kV). They are all sum of 100 scans.

should be 10 times that in Figure 5-3b. Comparing the intensities of the peaks in Figure 5-3a with 5-3b, leu-enkephalin is 12.0 times higher, angiotension II 10.9 times and LHRH 4.4 times. The calculated recoveries for these three peptides are 120%, 109% and 44%, respectively. An internal standard was not used here for quantitative comparison, so these numbers indicated the approximate preconcentration effects for these peptides. The more than one hundred percent recovery could result from experimental errors, such as errors from liquid volume pipetting or sample adsorption to the mixing tip. It could also originate from the differences in ionization efficiency under differing concentration conditions.³² Among the ten amino acids of LHRH, only leucine has a high hydrophobicity, so that LHRH is more hydrophilic than leu-enkephalin and angiotension II, and it is less retained in the reversed phase HLB beads.

Cytochrome c digest was also used as a sample for on-chip solid phase extraction. An 8 μM cytochrome c solution was digested overnight, then diluted to 100 nM in 20 mM ammonium bicarbonate. Then 80 μl of the 100 nM digest was passed through the solid phase extraction bed at 4 $\mu\text{l}/\text{min}$, followed by wash, elution and organic solvent evaporation. Finally, 6 μl of separation buffer was added to reservoir E and electroinfused for MS analysis. The mass spectrum is shown in Figure 5-4a. Seventeen cytochrome c fragments peaks were clearly identified, with a sequence coverage of 85.6%. Figure 5-4b shows the electroinfusion mass spectrum of a 100 nM cytochrome c digest in running buffer without preconcentration. Only 5 cytochrome c fragment peaks were seen, giving a sequence coverage of 41.3%. If we suppose the peak intensity is proportional to the sample concentration, the intensity of the corresponding peptide peaks in Figure 5-4a should be 13.3 times of that in Figure 5-4b. The comparison of the selected peaks is shown in Table 5-1. The estimated peptide recovery after solid phase extraction is between 41.4% and 106%, which means that this is an efficient way to preconcentrate peptides without much loss for many of them. Further, the peak intensities after solid phase extraction are much higher, providing much greater confidence in the determination of the protein. Since 0.5 mg of HLB beads can retain at least 18 μg of cytochrome c digest, then the solid phase extraction bed, with ~ 0.15 mg of beads, should have a capacity of at least 5.4 μg , which is much higher than the 0.1 μg used here. At 4 $\mu\text{l}/\text{min}$ sample pumping speed, no sample leakage past the bed was seen, as determined by testing the sample waste in reservoir E. The bed packing process took 5 min; 20 min was used for sample pumping, followed by about 8 min for sample washing and elution.

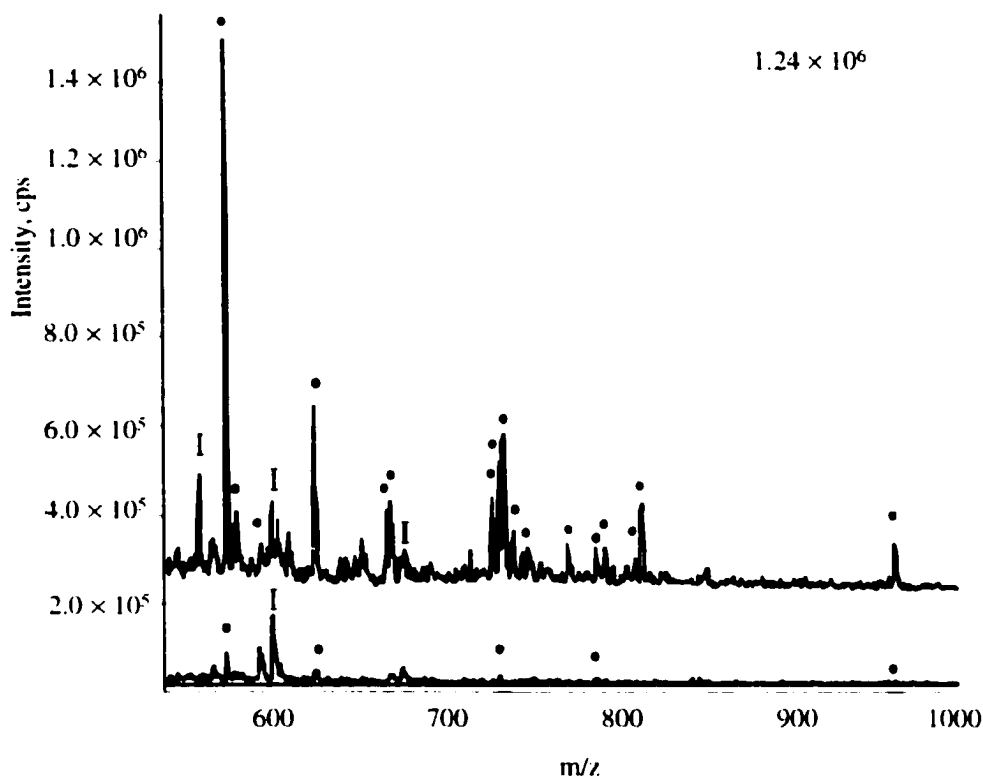


Figure 5-4. Comparison of 100 nM cytochrome c digest mass spectrum with and without SPE. 8 μ M cytochrome c was digested and diluted to 100 nM, (a) 80 μ l of 100 nM cytochrome c digested in 20 mM ammonium bicarbonate passed through the SPE bed at 4 μ l/min and finally conditioned in 6 μ l running buffer. (b) 100 nM cytochrome c in running buffer. For electroinfusion, voltage in reservoir E was -2 kV and electrospray tip was at 3 kV. All of the mass spectrum were sum of 30 scans. Black dot: cytochrome c fragment. I: impurity peaks.

Table 5-1. Comparison of 100 nM cytochrome c fragment intensity with and without SPE

m/z	585	634.5	740	795.5	964.5
Ratio of peak intensity before and after SPE ^{a)}	14.1	10.8	12.1	5.5	11
Recovery ^{b)}	106%	81.2%	91%	41.4%	82.7%

a). The numbers are calculate from the peptide peak intensities in Figure 5-4.

b). The numbers are calculated based on a theoretical value of 13.3.

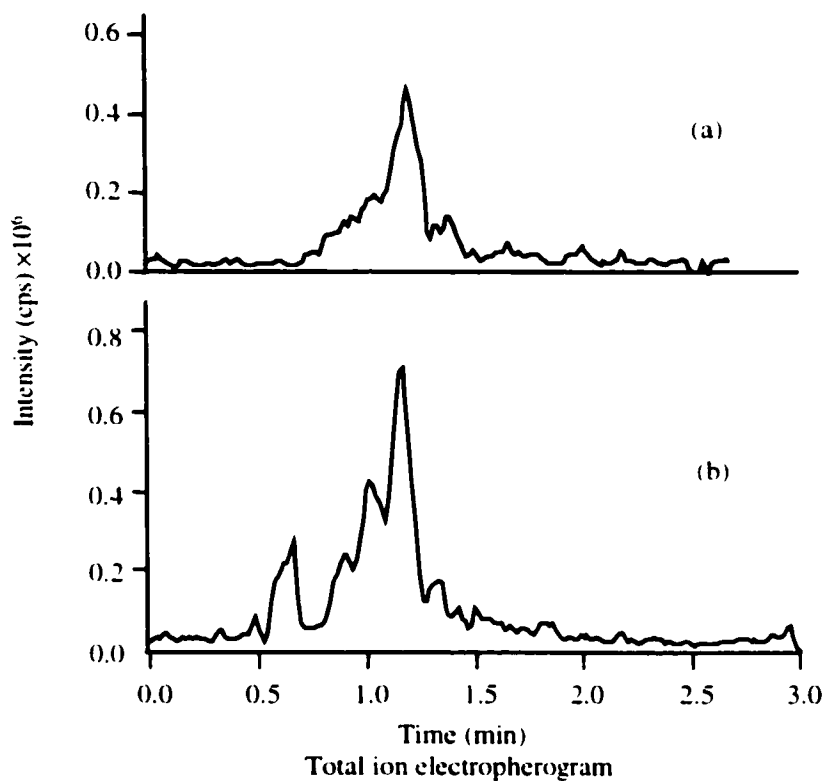


Figure 5-5. Comparison of separation TIE for cytochrome c digest with and without SPE. (a) 4 μM cytochrome c digest, diluted with separation buffer from 8 μM digestion. (b) SPE of 0.4 μM cytochrome c digest diluted with 20 mM ammonium bicarbonate from 8 μM digestion. A 120 μl 0.4 μM digest was flushed through a 4 mm long, on-chip preconcentration bed at 3 $\mu\text{l}/\text{min}$. Elution with 9 μl of methanol (3 $\mu\text{l}/\text{min}$) was followed by evaporation to dryness over 35 min, and addition of 6 μl of separation buffer (100 mM formic acid and 10 mM ammonium bicarbonate). Separation was performed as described in detail in section 5.2.7.

The evaporation took about 30 min, while 50 scans of the mass spectrum during electroinfusion took less than one min. The whole experiment required about 70 min.

Figure 5-5a shows the separation profile of a 4 μM cytochrome c digest. Nine cytochrome c fragments were extracted from this TIE, while 12 fragments were extracted from the pre-concentrated 0.4 μM digest in Figure 5-5b. Pre-concentrated sample shows about 50% higher intensity than the 4 μM sample, and much better resolved peak shape, despite it is ten times lower concentration. It is clear that this solid phase extraction on-chip can pre-concentrate peptides well.

5.3.3. Integrated Packed Beds for On-Chip Digestion and Solid Phase Extraction

At low protein concentration, the kinetics of the digestion reaction is reduced and extremely long digestion time is required. To avoid the very long digestion time a high concentration of enzyme can be used, but the high enzyme/sample ratio increases the chances of enzyme autodigestion. The enzyme fragments may give many peaks at high intensity that mask the sample peaks in the mass spectrum. To solve this problem, we used an immobilized trypsin bed to digest the protein. Immobilized trypsin undergoes less autodigestion than free trypsin. The high enzyme/protein ratio achieved in the packed bed makes digestion much faster, while fewer trypsin peaks will be seen in the peptide map. For submicromolar protein analysis, a pre-concentration method needs to be used before mass spectrometry detection. To improve detection limit, the digestion bed is followed by a solid phase extraction bed in our experiment, pre-concentrating the peptide fragments directly on chip. Figure 5-6 and Figure 5-7 shows a series of studies utilizing on-chip digestion and pre-concentration.

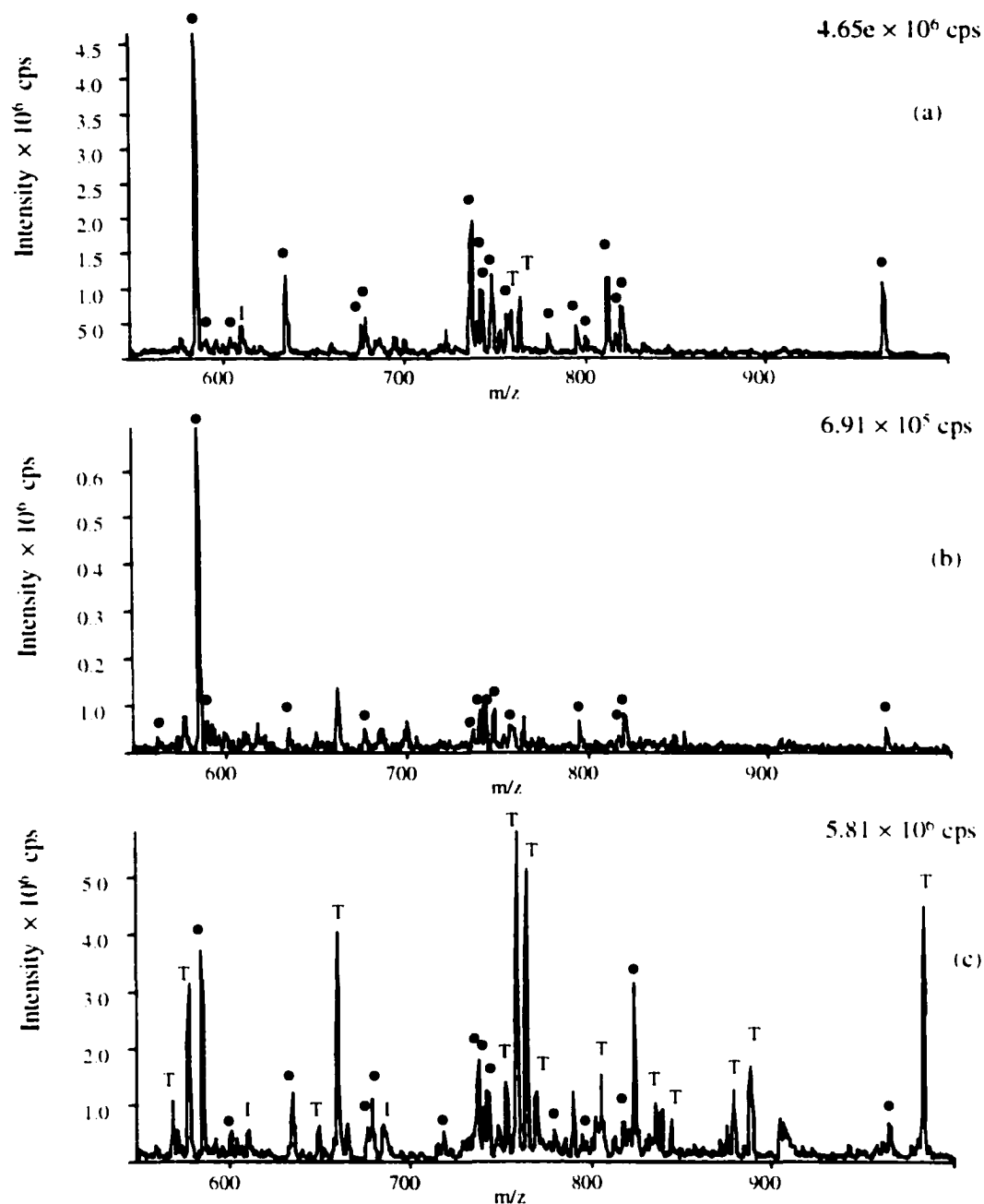


Figure 5-6. Comparison of 800 nM cytochrome *c* digest mass spectrum with and without SPE. (a) 60 μ l of 800 nM cytochrome *c* passed through the digestion bed and SPE bed at 0.5 μ l/min, finally conditioned in 6 μ l running buffer. (b) 5 μ l of 800 nM cytochrome *c* passed through only digestion bed at 0.5 μ l/min and later 5 μ l 200 mM formic acid was mixed. (c) 60 μ l of 800 nM cytochrome *c* passed through the SPE bed at 1.5 μ l/min followed by digestion with 100 ng/ μ l trypsin solution. The digest was eluted, evaporated and finally dissolved in 6 μ l running buffer. For all of these electroinfusion, voltage in reservoir *E* was -2 kV and electrospray tip was at 3 kV. All of the mass spectrum were sum of 50 scans. Black dot: cytochrome *c* fragment. T: trypsin peak. I: impurity peak.

Table 5-2. Comparison of 800 nM cytochrome c peptide recovery after digestion and SPE

m/z	585	634.5	676.5	743	964.5
Recovery from digestion and preconcentration ^{a), c)}	33%	110%	47%	59%	105%
Recovery from preconcentration and digestion ^{b), c)}	27%	110%	58%	59%	64.4%

- a). The numbers are calculated from the peptide peak intensities in Figure 5-6a and 5-6b.
 b). The numbers are calculated from the peptide peak intensities in Figure 5-6c and 5-6b.
 c). All of the recoveries were calculated based on a theoretical value of 20 times enrichment.

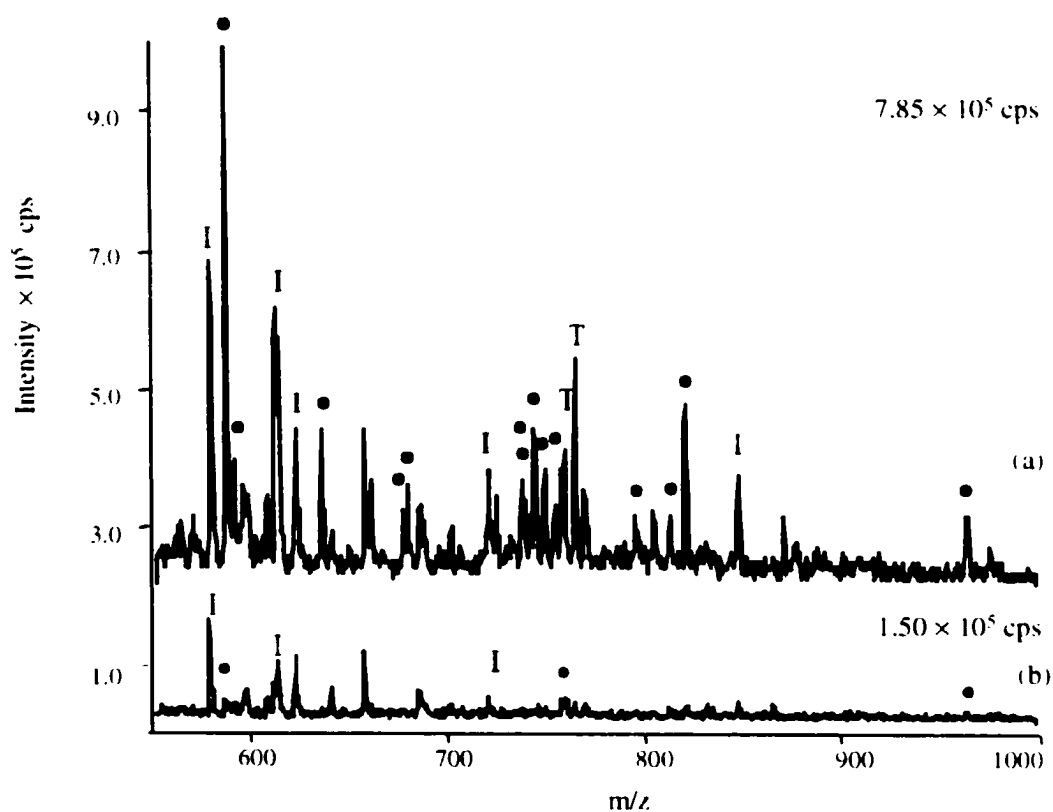


Figure 5-7. Comparison of 200 nM cytochrome c digest mass spectrum with and without SPE. (a) 80 μ l of 200 nM cytochrome c passed through the digestion bed and SPE bed at 0.5 μ l/min, finally conditioned in 6 μ l running buffer. (b) 5 μ l of 200 nM cytochrome c passed through only digestion bed at 0.5 μ l/min and later 5 μ l 200 mM formic acid was mixed. For all of the electroinfusion, voltage in reservoir E was -2 kV and electro spray tip was at 3 kV. All of the mass spectrum were sum of 50 scans. Black dot: cytochrome c fragment. T: trypsin peak. I: impurity peak.

Figure 5-6b shows the mass spectrum of 10 $\mu\text{g/ml}$ (800 nM) cytochrome c, passed through the digestion bed and mixed with 200 mM formic acid without preconcentration. Fourteen peptide peaks were seen and they gave a sequence coverage of 82.7%. When 60 μl of the same protein solution was passed through the digestion bed, followed by preconcentration in the next bed, and finally dissolved in 6 μl of running buffer for electrospray, the mass spectrum gave 18 peptide peaks and a sequence coverage of 85.6%, as shown in Figure 5-6a. After preconcentration, the peak intensity is clearly much higher. If the peak intensity is proportional to the sample concentration, the intensity of the corresponding peptide peaks in Figure 5-6a should be 20 times those in Figure 5-6b. The calculated recovery of the 5 selected peptides is listed in the second row of Table 5-2 to give an estimate of the preconcentration effect. When 200 nM cytochrome c was passed through the digestion bed, 3 tiny peptide peaks were observed, giving 29.8% sequence coverage, as shown in Figure 5-7b. Figure 5-7a shows the results for the same on-chip protein digestion followed by SPE preconcentration: 14 peptide fragments appeared and the sequence coverage increased to 76.0%. Theoretically, the intensity of the corresponding peptide peaks in Figure 5-7a should be 26.67 times of that in Figure 5-7b. The calculated recoveries for these three peaks (m/z 585, 757, 964.5) are 105%, 21% and 34% respectively (See Table 5-3). All of the above results show that preconcentration after digestion is an effective way to enrich a dilute sample.

At this low concentration chemical noise began to be important, with some impurity peaks from the buffer and the Crystal Bond seen in Figure 5-7a. The impurities are labeled I, and trypsin autodigestion peaks are labeled T, as m/z values at 758.5³⁺ and 764³⁺ became apparent. These trypsin peaks would also be preconcentrated on the SPE

beads. These impurity peaks do not constitute a significant interference at 200 nM cytochrome c, but could mask peptide fragments at lower protein concentrations.

The speed of this process is limited by the digestion and the evaporation steps. As we discussed in Chapter 4, when we used a 1.5 cm digestion bed, cytochrome c was completely consumed at flow rates below 1 $\mu\text{l}/\text{min}$. In this two bed system, the digestion

Table 5-3. Comparison of 200 nM cytochrome c peptide recovery after digestion and SPE

m/z	585	757	964.5
Ratio of peak intensity before and after SPE ^{a)}	28.0	5.6	9.1
Recovery ^{b)}	105%	21%	34%

a). The numbers are calculated from the peptide peak intensities in Figure 5-7.

b). The numbers are calculated based on a theoretical value of 26.67.

bed is 1.1 cm and the protein digestion flow rate was limited to no higher than 0.5 $\mu\text{l}/\text{min}$. With the current design, for 60 μl of protein solution delivered at 0.5 $\mu\text{l}/\text{min}$ digestion took two hours at room temperature. To get faster digestion, the digestion bed could be made longer in the future. The immobilization of the trypsin reduced the amount of autodigestion interference. Another advantage of this method is that the digestion and preconcentration were done at the same time, in the same flow path. Since the digest was adsorbed to the SPE bed immediately after digestion, there was no separate step for the SPE process, which avoids sample handling losses and saves time and effort.

5.3.4. Protein on Beads Preconcentration Followed by Trypsin Digestion within the Microchip

A. Doucette et al.¹⁴ have shown that protein may be preconcentrated directly, and then digested "in situ" on the beads by the introduction of trypsin. By raising the protein concentration before digestion, much better digestion kinetics may be achieved. We examined this process within a microchip device. There were three main steps involved. The first step was protein adsorption to HLB solid phase extraction beads. The second steps involved passing trypsin solution through the bead bed to digest the adsorbed protein. In the last step, the protein fragments were eluted with organic solvent to reservoir E, followed by evaporation, addition of separation buffer and mass spectral analysis.

It has been reported¹⁵ that the hydrophobic domains of proteins are bound to the sorbent surface, leaving the hydrophilic regions extending into the solution phase. This process is not protein selective, so that both sample and trypsin will adsorb. It is important to bind the sample protein quickly and to saturate the bead surface to avoid trypsin adsorption during the digestion step. Speed is important to shorten analysis time and also because adsorption seems less reversible over time. For cytochrome c, we found that the protein bound to the beads much faster in basic buffer, such as ammonium bicarbonate. When 100 µg/ml of protein in water was vortexed together with HLB beads for 30 min, the solution remained red, due to the heme group chromophore, while the beads were not stained red. Immediately after adding ammonium bicarbonate, the beads became red, indicating strong adsorption of cytochrome c. This could be because cytochrome c has a high pI of 9.6, so that in basic conditions it is less charged and less

hydrophilic, so it binds better to the reversed phase sorbent. For all of the following experiment, we dissolve the cytochrome c in 20 mM ammonium bicarbonate (pH 8.1) for the binding step.

Figure 5-6c shows the results for 800 nM cytochrome c analyzed using this protein adsorption followed by trypsin digestion procedure. Fourteen cytochrome c fragment peaks were identified. There were also many trypsin autodigestion peaks, many at higher intensity than the cytochrome c peaks. When we tried to reduce trypsin autodigestion by using low concentration of trypsin and shorter digestion time, we found that much of the cytochrome c was undigested. In MALDI, when a protein was not totally digested, its peak is usually far from the peptide peaks. In electrospray almost all of the peaks fall within the same window due to multiple charging, so that undigested cytochrome c may mask the fragment peaks. Although this method needs to be further optimized to reduce autolysis peaks, we can see that most of the cytochrome c fragments were preconcentrated and clearly identified. Theoretically, the intensity of the corresponding peptide peaks in Figure 5-6c should be 20 times of that in Figure 5-6b. The calculated recoveries for five of the selected cytochrome c peptides were listed in the third row of Table 5-2. Comparing the cytochrome c peptide intensities in Figure 5-6a with 5-6c and summary in Table 5-2, it is seen that the two digestion and preconcentration results are comparable, although the protein concentration-digestion method shows many more trypsin autodigestion peaks. Consequently, the latter procedure was not pursued further on chip with lower protein concentration.

Attempts were made to optimize the trypsin digestion of the preconcentrated cytochrome c. The results presented were about the best obtained for 800 nM cytochrome

c solutions. The use of lower trypsin concentration (the tested concentration range was between 40 ng/ μ l to 120 ng/ μ l) produced less digested cytochrome c for a one hour digestion time. A higher amount of trypsin simply increased the autodigestion problem. Reaction times from 30-120 min were tested using microcentrifuge tubes. Time proved to be less important than the amount of trypsin used in terms of cytochrome c consumption. In the chip 40-80 min reaction times were used but again changing the trypsin amount was more important for affecting the extent of protein digestion. Both the R2 beads and the HLB beads were tested for this procedure and the HLB beads were superior, binding the peptide fragment better.

In theory, the digestion/preconcentration method is still kinetically limited at lower concentrations. In contrast, the protein preconcentration/digestion method is always kinetically favored due to the accumulation of protein on the beads. With our current approach there are many trypsin autodigestion peaks observed, which limits the procedure's utility. However, it remains a potentially attractive alternative for dilute protein analysis, since this autodigestion problem might eventually be overcome. A possible method of improving the experimental design to reduce trypsin autodigestion will be discussed in Chapter 6.

In all of these digestion and/or preconcentration processes, we can see that reservoir E plays an important role. Open to the atmosphere, reservoir E acts as a decoupler, separating the hydraulic pressure stage and μ l volumes associated with the bed from the nl volume, electrokinetically pumped separation and ESMS stage. It also separates the basic digestion buffer and organic elution solvent from the BCQ coated CE channel and ES analysis, which needs acidic buffer. The beds were fabricated directly in the cover

plates, and no frits were needed for bed packing. The packed bead beds could be clearly seen in the transparent glass chip, making it easy to inspect the bed packing quality. Several steps, including protein digestion, peptide preconcentration, washing, elution, sample infusion and electrospray detection were all integrated within the 2 cm × 6 cm chip, minimizing sample transfer steps. This reduced the sample loss and effort by the experimentalist. Currently, reservoir E requires several microliters of sample for analysis. Better preconcentration effect could be achieved by decreasing the volume of the sample reservoir and reducing the volume needed in reservoir E. Time could also be saved by developing a better method for evaporating the elution solvent in the reservoir.

5.4. Conclusions

We have designed an integrated system on microchip for protein digestion, solid phase extraction, capillary electrophoresis and electrospray mass spectrometry analysis. This is the first report which includes so many protein processing steps within a microfluidic device for MS detection. Unlike previous reports, in which the microchip was used as a capillary to feed sample to a mass spectrometer, we have tried to make great use of the advantages of the microfluidic systems. Protein may be rapidly digested, and also preconcentrated, in a convenient integrated set of steps in the chip. Longer digestion beds can be used in the future to further increase the digestion speed and reduce the total time needed. In the future complex protein digests adsorbed in the solid phase extraction bed can be later eluted using a gradient elution method with a similar, but different, chip design, which will be shown in the next chapter. By using on line gradient elution, much less elution solvent could be used and preconcentration factors could be

much higher. The current results show the significant promise of integration of protein processing steps, identify areas that need improvement, yet clearly establish the feasibility of this approach.

5.5. References

1. Jensen, O.N.; Podtelejnikov, A.V.; Mann, M. *Anal. Chem.* **1997**, 69, 4741-4750.
2. Borchers, C.; Peter, J.F.; Hall, M.; Kunkel, T.A.; Tomer, K.B. *Anal. Chem.* **2000**, 72, 1163-1168.
3. Li, J.; Kelly, J.; Chernushevich, I.; Harrison, D.J.; Thibault, P. *Anal. Chem.* **2000**, 72, 599-609.
4. Xiang, F.; Lin, Y.; Wen, J.; Matson, D.W.; Smith R.D. *Anal. Chem.* **1999**, 71, 1486-1490.
5. Xue, Q.; Dunayevskiy, Y. M.; Foret, F.; Karger, B. L. *Rapid. Commun. Mass Spectrom.* **1997**, 11, 1253-1256.
6. Wang, C.; Oleschuk, R.; Ouchen, F.; Li, J.; Thibault, P.; Harrison, D. J. *Rapid Commun. Mass Spectrom.* **2000**, 14, 1377-1383.
7. Zhang B.; Liu H.; Karger B. L.; Foret F. *Anal. Chem.* **1999**, 71, 3258-3264.
8. Li, J.; Wang, C.; Kelly, J. F.; Harrison, D. J.; Thibault, P. *Electrophoresis* **2000**, 21, 198-210.
9. Wen, J.; Lin, Y.; Xiang, F.; Matson,D.; Udseth, H.R.; Smith, R.D. *Electrophoresis* **2000**, 21, 191-197.
10. Voyksner, R.D.; Chen, D.C.; Swaisgood, H.E. *Anal. Biochem.* **1990**, 188, 72-81.
11. Davis, M.T.; Lee, T.D.; Ronk, M.; Hefta, S.A. *Anal. Biochem.* **1995**, 224, 235-244.
12. Gobom, J.; Nordhoff .E.; Ekman, R.; Roepstorff, P. *International Journal of Mass Spectrometry and Ion Processes* **1997**, 169/170, 153-163.
13. Blackburn, R.K.; Anderegg, R.J. *J. Am. Soc. Mass Spectrum.* **1997**, 8, 483-494.
14. Doucette, A.; Craft, D.; Li, L. *Anal. Chem.* **2000**, 72, 3355-3362.
15. Aguilar, M.; Clayton, D. J.; Holt, P.; Kronina, V.; Boysen, R. I.; Purcell, A. W.; Hearn, M. T. W. *Anal. Chem.* **1998**, 70, 5010-5018.

16. Guzman, N. A.; Trebilcock, M. A.; Advis, J. P. *J. Liq. Chromatogr.* **1991**, 14, 997-1015.
17. Tomlinson, A. J.; Benson, L. B.; Johnson, K. L. *J. Chromatogr.* **1993**, 621, 239-248.
18. Tomlinson, A. J.; Benson, L. B.; Naylor, S. *J. Cap. Elec.* **1994**, 2, 127-135.
19. Tomlinson, A. J.; Benson, L. B.; Oda, R. P.; Braddock, W. D. *J High Resol. Chromatogr.* **1994**, 17, 669-673.
20. Tomlinson, A. J.; Naylor, S. *J High Resol. Chromatogr.* **1995**, 18, 384-386.
21. Tomlinson, A. J.; Benson, L. B.; Jameson, S.; Naylor, S. *J. Am. Soc. Mass Spectrum.* **1996**, 8, 15-24.
22. Strausbauch, M. A.; Landers, J. P.; Wettstein, P. J. *Anal. Chem.* **1996**, 68, 306-314.
23. Tong, W.; Link, A.; Eng, J. K.; Yate, J. R. *Anal. Chem.* **1999**, 71, 2270-2278.
24. Bonneil, E.; Waldron, K. C. *J. Chromatogr. B* **1999**, 736, 273-287.
25. Herring, C. J.; Qin, J. *Rapid. Commun. Mass Spectrom* **1999**, 13, 1-7.
26. Osbourn, D. M.; Weiss, D. J.; Lunte, C. E. *Electrophoresis* **2000**, 21, 2768-2779.
27. Figeys, D.; Ducret, A.; Yates, J. R.; Aebersold, R. *Nature Biotechnology* **1996**, 14, 1579-1583.
28. Figeys, D.; Ducret, A.; Aebersold, R. *J. Chromatogr. A* **1997**, 763, 295-306.
29. Figeys, D.; Aebersold, R. *Electrophoresis* **1997**, 18, 360-368.
30. Figeys, D.; Zhang, Y.; Aebersold, R. *Electrophoresis* **1998**, 19, 2338-2347.
31. Figeys, D.; Aebersold, R. *Anal. Chem.* **1998**, 70, 3721-3727.
32. Kebarle, P.; Tang, L. *Anal. Chem.* **1993**, 65, 972A-986A.

Chapter 6

Summary and future outlook

Table of Contents	Page
6.1. Further Development of Microchip-ESMS Interface.....	151
6.2. Improvement for Integrated Packed Bed Protein Digestion on Chip.....	152
6.3. More Thinking about Solid Phase Extraction on Microchip.....	153
6.4. References.....	158

6.1. Further Development of Microchip-ESMS Interface

In Chapter 2, we discussed different designs for the microchip-ESMS interface. Direct electro spray from the flat edge of the chip at the channel outlet suffered from liquid spreading and difficulty of forming stable spray. Small nozzles fabricated in silicon,¹ sharp ends made from plastic^{2,3} and capillary tips⁴⁻¹⁰ coupled to a microchip were all used to generate stable electro spray for MS analysis in different groups. We used a gold coated capillary tip coupled at the end of the channel in the microchip, which proved to be a reliable interface. Protein and peptide separations were achieved using this setup and it provided a convenient way of sample EOF infusion and separation for MS detection. The gold tip could be used for days without showing deterioration. However there are still problems with this interface. The connection hole fabrication is a laborious process. The Crystal Bond used to glue the capillary tip to the chip can be easily dissolved in an organic solvent such as acetonitrile, which limits the solvent that can be used on microchip.

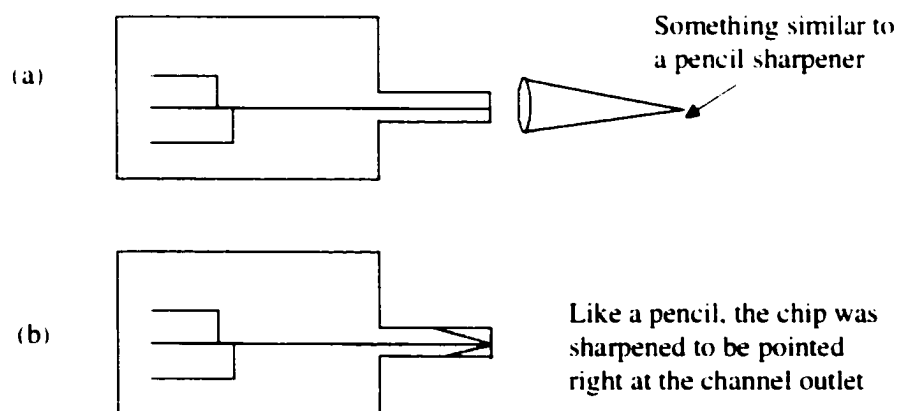


Figure 6-1. Schematic of the possible way for making a direct electro spray tip from a chip. (a) The chip is cut to have a narrow end at the exit channel section and it is inserted to the sharpener. (b) The chip is sharpened right at the channel outlet (see the dot line). Gold coating could be applied at the tip for voltage application.

I had been thinking about how to get a pointed tip directly from a chip. When I used a pencil sharpener and saw that pencil was inserted, rotated and came out as a beautiful cone shape with a very sharp tip, I wondered if our chip might also be sharpened like this. Figure 6-1 shows the basic idea. The chip was cut to a shape as in Figure 6-1a, so that the end part that includes the channel was narrowed for further fabrication. Then the narrow part is inserted to the tool that could sharpen the chip like a pencil sharpener. The possibility of making this kind of sharpener plays an important role for this idea. The key point is to have a very good blade or something extremely sharp, and to position the channel outlet precisely at the center of the cone. This method relies on mechanical work and may prove to be very challenging practically. But once this sharpener could be made, it could be used for glass and plastic. It could also be mass produced. Another possibility is to sand the end of the chip, as shown in Figure 6-1a. A piece of sand stone could be made to be cone shaped inside. The slim end of the chip was inserted into the sand stone which is rotating, so that a pointed tip could be made. After the tip is made, it can be deposited with gold for voltage application.

6.2. Improvement for Integrated Packed Bed Protein Digestion on Microchip

In Chapter 4, we described how an immobilized trypsin bed was used for fast protein digestion. The integrated packed bed appeared to be the fastest digestion method comparing to reservoir digestion and traditional solution phase digestion. At a flow rate of 0.5 $\mu\text{l}/\text{min}$, only 6 min. was needed to digest 3 μl cytochrome c solutions. But when larger volumes of protein solutions need to be digested, such as 100 μl , more than 200 min. is needed. To get faster digestion, the immobilized trypsin bed could be made

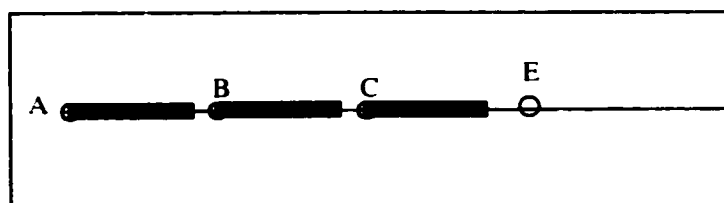


Figure 6-2. Design of making multiple digestion beds to increase the total bed length.

longer, so that the protein solution pumping speed could be increased, while ensuring that the protein has the same contact time with the enzyme. However, packing a bed longer than 2 cm with vacuum alone could be challenging. Once some beads are packed in the column, they build up the resistance and slow further packing. To solve this problem, a multiple bed system could be used. Figure 6-2 shows a three-bed system. The beds could be fabricated as described in Chapter 4 and Chapter 5, with each bed ~1.5 cm long. First, bed A could be packed by sucking at reservoir B while bead suspension is in reservoir A. Then bed B could be packed by sucking at reservoir C while having the bead suspension in reservoir B. A similar process could be done for the continuous bed packing. After packing, reservoir B and C could be capped and the operation of the multiple bed system works like the one bed system discussed in Chapter 4. This design gives the flexibility of choosing a long or short bed according to experimental needs. When a short bed is needed, less beds could be packed and the other beds left empty. This design solves the packing problem and provides whatever long bed we need for fast protein digestion.

6.3. More Thinking about Solid Phase Extraction on Microchip

In this thesis, we described two sample preconcentration methods adapted into the microchip device: one is large volume sample stacking (Chapter 3) and the other is solid phase extraction (Chapter 5). Large volume sample stacking with polarity switching is a

useful way to enrich analyte ions with high electrophoretic mobilities in the direction opposite to EOF. Compared to normal double T injection, significant improvements in sensitivity were achieved for peptides of higher mobility, such as bradykinin (50-fold). Reversed phase solid phase extraction is good for hydrophobic sample preconcentration. The latter has been widely used and is relatively easy to operate, especially as it provides a convenient way for sample clean up.¹¹⁻¹⁴ Using a solid phase extraction bed fabricated into the microchip device, standard peptides and cytochrome c fragments were all preconcentrated well. Continuous protein digestion and preconcentration was achieved by using the immobilized trypsin bed connected with a solid phase extraction bed in a microchip. Compared to integrated packed digestion without an SPE step, eleven more peptide fragments appeared and sequence coverage increased from 29.8% to 67% for 200 nM cytochrome c solutions.

For solid phase extraction in Chapter 5, adsorbed peptides were eluted with 9 μ l of methanol, evaporated and dissolved in 6 μ l of running buffer for further sample infusion or separation. The preconcentration factor could be increased by reducing the buffer volume needed to finally dissolve the sample. Here we introduce another design to increase the preconcentration effect and to eliminate the organic solvent evaporation time. The chip layout is shown in Figure 6-3. The solid phase extraction bed is in the

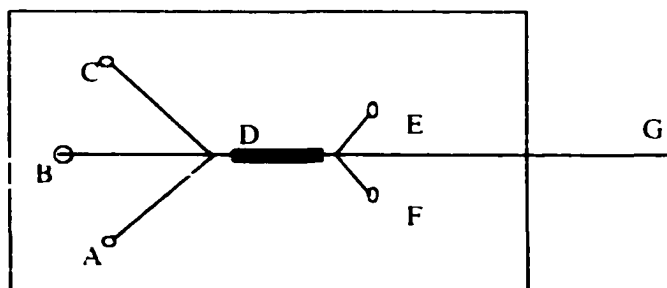


Figure 6-3. Solid phase extraction of peptides followed by gradient elution.

middle and is directly connected with reservoir D. The solid phase extraction bed could be packed by sucking at reservoir E or F while a bead suspension is in reservoir D. Reservoir F is optional and could be removed. After packing, reservoir D is capped. During the sample loading step, reservoir A and C are also sealed using a septum. A peptide mixture is introduced to the bed through reservoir B by pumping and by applying vacuum through reservoir E and F. In this way, sample waste would be removed through reservoir E and F. After sample loading and washing, reservoir A and C are opened. An organic solvent, such as methanol, is put in reservoir A and aqueous buffer is put in reservoir C. Voltage is applied to reservoir A, C and electrospray tip G. A solvent gradient could be generated by ramping voltages in reservoirs A and C. Peptides in the solid phase extraction bed could be gradiently eluted and separated before MS detection. The volume of solvent used for elution could be very small and a much better preconcentration effect could be achieved. Figeys et al.¹⁵ have demonstrated this using a microchip to generate solvent gradient and sequentially elute peptides absorbed on an off-chip SPE cartridge. In our new design, everything is in the chip and which makes it more compact and integrate.

The gradient elution design discussed above could also be coupled to the integrated packed bed digestion. The chip layout is shown in Figure 6-4. The immobilized trypsin

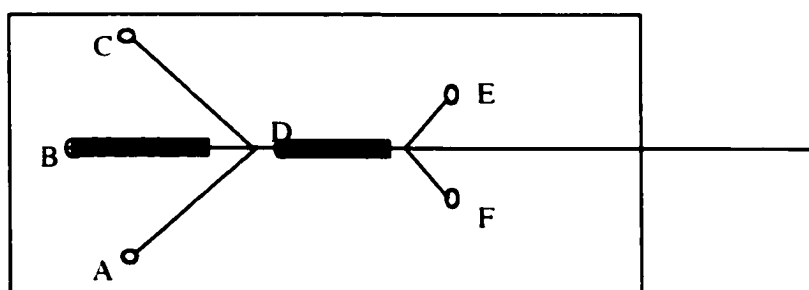


Figure 6-4. Design for digestion and SPE followed by gradient elution.

bed is connected to reservoir B and the SPE bed is connected to reservoir D. In the bead packing process, reservoir A and C are sealed. The immobilized trypsin bed could be packed by sucking at reservoir D while trypsin bead suspension is in reservoir B. The solid phase extraction bed is packed as described above. After packing, reservoir D is also capped. A protein solution is pumped through reservoir B into the digestion bed, then into the solid phase extraction bed. Vacuum could be applied at reservoir E and F to get rid of sample waste. After passing sample and washing, reservoir A and C would be opened to introduce organic solvent and aqueous buffer, respectively. Gradient elution would then be done as described above. In this way, immobilized trypsin digestion, solid phase extraction and gradient solvent elution are all combined together on a microchip before ESMS analysis. There is no organic solvent evaporation step involved and much time could be saved. Several continuous digestion beds could be used and the digestion speed could also be increased to save time.

In Chapter 5, we also tried to preconcentrate cytochrome c on the solid phase extraction bed, followed by passing trypsin solution to digest the protein adsorbed. The peptide peak intensities were clearly increased and the recovery ranged between 33% - 100%. At the same time, many trypsin autodigestion peaks appeared. In the design used in Chapter 5, trypsin was dissolved in the digestion buffer and gradually passed through the bed. Before the trypsin digested the protein in the bed, it had gone through a certain amount of autodigestion in the digestion buffer, especially when a long digestion time, such as one hour, needed to be used. The design in Figure 6-3 could be used to reduce the trypsin autodigestion before it digests the proteins. The solid phase extraction bed is packed as described above. After packing reservoir D is capped. During the sample

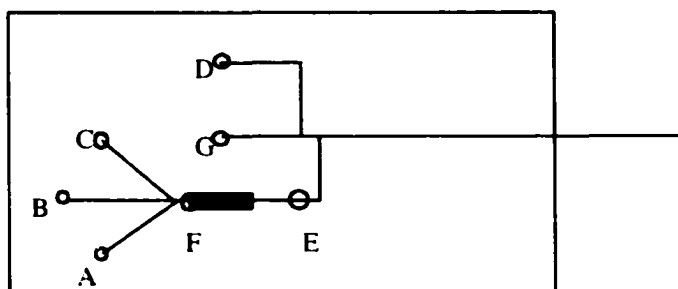


Figure 6-5. Solid phase extraction and CE elution or separation design.

loading step, reservoir A and C are also sealed using septa. Protein solution is introduced to the bed through reservoir B by pumping and by vacuum through reservoir E and F. In this way, sample waste is removed through reservoir E and F. After sample loading and washing, reservoir A and C are opened and reservoir B is sealed. A trypsin solution in water is placed in reservoir A and the digestion buffer is placed in reservoir C. Trypsin undergoes less autodigestion when it is in water. Pressure is applied to reservoir A and C to drive the solutions to mix in the solid phase extraction bed. The waste is collected through reservoir E and F by slightly applying vacuum. In this way, the trypsin solution is mixed with the digestion buffer right before it goes to the bed and the chances of autodigestion could be reduced. After digestion, the peptides could be gradually eluted as we described above or they could be electroinfused or separated by EOF as described in Chapter 4 and Chapter 5. The design could be like the layout shown in Figure 6-5. The peptides are eluted to reservoir E. After organic solvent evaporation, running buffer would be added for electroinfusion or separation.

6.4. References

1. Schultz G. A.; Corso T. N.; Prosser S. J.; Zhang S. *Anal. Chem.* **2000**, 72, 4058-4063.
2. Wen, J.; Lin Y.; Xiang, F.; Matson, D.W.; Udseth, H.R.; Smith, R.D. *Electrophoresis*, **2000**, 21, 191-197.
3. Yuan C.; Shiea, J. *Anal. Chem.* **2001**, 73, 1080-1083.
4. Bings, N.H.; Wang, C.; Skinner, C. D.; Colyer, C.; Thibault, P.; Harrison, D. J. *Anal. Chem.* **1999**, 71, 3292-3296.
5. Li, J.; Kelly, J.; Chernushevich, I.; Harrison, D. J.; Thibault, P. *Anal. Chem.* **2000**, 72, 599-609.
6. Li, J.; Wang, C.; Kelly, J.; Harrison, D. J.; Thibault, P. *Electrophoresis* **2000**, 21, 198-210.
7. Zhang, B.; Liu, H.; Karger, B.L.; Foret .F. *Anal. Chem.* **1999**, 71, 3258-3264.
8. Zhang, B.; Karger, B.L.; Foret, F. *Anal. Chem.* **2000**, 72, 1015-1022.
9. Figeys, D.; Ning, Y.; Aebersold, R. *Anal. Chem.* **1997**, 69, 3153-3160.
10. Figeys, D.; Gygi, S.P.; McKinnon, G.; Aebersold, R. *Anal. Chem.* **1998**, 70, 3728-3734.
11. Gobom, J.; Nordhoff, E.; Ekman, R.; Roepstorff, P., *International Journal of Mass Spectrometry and Ion Processes* **1997**, 169/170, 153-163.
12. Blackburn, R.K.; Anderegg, R.J. *J. Am. Soc. Mass Spectrum.* **1997**, 8, 483-494.
13. Tomlinson, A. J.; Benson, L. M.; Jameson, S.; Johnson, D. H.; Naylor, S. *J. Am. Soc. Mass. Specrom.* **1997**, 8, 15-24.
14. Bonneil, E.; Waldron, K. C. *J. Chromatogr. B* **1999**, 736, 273-287.
15. Figeys, D.; Abersold, R. *Anal. Chem.* **1998**, 70, 3721-3727.